An-Najah National University

Faculty of Graduate Studies

MODELING OF GROUNDWATER RECHARGE IN THE EOCENE AQUIFER (PALESTINE) USING THE USGS SOIL WATER BALANCE (SWB) SOFTWARE

By

Amr Adel Deeb

Supervisor

Dr. Mohammad N. Almasri

This Thesis is Submitted in Partial Fulfillment of the Requirements for the Degree of Master of Water and Environmental Engineering, Faculty of Graduate Studies, An-Najah National University, Nablus, Palestine

2021

MODELING OF GROUNDWATER RECHARGE IN THE EOCENE AQUIFER (PALESTINE) USING THE USGS SOIL WATER BALANCE (SWB) SOFTWARE

By

Amr Adel Deeb

This Thesis was defended successfully on 18/11/2021 and approved by:

Dr. Mohammad N. Almasri	
Supervisor	Signature
Dr. Fayez Abuhelou	
External Examiner	Signature
Dr. Abdelhaleem Khader	
Internal Examiner	Signature

Dedication

I dedicate my thesis to my parents, brother and sister

With all respect

Amr

Acknowledgements

I would like to express great thanks to my supervisor Dr. Mohammad N. Almasri for his continuous support, suggestions, guidance, and assistance during preparing this thesis.

Deep grateful to Stephen M. Westenbroek of the U.S. Geological Survey for his assistance in the SWB code.

I express my sincere thanks to the Palestinian Water Authority (PWA) especially to Omar Zayed and Ibrahim Hantash for helping me obtain the necessary data for this thesis.

I would like to thanks the Palestinian Meteorological Department (PMD), Jenin Municipality, and the Ministry of Agriculture (MoA) especially Ghassan Nairat, Rima Dallal, Naser Attari, and Dr. Ahmad Jaradat for their cooperation in providing me with the necessary data for this thesis.

Declaration

I, the undersigned, declare that I submitted the thesis which is titled:

MODELING OF GROUNDWATER RECHARGE IN THE EOCENE AQUIFER (PALESTINE) USING THE USGS SOIL WATER BALANCE (SWB) SOFTWARE

I declare that the work provided in this thesis, unless otherwise referenced, is the researcher's own work, and has not been submitted elsewhere for any other degree or qualification.

Student's Name: **Amr Adel Deeb**

Signature: 

Date: **18/11/2021**

Table of Contents

List of Tables

List of Figures

List of Appendices

MODELING OF GROUNDWATER RECHARGE IN THE EOCENE AQUIFER (PALESTINE) USING THE USGS SOIL WATER BALANCE (SWB) SOFTWARE

By

Amr Adel Deeb

Supervisor

Dr. Mohammad N. Almasri

Abstract

Groundwater is the main source of freshwater in Palestine. Groundwater recharge is a hydrological process that occurs when the water seeps to the subsurface and reaches the saturation zone. This process begins with the occurrence of rainfall on the ground surface, followed by the process of water infiltration into the root zone. Groundwater recharge is one of the components of the hydrological cycle, but it is the least understood one; because it is highly variable in space and time and is difficult to measure directly. However, knowing and measuring the recharge of the aquifer is vital and extremely important for the groundwater management process. This research had used the Soil Water Balance (SWB) code developed by the U.S. Geological Survey (USGS), to simulate the potential groundwater recharge for the Eocene Aquifer for the year 2020. The Eocene Aquifer is located in the northern part of the West Bank, Palestine. The features of SWB code are that it is the input that the code needs are easy to get, and estimates the amount of groundwater recharge with accuracy based on spatial and temporal distributions. The SWB model spatial resolution was selected with a 30 m × 30 m uniform cells. In order to model recharge, the aquifer domain was discretized into regular square cells. The SWB model succeeded in estimating the amount of recharge based on spatial and temporal variations for 2020 with a value of 50.70 mm/year (1.996 in/year) and the total annual recharge of the entire Eocene Aquifer during the study period is 23.25 million cubic meters (MCM). The recharge amount was about 10.07% of the rainfall volume. Recharge rate varies among land use types. The SWB model was verified using the Water Table Fluctuation Method (WTF) and the Water Demand Calculation Method (WDC) by comparing the results of the potential recharge values obtained from the SWB model with the recharge values obtained from the WTF and the WDC methods.

The research showed significant conformity between the SWB model and the verification methods. The curve number values were manually adjusted by -2%, -1%, and -0.5% for land use types, and the curve runoff number values with the best fit to the WTF method to get more realistic results. The performance of the SWB model was evaluated after the verification process using relative error (RE) and goodness of fit between the simulated recharge values generated by SWB model and the observed recharge values resulting from the WTF method. The total annual amount of water demand for the Eocene Aquifer was estimated about of 28.29 MCM, where the results of the research proved that the groundwater level in the Eocene Aquifer is decreasing with time due to the annual water deficit, which was estimated at about of 5.04 MCM. Sensitivity analysis was performed to examine how the percentage change in the curve number affects the percentage change in the corresponding recharge. The curve number values have been adjusted for all land use by ± 5% and ± 10%. The results show that groundwater recharge is highly sensitive to small variations in the curve number values and have a large impact on model results. The highest recharge rates occur in the southern and northwestern parts of the Eocene Aquifer. The lowest rates of recharge are distributed in the center and north of the aquifer. This corresponds to the spatial distribution of rainfall and the land use types in the area. The research recommended that a groundwater management plan should be made in the Eocene Aquifer based on the results of the SWB model in order to manage and maintain renewable and sustainable water resources in this aquifer and to increase the groundwater level by achieving a balance between recharge and total pumping, develop precautionary plans to protect the groundwater from pollution, and understand the negative impact of the transformation of highly recharge areas to residential areas on the water situation in the aquifer.

Chapter One
Introduction

1.1 General Background

Groundwater is one of the main sources of freshwater that is found in the subsurface within the rock formations and between the porous spaces in the soil and in the form of basins called aquifers (Groundwater Foundation, 2005). It is stored and moves slowly in these aquifers. Groundwater moves within an aquifer at different speeds and its speed depends on many factors and characteristics of the aquifer. The groundwater level may rise or fall depending on recharge. Heavy rains cause the groundwater level to rise, while the heavy continuous pumping of water from wells reduces the water level in the aquifer (Groundwater Foundation, 2005). The amount of groundwater recharge is directly proportional to the rate of rainfall (Owor et al., 2009). In addition to the effect of the topographic nature on groundwater recharge. The increase in the ground surface slope leads to an increase in the amount of runoff and a decrease in the amount of infiltration, which leads to a decrease in the amount of recharge. In general, the recharge maps show that the amount of groundwater recharge is low in urban and mountainous areas, and is high in coastal and low-elevation areas (Singh et al., 2018; Healy and Scanlon, 2010).

Given the great importance of groundwater, it is necessary to achieve a sustainable groundwater utilization through proper management and by considering the safe extraction of water (Fetter, 2001; Komakech and Bont, 2018). The most important conditions in managing the sustainability of groundwater are the calculations, estimations, and detailed knowledge of the quantities of potential groundwater recharge. Needless to mention that the groundwater recharge is an important aspect of the hydrological cycle, and it is necessary for water balance calculations (Lentswe and Molwalefhe, 2020).

Groundwater recharge occurs when water seeps into the subsurface and supplies the aquifer with water (Jezdimirovic et al., 2019). Freeze and Cherry (1979) defined recharge as the process of entering the water from the unsaturated zone into the saturated zone. Groundwater recharge is a basic component to the global water balance; because it supplies and recharges groundwater aquifers and thus provides freshwater to large parts of the world (Hartmanna et al., 2017). A recharge is a tool for managing water resources

and is necessary to create a balance between water supply and water consumption (Jhariya et al., 2016).

For efficient management of groundwater, the quantity of groundwater recharge must be determined, especially in the areas which depend on groundwater as the main source of freshwater (Kumar, 2003; Koussis et al., 2010) and to properly achieve the water balance and assess water vulnerability to contamination (Singh et al., 2018; Healy and Scanlon, 2010).

Groundwater in Palestine is the main source of freshwater (PWA, 2018). Palestine is considered one of the region's most vulnerable to water problems in terms of quantity due to restrictions imposed on the access to water resources due to political factors and the shortage of water quantity resulting from the imbalance between water supply and water consumption. Therefore, it is necessary to know, evaluate and calculate the amount of available water from recharge, as the amount of the aquifer yield depends mainly on the amount of recharge (Salim and Wild, 2003; Sahuquillo, 2017).

The increase in population and intensive agriculture in the Eocene Aquifer area caused an increase in the water demand, followed by a decline in the water table. This decline led to dryness and abandonment of many wells, especially in the summer where the water demand is high and the recharge is at a minimum (Almasri et al., 2020).

Groundwater recharge estimations that take into consideration the spatial and temporal variations are necessary for many hydrological assessments. They assist in developing and constructing groundwater flow models where the recharge model outputs are used as inputs to the groundwater flow model, transport of contaminants, and groundwater replenishment. Recharge is impacted by many land use activities such as urban, agricultural, and industrial development (Scanlon et al., 2002; Manna et al., 2019).

Figure 1.1 illustrates the features of groundwater recharge along with the factors that affect this process, which are spatially and temporally variable and difficult to evaluate. It is also sensitive to many different activities such as urban, agricultural, and industrial development. It depends on many factors including temperature, rainfall pattern, classification of land use, land cover, hydrologic soil group, available soil-water capacity, and surface water flow direction (see figure 1.1). In addition, the recharge has a great role

in the transport of contaminants. The regional importance of recharge is apparent as it determines the safe yield of the groundwater aquifers (Sharma, 1986; Yenhun et al., 2017; Hartmanna et al., 2017; USGS, 2016; Meyland, 2011).

Figure 1.1:

Features and factors affecting the groundwater recharge.

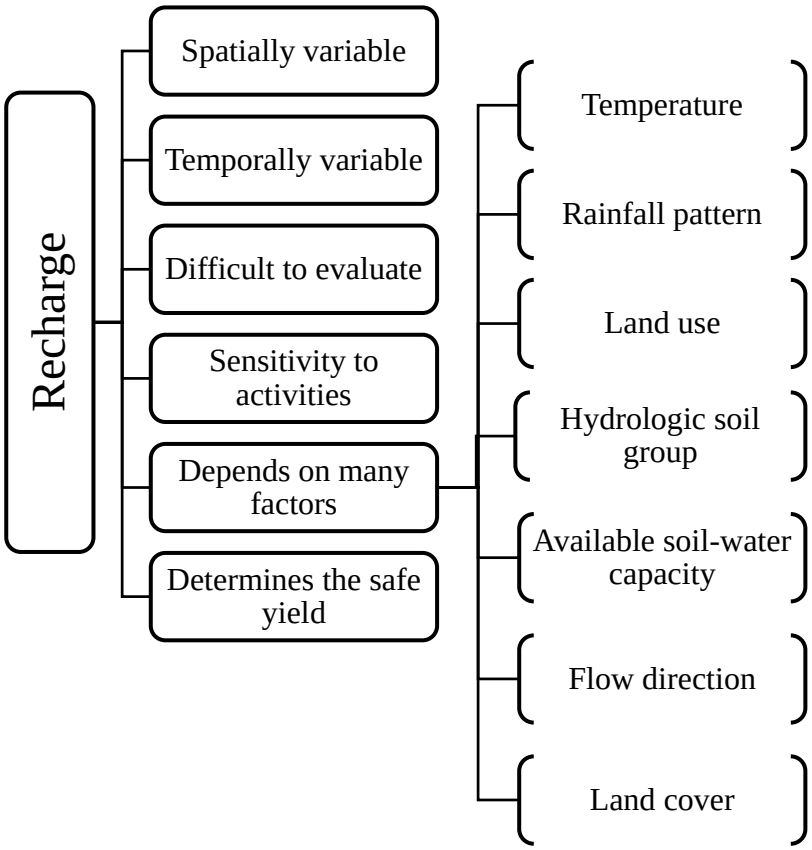

There are many codes used to estimate the amount of groundwater recharge (ESPERE[1] code, SWAP[2] code, EARTH[3] code), but some of them do not take into consideration the spatial and temporal variations in recharge amount, and others do not perform the calculations based on the daily timestep. Therefore, the soil water balance (SWB)[4] code was used (Day, 2019; Smith and Westenbroek, 2015; Metropolitan Council, 2014; Harlow and Hagedorn, 2018; Hart et al., 2012).

[1] ESPERE: estimating effective rainfall and aquifer recharge by different methods
[2] SWAP: soil-water-atmosphere-plant
[3] EARTH: the extended model for aquifer recharge and soil moisture transport through the unsaturated hardrock
[4] https://www.usgs.gov/centers/umid-water/science/swb-modified-thornthwaite-mather-soil-water-balance?qt-science_center_objects=0#qt-science_center_objects

The SWB code was used intensively in many sites in the U.S. but, to our best knowledge, was never used in Palestine before.

This research aims to apply the SWB code developed by the U.S. Geological Survey (USGS), to simulate the potential groundwater recharge for the Eocene Aquifer, which is located in the northern part of the West Bank, Palestine.

In this research, groundwater recharge will be estimated based on spatial and temporal distributions. The high potential recharge zones that are important in defining zones vulnerable to contamination will be delineated by building a groundwater recharge model for the Eocene Aquifer by SWB code. The percentage of annual recharge from annual rainfall will be estimated. The verification of the developed model will be carried out using the water table fluctuation method (WTF) and water demand calculation method (WDC). The performance of the developed model will be evaluated by calculating the relative error and goodness of fit between the simulated recharge rates resulting from the SWB model and the calculated recharge rates resulting from the WTF method. A sensitivity analysis for recharge and curve number will be done, and the relationships between recharge, climate, land use, and curve number will be studied.

1.2 Research Questions

The main purpose of this research is to answer the following questions:

1. What is the amount of annual average total recharge in the Eocene Aquifer?
2. Which zones in the Eocene Aquifer have the high potential for recharge?
3. What is the percentage of annual recharge from annual rainfall?

1.3 Research Objectives

The objectives of this research are as follows:

1. To estimate the spatial and temporal variations in groundwater recharge for the Eocene Aquifer.
2. To delineate the high potential recharge zones.

1.4 Research Outputs

The main outputs of this research are:

1. Maps of the spatial and temporal variations in groundwater recharge for the Eocene Aquifer.
2. A readily available recharge model for the Eocene Aquifer.

1.5 Research Motivations

The following are the research motivations:

1. Groundwater in Palestine is the main source of freshwater, and thus it is necessary to quantify groundwater recharge using a reliable method.
2. This is the first time that a model has been made to simulate groundwater recharge for the Eocene Aquifer based on spatial and temporal distributions. This will help and facilitate the work of other researchers in knowing and evaluating the quantity and quality of water, groundwater modeling, pollutant transport, understanding the impact of urbanization, agricultural activities and industrial development on the recharge quantity. In addition, the recharge model helps in developing plans to protect the groundwater from pollution and the decline in the water table of the Eocene Aquifer.

1.6 Research Methodology

The overall research methodology is divided into six basic stages (see figure 1.2): literature review, data collection, data processing, model development, analysis of model output and the preparation of the conclusions and recommendations.

Figure 1.2:

The Methodology.

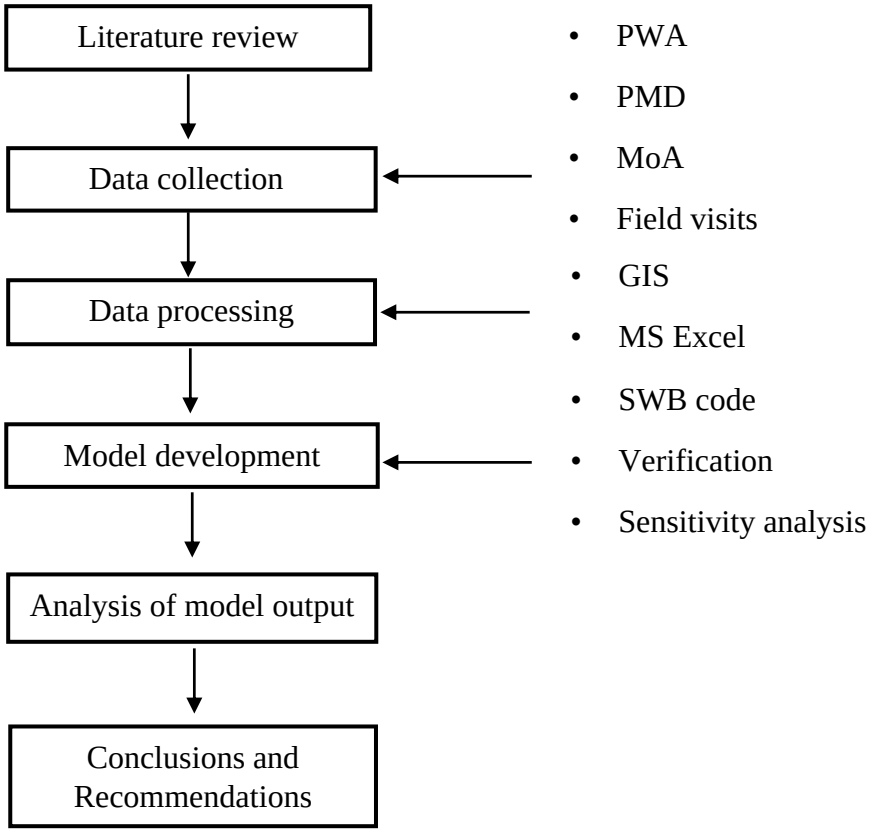

The first stage in the methodology is the literature review in order to know and study the methods and theories that have been followed and adopted in previous studies related to groundwater recharge. We can know the processes that affect recharge, and therefore to highlight the tools that were used to confront the problems that were encountered in the previous studies. In addition, the tutorial of the SWB code was studied to understand the mechanism of code functionality and to know the required inputs and outputs of the model; to obtain correct results, and to understand the equations and theories on the basis of which the code was developed.

The second stage of the research methodology includes collecting basic information and data necessary for the modeling of groundwater recharge. This information and data were obtained from the Palestinian Water Authority (PWA), previous related studies, the Palestinian Meteorological Department (PMD), the Ministry of Agriculture (MoA), reports, and the visits to the study area. The following required data were used:

1. Topographic maps.

2. Climatic data including temperature and rainfall.
3. Hydrologic soil group map.
4. Land use map.
5. Available water capacity.

The third stage includes processing the obtained data. The processing includes converting the data from shapefiles using ArcMap (GIS) software to tabular and gridded data (ASCII files). The SWB code supports tabular and gridded data that are used as input to the SWB code.

The fourth stage involves building a groundwater recharge model for the Eocene Aquifer by SWB code based on the gathered data and information and based understanding and solving the problems encountered in the stage of model development. After the verification of the developed model was carried out using the water table fluctuation method (WTF) and water demand calculation method (WDC). The performance of the resulting model was evaluated by calculating the relative error and goodness of fit between the simulated recharge rates resulting from the SWB model and the calculated recharge rates resulting from the WTF method. Also, a sensitivity analysis for recharge and curve number was carried out to examine how the percentage change in the curve number affects the percentage change resulting in the recharge.

In the fifth stage, the developed model was used to study the spatial and temporal variations in the amounts of groundwater recharge. At this stage, the total annual recharge amount was calculated, the results of the SWB model were reviewed, maps were made to show the recharge zones, and the relationships between recharge, climate, land use, and curve number were studied.

In the sixth and final stage, conclusions and recommendations for future work were made based on the results of this research.

1.7 Groundwater Recharge: A General Overview

Recharge is a hydrological process that occurs when the water seeps to the underground and reaches the saturation zone (Yeh et al., 2016). This process (see figure 1.3) begins with the occurrence of rainfall on the ground surface, followed by the process of water infiltration into the root zone. The water that was not consumed by the plants and did not

evaporate will continues to infiltrate by a process called percolation (recharge) and supplies the groundwater aquifer with water (Freeze and Cherry, 1979; Anderson et al., 2015).

Groundwater recharge is one of the components of the hydrological cycle, but it is the least understood one; because it is highly variable in space and time, and is difficult to measure directly (Lentswe and Molwalefhe, 2020). However, knowing and measuring the recharge of the aquifer is vital and extremely important for the groundwater management process (Simmers, 1990; Adane et al., 2018). There are many methods that are used for the process of determining the recharge of groundwater, including: (1) Physical methods that depend in their calculations on the water balance and soil physics; (2) Chemical methods that use water-soluble materials such as tracer; (3) Hydrological modeling methods that work to develop an approximate model by using water balance calculations to simulates the real situation (Melati et al., 2019; Healy and Scanlon, 2010).

Figure 1.3

The hydrological cycle process (Adhikari, 2020).

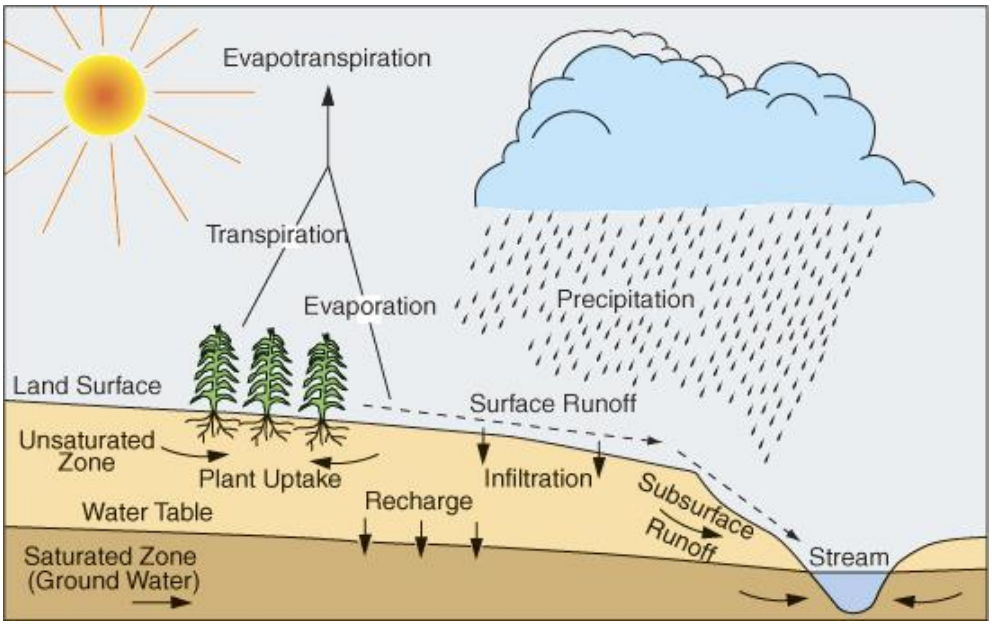

The process of groundwater recharge occurs slowly and depletion of groundwater resources may occur if they are exploited in the long term at rates greater than the recharge rates. This leads to a decrease in the level of water table. Therefore, it is necessary to make estimations of recharge quantities to achieve the water budget in groundwater aquifers and appropriate utilization of groundwater in quantities (Jemal, 2006).

The main factors that affect the amount and movement of recharge are:

1. Geology: the amount of recharge is affected by the geological formations of the aquifer. The aquifers with highly permeable geological formations are the best aquifers. Water moves easily within the aquifer when internal voids and fractures are well connected. The aquifer contains sufficient and connected voids and fractures that make it a good aquifer in terms of storage capacity and ease of water passage. This leads to an increase in the recharge amounts. Some sedimentary rocks such as limestone and sandstone are good aquifers; due to containing fractures and voids of high permeability. Igneous and metamorphic rocks such as granite and quartz have a low porosity, which makes them poor aquifers and their recharge amount is low (Vandas et al., 2002);
2. Rainfall: groundwater recharge rates are highly affected by the amount, duration, distribution, and intensity of rainfall. There is a direct relationship between infiltration and recharge. The duration of the rainfall has a great influence on the infiltration rate. When the rainfall occurs, infiltration occurs rapidly because the soil is unsaturated, and with time the rate of infiltration begins to slow until the soil reaches saturation conditions and the surface runoff begins to increase, accompanied by a decrease in groundwater recharge rates. Rainfall occurrence over a short period of time results in low recharge quantities; because the soil did not take enough time for the water to pass through. On the contrary, the occurrence of rainfall over a longer period of time is accompanied by higher rates of infiltration and recharge rates (USGS, 2019);
3. Soil type: it is one of the factors that have a great impact on the recharge rate. Water moves and seeps faster within sandy soils due to its large pores, which increase the recharge rate, but in clay soils, the pores are small and cause a decrease in infiltration rates. This leads to an increase in surface runoff and decrease in groundwater recharge rates (USDA, 2011);
4. Slope: when the slope of the land surface is high, surface runoff occurs more easily, which leads to a decrease in infiltration rates due to decrease in water ponding on the surface, and thus the groundwater recharge rate is reduced (USGS, 2019);
5. Soil compaction: it occurs when the space between soil particles is reduced due to the compression of soil particles together, as a result, the permeability of the soil

decreases, which leads to a decrease in the infiltration rate, soil drainage and leads to a decrease in the recharge rate (University of Minnesota Extension, 2018);

6. Weather conditions: the amount of groundwater recharge is affected by weather changes, where the highest rates are during the winter due to rainfall and low temperatures, which are followed by fewer evaporation rates. Lower recharge rates in the summer are due to high temperature and absence of rainfall (Kotchoni et al., 2018);
7. Land use: this has a significant impact on the rate of groundwater recharge. Urban, industrial and agricultural development, followed by increasing the areas of buildings and paved streets (impervious areas), causes an increase in water demand and a decrease in the areas exposed to infiltration, which leads to a decrease in groundwater recharge rates (Yang and Zhang, 2011);
8. Permeability: the increase in the pore size in the soil leads to an increase in the permeability of the soil (the ability of the soil to transmit a fluid). This leads to an increase in the infiltration rates, which increases the groundwater recharge rates (USGS, 2018); and
9. Soil moisture content: groundwater recharge rates are affected by soil moisture content. Saturated soil loses its ability to hold more water where infiltration rates reach its maximum capacity. This leads to an increase in runoff and reduced recharge rates (Silva and Rushton, 2007).

It is important to take these factors into consideration when estimating groundwater recharge (Thapa et al., 2017; Rukundo and Doˇgan, 2019; Lwasaki et al., 2014).

Chapter Two
Literature Review

2.1 Introduction

Due to the importance of groundwater, many studies have been concerned with estimating the amount of recharge locally and worldwide. Groundwater recharge is the main factor that determines the sustainability of groundwater aquifers because it determines the maximum amount of water that may be withdrawn from the aquifers without depleting it (Döll and Fiedler, 2008). For effective and sustainable groundwater management, the groundwater recharge must be modeled based on the spatial and temporal distribution in order to be used in groundwater flow models and to be employed in making administrative decisions related to the water. In addition, it contributes to preparing maps of groundwater recharge zones and determining recharge rates (Dripps and Bradbury, 2007).

The following are studies to estimate the amounts of groundwater recharge.

2.2 Worldwide Studies of Groundwater Recharge Estimation

Hatfield et al. (1999) used the water budget method (see equation 2.1) to calculate the amount of potential recharge to the Walnut creek watershed located in the southern part of the Iowa State, U.S. The amount of recharge was calculated for the time period from 1992 to 1995 and the results were 0.04 in, 2.2 in, 4 in, and 3.7 in, respectively. The study showed that the average amount of recharge for the study period was less than 5% of the annual rainfall for the same period.

$$Recharge = (Precipitation - Evapotranspiration) + Stream\ discharge \qquad (2.1)$$

Where each term in equation 2.1 has the same units (inches per year).

Hart et al. (2012) used the SWB model to estimate groundwater recharge based on spatial and temporal variations in Dane County, Wisconsin, U.S. They also used the resulting maps (groundwater recharge maps) to identify areas that contribute significantly to recharge for the study area. The annual variation rate of recharge for the study area was from less than 5 in/year to more than 20 in/year in the period from 1950 to 2008. They showed that the temporal variations in the recharge value were due to annual climate

changes, while the spatial variations were due to land use, soil type, and topography of the area. Their results demonstrate that applying the SWB model gives very consistent and reasonable results compared to various other methods for estimating the amount of recharge, and the SWB model gives high accuracy in results with low effort.

Metropolitan Council (2014) recommended a study using the SWB model with a groundwater flow model for regional water supply planning for the Twin Cities metropolitan area (Minneapolis - Saint Paul), U.S. The main objective of the research was to estimate the spatial variations of the groundwater recharge. This study, using the SWB model, estimated the recharge rates for the entire area for the period 1988-2011, which averaged about 8.2 in/year. The study worked on the overlap of the SWB recharge grids and the MODFLOW grids for groundwater modeling. Finally, the results of the study showed that the SWB model is a good application that allows the estimation of spatially and temporally variable recharge quantities that reflect changes in climate, soil, and land use.

Smith and Westenbroek (2015) estimated groundwater recharge for the entire state of Minnesota, U.S. using the SWB model, as they found that the potential annual rate of groundwater recharge for the entire study area for a period of 15 years is estimated to be about 4.9 in/year. The study showed that the lowest recharge area was in the western part of the state where the rainfall is low, and also because of its clayey soil with lower permeability. The model was calibrated using baseflow separation techniques for 35 watersheds within the state; to provide separate recharge values for each area. The calibrated model showed a good correlation with baseflow recharge estimates and concluded that the SWB model gives reasonable spatial and temporal recharging estimates that can be incorporated into water balance calculations and groundwater modeling.

Harlow and Hagedorn (2018) applied the SWB model to simulate groundwater recharge on Catalina Island, California, U.S. for the years 2008-2014. The study showed that the annual groundwater recharge rate was the lowest in 2013 about 0.05 mm/year, the highest in 2008 about 82.3 mm/year, and the annual recharge rate for all years during the study period was 23 mm/year. The research proved that the percentage of recharge to gross precipitation for all years was 6.55%. The study clarified that in the years 2009, 2011,

2012, 2013, and 2014, significant parts of the island did not receive any groundwater recharge. This indicated the severity of the recent drought in this state. The research recommended the need to pay attention to the application of methods that highlight groundwater sustainability, use the outputs of this study as inputs in the groundwater flow model, and test the response of the groundwater system for Catalina Island in different groundwater use scenarios.

Day (2019) estimated the mean annual potential recharge (MAPR) for the Des Moines lobe in central Iowa, U.S. during the 20-year period from 1996-2015 using the SWB model and calibrated the estimates of the MAPR value with the values derived from the baseflow separation analysis process, in addition to estimating the sensitivity of the MAPR to curve number values. The results of this study showed that the MAPR for 20 years was 6.3 in/year. During the same period, the average precipitation was 36 in, and the study indicated that the estimate of recharge represents 17% of the precipitation value. In addition to finding a strong relationship between precipitation and recharge. Significant differences in recharge values were observed based on surficial geology.

Cambraia Neto and Rodrigues (2020) evaluated methods for estimating groundwater recharge of watersheds located in the Brazilian Savannah region. The recharge rates for this region were calculated using several methods, including baseflow separation (BFS) (see equation 2.2), water table fluctuation (WTF) (see equation 2.3), and a sequential water balance (BALSEQ) (see equation 2.4) for the period from October 2009 to September 2011. The results showed that the groundwater recharge rates resulted from these methods were estimated as a percentage of the total rainfall, as it constituted 23.7% using the baseflow separation method, 26.6% using the water table fluctuation and by using the BALSEQ method, the amount of recharge was estimated at 31.5% of the annual rainfall rate. The study proved that the calculated estimates of the amount of groundwater recharge by the methods used were consistent with the values observed in other agricultural watersheds, in addition, that they proved that the methods used can be used to work on sustainable management of groundwater aquifers within the study area.

$$Recharge = Q_{off} - Q_{on} + BF + ET + \Delta S \quad (2.2)$$

Where;

Q_{off} is groundwater off the watershed;

Q_{on} is groundwater onto the watershed;

BF is baseflow discharge;

ET is evapotranspiration from groundwater;

ΔS is the change in groundwater storage?

$$Recharge\ (m) = S_y \frac{\Delta h}{\Delta t} \quad (2.3)$$

Where;

S_y is specific yield (unitless);

h is water table height (m);

t is time.

$$RAQ = PRC - SR - EVR \quad (2.4)$$

Where;

RAQ is the aquifer recharge (mm);

PRC is the daily precipitation (mm);

SR is the daily surface runoff (mm);

EVR is the evapotranspiration (mm).

By reviewing the worldwide studies, it was noticed that the SWB model is widely used and applied for estimating groundwater recharge based on spatial and temporal variations. The results of these studies were proved that the application of the SWB model gives very reasonable and consistent results compared to the various other methods used to estimate

the amount of recharge (Hart et al., 2012; Metropolitan Council, 2014; Smith and Westenbroek, 2015; Harlow and Hagedorn, 2018; Day, 2019). These studies showed that the SWB code gives close results for recharge values calculated using the streamflow method. The SWB code was used intensively in many sites in the U.S. but, to our best knowledge, was not used in Palestine.

2.3 Local Studies of Groundwater Recharge Estimation

The estimates of groundwater recharge are very important due to the reliance of many studies of water resources in Palestine on it (KHALAF, 2010).

SUSMAQ project (2004) developed a groundwater flow model for the Eocene Aquifer, West Bank, Palestine. The aim of the research was to understand and evaluate the availability and flow of groundwater in the Eocene Aquifer. The resulting model was used to manage the water resources and to assess the variations and factors affecting the quality and quantity of water for the study area. This work estimated the amount of recharge based on empirical equations taken from previous studies (see equations 2.5, 2.6 and 2.7).

$$For\ Ra < 300\ mm/yr, Re = 0.15 \times Ra \quad (2.5)$$

$$For\ Ra \geq 300\ mm/yr\ and \leq 650\ mm/yr, Re = 0.534 \times (Ra - 216) \quad (2.6)$$

$$For\ Ra \geq 650\ mm/yr, Re = 0.8 \times (Ra - 360) \quad (2.7)$$

Where;

Re is the recharge in mm;

Ra is the rainfall in mm.

These equations were adapted through steady-state simulation for this study by adjusting the coefficients according to the amount of rainfall. By using the previous equations, the amount of recharge was obtained as a percentage of the amount of rainfall for each year of study period. The resulting model was calibrated against the transient state condition and the annual differences between the measured water level and the simulated hydraulic head were ranged between (2-5) meters. Through the work on this project, it was noticed that some parts of the Eocene Aquifer work as a confined aquifer and other parts work as

an unconfined aquifer. This reflects the natural formations of the Eocene Aquifer. The resulting model indicated that the most sensitive factors were recharge variations and aquifer geometry. The results of the study recommended that the sustainable yield in the transient state of the Eocene Aquifer should not exceed 29 mcm/year.

Asbah (2004) estimated monthly groundwater recharge of the Auja-Tamseeh catchment, Palestine. The aim of the study was to develop a model for the monthly distribution of recharge quantities based on the hydrological observations that were developed through analyzing the quantities of rainfall and studying its effect on the rise of the groundwater level in the aquifer. Through the observations and assumptions, the numerical recharge equation was developed for the monthly estimate of the recharge on the Auja-Tamseeh catchment (see equation 2.8), as this equation took into consideration the spatial and temporal distributions of rainfall quantities for the study area.

$$R_i = \frac{P_{ci}}{P_a} \times R_a \qquad (2.8)$$

Where;

R_i is the monthly recharge in mm;

P_a is the annual rainfall in mm;

R_a is the annual calibrated recharge in mm;

P_{ci} is the accumulated rainfall from pervious months to current month in mm.

The study proved that the percentage of groundwater recharge from the amount of rainfall was equal to 21%, which is a value close to results of other studies like SUSMAQ study of Wadi-Natuf were this percentage was equal to 25.7 %.

Baalousha (2005) estimated groundwater recharge using cumulative rainfall departure method (CRD) for the coastal aquifer of Gaza Strip, Palestine. The method used in the calculations is based on the principle of water balance. The study showed that the method used does not require much data compared to other methods used to estimate recharge. The CRD method was carried out using optimization approach to minimize the root mean square error (RMSE) between the measured and the simulated groundwater head. After

making comparisons with other studies, the results of this study proved that the CRD method used gave results very close to the results of other methods, but with less data requirements and greater ease of application compared to other methods. One of the results of the study was to find the annual amount of groundwater recharge that results from rainfall in the Gaza Strip, which was 43 MCM.

Tubeileh et al. (2006) used the MODFLOW software to develop a groundwater model to assess the water budget, groundwater movement, and annual yield of the Eocene Aquifer, West Bank, Palestine. The study concluded that the most influencing and sensitive factors for the Eocene Aquifer are recharge and hydraulic conductivity. The study relied on previous relevant studies in the estimates of the amount of recharge. These previous studies estimated the amount of recharge as a percentage of rainfall based on the distribution of rainfall intensity, topography, soil characteristics, and land use. The study showed that the sustainable yield of the Eocene Aquifer is about 72 MCM.

Kharmah (2007) used Groundwater Management (GWM) software to develop a management tool to determine the spatial distribution of sustainable pumping rates in the Eocene Aquifer, West Bank, Palestine. The study used the modified empirical equations by Guttman (1998) to estimate recharge for the Eocene Aquifer. The average annual groundwater recharge from rainfall was about 78 MCM. The groundwater model was developed by using the MODFLOW software and calibrated under steady-state conditions. It showed that the annual discharge from the Eocene Aquifer outside the West Bank is around 55 MCM, and then the study used this resulting simulation model in developing the GWM model to find out the sustainable pumping rates that the aquifer can sustain without causing its depletion (safe yield). The results of the study showed that the safe yield from the Eocene Aquifer was about 23 MCM.

Juaidi (2008) estimated the amount of groundwater recharge for the entire area of the West Bank, Palestine, using the soil moisture deficit method (SMD). The ModelBuilder of GIS was used to develop a model for groundwater recharge based on the SMD method, and the aim of the study was to develop a readily available recharge model for the West Bank based on spatial and temporal variations in the amount of groundwater recharge. The highest recharge rates occurred in the north-western parts of the West Bank, while the lowest rates of groundwater recharge occurred in the south-eastern parts, and this was

according to the spatial distribution of rainfall and potential evaporation. The study showed that the total annual recharge for the year 2004 was 852 MCM for the entire study area. The long-term groundwater recharge rate was estimated for the period 1975-1997 was 610 MCM for the entire study area.

By reviewing previous local studies, it was noticed that these studies focused on developing models of groundwater flow. However, these were based on their estimate of the amount of recharge for the Eocene Aquifer area on annual or monthly rainfall rates, and on empirical equations obtained from other areas (SUSMAQ, 2004; Asbah, 2004; Tubeileh et al., 2006; Kharmah, 2007). These studies did not take into account many of the basic factors. These factors have a significant effect on recharge values. Among these factors are the hydrological soil group (HSG), spatial and temporal distribution of daily rainfall values, flow direction, change in soil moisture, available water capacity (AWC), evapotranspiration, root zone depth, interception, and land use types. This proves that estimating recharge based only on the amount of rainfall gives inaccurate results (Westenbroek et al., 2010). This approach of estimating recharge proves to be inappropriate for developing groundwater flow models and for pollution models. As this gives inaccurate results compared with models based on daily rainfall data and spatial and temporal distributions of the recharge amount (Westenbroek et al., 2010).

This research aims to develop a recharge model for the Eocene Aquifer area based on spatial and temporal variations and based on daily rainfall data. This provides accurate and reasonable values for recharge and contributes to assessing the water situation in this aquifer.

Chapter Three
The Swb Code

3.1 General Background

The estimates of the amount of groundwater recharge based on spatial and temporal variations are very important for many hydrological assessments such as water quality protection, stream flow management, replenishment of groundwater aquifers, groundwater flow modeling, and pollutant transport. Also, it helps in understanding and studying the impact of urban, industrial, and agricultural development (Scanlon et al., 2002).

The SWB code is a computer code developed by the USGS to calculate spatial and temporal variations in groundwater recharge (Westenbroek et al., 2010). It was developed to quickly and easily estimate the amount of groundwater recharge. The SWB code does not have a graphical user interface (GUI), but is a control file that reads the control statements that have been programmed by the code developers to model the groundwater recharge. The SWB code calculates the components of water balance at a daily timestep based on a modified version of the Thornthwaite-Mather soil water balance approach (Thornthwaite, 1948; Thornthwaite and Mather, 1957). The USGS personnel developed and modified the SWB code to allow the use of available GIS datasets to estimate the amount of recharge (Westenbroek et al., 2010) based on the code written by Weston Dripps (2003) as part of his doctoral dissertation at the University of Wisconsin-Madison that was subsequently published by Dripps and Bradbury (2007). Groundwater recharge is highly variable with respect to time and space (Jyrkama and Sykes, 2007). Many groundwater modelers assume the value of groundwater recharge as a percentage of the rainfall (Jyrkama and Sykes, 2007). This assumption gives inaccurate results; because it does not take into account the spatial distributions that have a significant impact on the value of recharge and that improve the performance of the model.

3.2 SWB Theory

The SWB code uses a modified version of the Thornthwaite-Mather method (Thornthwaite and Mather, 1957) to estimate the amount of groundwater recharge. The SWB code calculates the amount of groundwater recharge separately for each grid cell in

the model domain. The SWB code requires entering all input data (climate data and landscape characteristics) as gridded data in the form of American Standard Code for Information Interchange (ASCII) file in order to make calculations of groundwater recharge for each grid cell in the model domain separately. The sources and sinks of water are calculated in each grid cell and the recharge is calculated based on the difference between these sources and sinks and the change in soil moisture according to equation 3.1 (Westenbroek et al., 2010). The SWB code imposes a restriction on the outline of the study area to be rectangular or square shape to avoid the presence of grid cells with missing data that causes errors in the model run. The outline of the study area is defined for the SWB code by entering the coordinates (from GIS) of the corners of the square or rectangular study area and entering the grid cell size (Westenbroek et al., 2010).

$$Recharge = (Precipitation + snowmelt + inflow) - (interception + outflow + ET) - \Delta soil\ moisture \quad (3.1)$$

3.3 Input data

All the input data that the model requires are available and easy to obtain. The SWB code requires climatic data (rainfall and temperature data), soil characteristics maps (land use/land cover), study area boundaries, and elevation maps (contour maps). All of this data is easy to provide and obtain from the related local authorities or from the related websites, the SWB code allows processing this data using a geographic information system (GIS) to convert it into a format that the code can reads (ASCII files). Therefore, the SWB model does not require field data. The SWB model requires seven types of data (see table 3.1), including gridded and tabular data. The required gridded data (ASCII) includes land cover/land use data, flow direction, hydrological soil group (HSG), available water capacity (AWC), climatic data. The tabulated data, includes the soil moisture retention table and the soil and land use properties lookup table (Westenbroek et al., 2010).

Table 3.1

Required input data for SWB model.

Required Data	Data Type	Description
Land use	Gridded	ASCII file contains integer values for each grid cell in the model domain, that were assigned to describe the land use type and soil properties present in the study area based on the land use and soil lookup table used as an input.
Hydrological soil group (HSG)	Gridded	ASCII file contains integer values (1 - 4) for each grid cell in the model domain, that were assigned to describe the hydrological soil groups (A, B, C, D) present in the study area, where these groups ranging from 1 (soil group A) to 4 (soil group D).
Flow direction (D8)	Gridded	ASCII file contains integer values (1, 2, 4, 8, 16, 32, 64, 128) for each grid cell in the model domain, that were diverted from the digital elevation model (DEM) for the study area, to determine how to route overland flow between cells.
Available water capacity (AWC)	Gridded	ASCII file contains real number values for each grid cell in the model domain, that estimated by Dripps (2003) for various soil texture groups, which range from 1.20 for sand soil to 3.6 in/ft for clay soil, that were assigned to describe the amount of water holding capacity in inches per foot of soil thickness.
Climate data	Gridded	The SWB code requires about 1,098 ASCII climate files, 366 containing the daily precipitation values in inches and the others for the daily maximum and minimum temperature values in Fahrenheit, for each grid cell in the model domain.

Land use and soil lookup table	Tabular	Table in a tab-delimited text file format containing land use codes, curve number values, interception values, root depth, and maximum daily recharge (max infiltration) for each land-use type in the study area to calculate model parameters on the basis of grid cell properties.
Soil moisture retention table	Tabular	The table attached with SWB code developed by Thornthwaite and Mather (1957), used to calculate the change in soil moisture during the periods of unsatisfied potential evapotranspiration.

The SWB code uses the input parameters to calculate the amount of groundwater recharge, including precipitation, snowmelt, and inflow.

3.3.1 Precipitation

The daily precipitation is previewed from the SWB code in order to determine whether the precipitation will take the form of rain or snow. The amount of precipitation is entered for each cell in the model domain in the form of ASCII grid files for each day of the study year, in inches (Westenbroek et al., 2010).

3.3.2 Flow direction

The SWB code uses a flow direction grid derived from a digital elevation model (DEM) to calculate the inflow (surface runoff supplied to a grid cell from upslope cell) for each cell in the model domain. The outflow (surface runoff leaving a grid cell to an adjacent downslope cell) is routed to adjacent downslope grid cells based on flow direction input. The inflow is optional in the SWB code and can be turned off and considered as zero if the flow routing is turned off (Westenbroek et al., 2010).

The parameters that reduce the amount of water that is computed as groundwater recharge include interception, outflow, evapotranspiration, and change in soil moisture.

3.3.3 Interception

The interception values are manually entered in inches (in) for each land use type and for each season (growing and dormant). The SWB code allows the user to enter the interception value from any reference. The code assumes that the water does not reach the surface of the soil until the daily precipitation value exceeds the specified interception value.

3.3.4 Hydrological soil group (HSG)

The SWB code uses the HSG as an input to understand the group of soil present in the study area based on the infiltration capacity. The U.S. Department of Agriculture (USDA), Natural Resource Conservation Service (NRCS) has divided about 14,000 soil series into four groups (A, B, C, and D) based on the infiltration capacity. These groups are defined for the code in the form of integer grids ranging from 1 (soil group A) to 4 (soil group D), where the soil group A constitutes the highest infiltration capacity and the lowest potential surface runoff, and the soil group D has the lowest infiltration capacity and the highest potential surface runoff (see table 3.2). The SWB code allows assigning the daily maximum recharge values for each soil group in the study area according to table 3.2. Any value that exceeds the daily maximum recharge value is considered by the code as a rejected recharge.

Table 3.2:

Infiltration rates for NRCS hydrological soil group (Cronshey et al., 1986).

Soil Group	Infiltration Rate (inches/day)
A	> 7.2
B	3.6 - 7.2
C	1.2 - 3.6
D	< 1.2

3.3.5 Available water capacity (AWC)

Each soil type within the study area must be assigned values of AWC and the depth of the root zone in order to calculate a value of maximum soil water capacity (MSWC) (see equation 3.2). The AWC is the amount of water holding capacity in inches per foot of soil thickness. The SWB code allows the use of the soil texture to assign the AWC values as in a table 3.3 (Dripps, 2003; Thornthwaite and Mather, 1957). The value of MSWC expresses the maximum amount of soil water storage and the SWB code assumes that any

amount of water added to the soil column in excess of this value becomes a recharge (Westenbroek et al., 2010).

$$\text{MSWC (in)} = \text{AWC (in/ft)} \times \text{RZD (ft)} \quad (3.2)$$

Where;

MSWC is the Maximum soil water capacity;

AWC is the Available water capacity;

RZD is the Root zone depth.

Table 3.3:

The estimated available water capacities for various soil texture groups (Dripps, 2003; Thornthwaite and Mather, 1957).

Soil texture	AWC (in/ft)
Sand	1.20
Loamy sand	1.40
Sandy loam	1.60
Fine sandy loam	1.80
Very fine sandy loam	2.00
Loam	2.20
Silt loam	2.40
Silt	2.55
Sandy clay loam	2.70
Silty clay loam	2.85
Clay loam	3.00
Sandy clay	3.20
Silty clay	3.40
Clay	3.60

3.3.6 Inflow and Outflow

The SWB code calculates the amount of inflow and outflow for each cell within the model domain using the USDA-NRCS curve number rainfall-runoff relationship (Cronshey et al., 1986). This rainfall-runoff relation depends on four properties: land use, soil type, surface condition, and antecedent runoff condition. The curve number (CN) method defines runoff as the difference between precipitation (P) and initial abstraction (I_a). The initial abstraction is the amount of precipitation that must fall before runoff is generated. It expresses the summation of all processes that may cause a reduction in the amount of surface runoff, including depression storage, infiltration, and an interception by plant and fallen leaves (Woodward et al., 2003). Runoff volumes are calculated by using equation 3.3 (Woodward et al., 2002):

$$R = \frac{(P-I_a)^2}{(P+[S_{max}-I_a])} \quad P > I_a \tag{3.3}$$

Where;

R is runoff (L);

P is daily precipitation (L);

S_{max} is maximum soil-moisture holding capacity (L);

I_a is initial abstraction (L).

I_a is related to S_{max} (see equation 3.4):

$$I_a = 0.2S_{max} \tag{3.4}$$

For the land cover type, the max storage term in the SWB code was defined by the CN (see equation 3.5)

$$S_{max} = \left(\frac{1{,}000}{CN}\right) - 10 \tag{3.5}$$

The SWB code adjusts the CN upward or downward depending on the amount of precipitation that occurred in the previous five-day period. This precipitation value is also used to describe the soil moisture conditions and determine their classes. There are three classes of moisture condition called antecedent runoff condition (ARC) I, II, and III (see table 3.4) (Westenbroek et al., 2010). The curve number values that are provided to the model in the land use lookup table are normal conditions (ARC II) where the SWB code automatically adjusts the CN values based on the moisture conditions by using certain equations. When the soil is nearly at saturation, the CN is automatically adjusted upward (see equation 3.6) from the normal conditions (ARC II) to the nearly saturated conditions (ARC III), because in saturated soil the amount of surface runoff is higher (Mishra et al., 2003; Westenbroek et al., 2010).

$$CN_{ARC(III)} = \frac{CN_{ARC(II)}}{(0.427+0.00573*CN_{ARC(II)})} \tag{3.6}$$

When the soil is dry (ARC I), the SWB code automatically adjusts the curve number downward (see equation 3.7), because in dry soil the runoff will be reduced and the infiltration will be increased (Mishra et al., 2003; Westenbroek et al., 2010).

$$CN_{ARC(I)} = \frac{CN_{ARC(II)}}{(2.281+0.01281*CN_{ARC(II)})} \quad (3.7)$$

The CN range from 0 to 100, where 0 indicating no surface runoff (pervious surface), and 100 indicating the highest value of surface runoff (impervious surface) (Mockus, 1964). The initial abstraction value used by the SWB code indicates that the surface runoff does not occur until precipitation falls between 1 to 117 mm (0.04 to 4.6 in), where the 1 mm is expressed as the minimum precipitation when the CN is equal to 100 and the minimum precipitation is 117 mm when the CN is equal to 0 (Westenbroek et al., 2010).

Table 3.4:

Definition of antecedent runoff conditions used in the SWB code [Precipitation in preceding 5 days, in inches].

Condition	Soil Wetness	Dormant Season	Growing Season
I	Dry	< 0.05	< 1.4
II	Average	0.5 - 1.1	1.4 - 2.1
III	Near saturation	> 1.1	> 2.1

3.3.7 Evapotranspiration (ET)

ET defined as the sum of the water that leaves the system as water vapor through evaporation from water bodies, snow, and ice, as well as the evaporated water resulting from plant respiration (transpiration) (Dingman, 2015). The SWB code uses the Hargreaves-Samani method in calculating the ET, as this method was developed based on 8-years of lysimeter measurements for ET and by deriving an equation to produce ET estimates (see equation 3.8) (Hargreaves and Samani, 1985). In order to produce spatially distributed estimation for potential-evapotranspiration (PET), the SWB needs to be supplied with the input of the daily maximum and minimum temperature grids. The SWB code deals with the interception value as ET. As for the calculation of actual ET, when precipitation minus potential evapotranspiration (P-PET) is negative, the actual evapotranspiration (AET) equals the change in soil moisture. When P-PET is positive then the AET equals PET (Westenbroek et al., 2010).

$$ET = 0.0135\ (KT)(R_a)(TD)^{0.5}(TC + 17.8) \quad (3.8)$$

Where;

TD = T_{max} -T_{min} (°F);

TC = the average daily temperature (°F);

R_a = extraterrestrial radiation (in/day);

KT = empirical coefficient (KT = 0.162 for interior regions, KT = 0.19 for coastal regions).

3.3.8 Initial soil moisture (ISM)

The ISM expresses the percentage of saturation of the AWC. The ISM is one of the basic inputs required for the SWB code. The code allows the user to enter it either as a single constant value for each study area or as a grid value that depends on land use, soil type, and rainfall distribution. To obtain a realistic values and accurate results, the ISM value must be entered as grid data.

3.3.9 Change in soil moisture (∆ soil moisture)

Soil moisture represents the amount of water infiltrated into the soil and held in soil storage in each grid cell. The SWB code uses input soil information, the land cover information, and the Thornthwaite-Mather (T-M) tables to calculate the MSWC (maximum soil water holding capacity that roughly equivalent to field capacity) (in/ft) using equation 3.2. The minimum value of soil moisture corresponds to the soil's wilting capacity (Westenbroek et al. 2010). The SWB code uses the Thornthwaite and Mather (1957) soil-water-balance method to calculate the change in soil moisture storage per day for each grid cell in the model domain. The first step in calculating the soil moisture value for any grid cell is the calculation of the Precipitation minus Potential Evapotranspiration (P – PET). In the second step the accumulated potential water loss (APWL) is calculated, which is a running sum of the P – PET values and represents the total amount of unsatisfied PET to which the soil has been subjected. Increasing the value of APWL results from a negative value of P-PET. As the APWL increases, soil moisture is less readily given up to ET or recharge. The decrease in the value of the APWL results from the positive value of P-PET, and this leads to an approach to the maximum soil-water capacity (storage is full) and the excess soil moisture will be considered as groundwater recharge and the APWL is reset to zero (Westenbroek et al. 2010).

To avoid the occurrence of error messages in the running of SWB code, the grid cell size and the grid extent for all gridded inputs must be the same and perfectly aligned. The grid

cell size should be chosen based on the accuracy of the features available data. The smaller grid cell size gives more accurate results yet the code will take more time to give the outputs, and vice versa (Westenbroek et al. 2010).

3.4 Output data

The SWB code provides the user with different types of daily, monthly and annual output as needed, and these outputs include tabular files, gridded files, and images. The tabular files are in Excel format and contain a summary of the daily calculations that the code has made, while the output gridded files and images allow the user to obtain it at a daily, monthly, or yearly frequency, according to the user's need, and from these outputs, gross precipitation, snowfall, snow cover, minimum daily air temperature, mean daily air temperature, maximum daily air temperature, interception, net precipitation (gross precipitation minus interception), runoff outside (surface flow that's flow out of the model domain), rejected recharge (recharge in excess of the daily maximum recharge rate), inflow (surface flow supplied to grid cell), outflow (surface flow leaving a grid cell), potential evapotranspiration, actual evapotranspiration, soil moisture, change in soil moisture, and recharge. The code also provides outputs in the form of a grid file for the final soil moisture (FSM), which the code produces automatically to allow the user to use as an input for the ISM to get realistic results (Westenbroek et al. 2010).

Chapter Four

Description of the Study Area

4.1 Location

The aquifers in the West Bank, Palestine are divided into three main aquifers: the eastern aquifer, the northeastern aquifer, and the western aquifer (see figure 4.1) (PWA, 2001b).

Figure 4.1:

The aquifers located within the West Bank, Palestine.

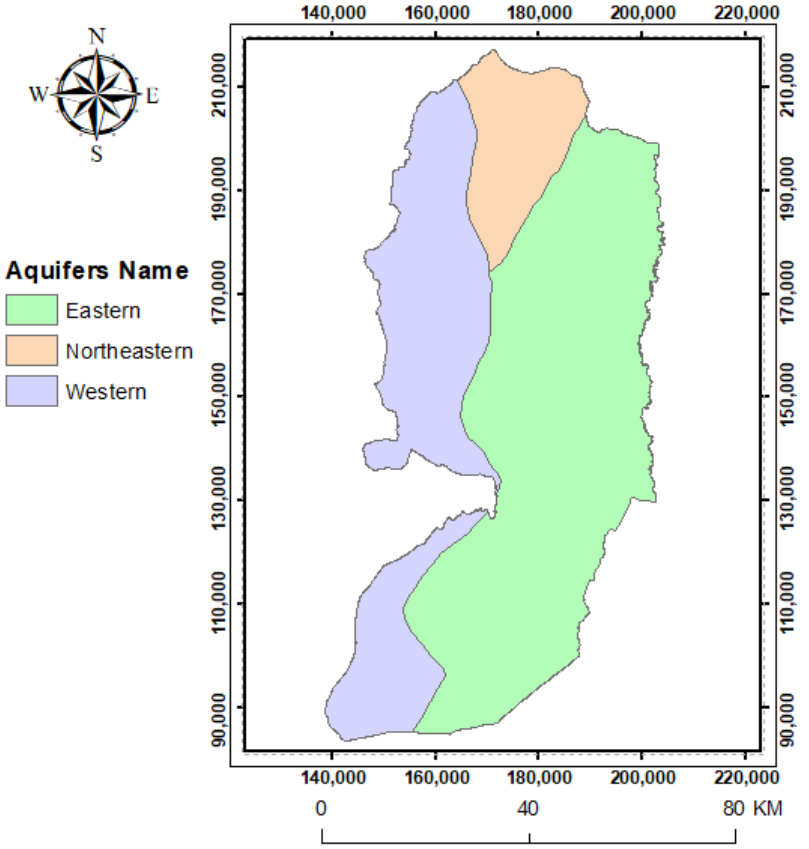

The Eocene Aquifer is one of the main sources of water in the West Bank, Palestine (PWA, 2018). This aquifer is located in the northeastern aquifer (the northern part of the West Bank, Palestine) (see figure 4.2). The Eocene Aquifer covers Jenin District, part of Nablus District and part of Tubas District (see figure 4.3). It has a total area of about 648 km^2, of which 458.6 km^2 are located inside the West Bank (see figure 4.4). The Eocene Aquifer was chosen as the study area for this research because: 1) this aquifer serves 43 communities with a total population of about 203,400 persons (Almasri et al., 2020); 2) the intense agriculture in the study area, which depends on irrigation from the

groundwater wells; and 3) dry and abandonment of many groundwater wells in the area especially in the summer season that resulted from declining the water table in the aquifer where water demand is high and groundwater recharge is at minimum (Almasri et al., 2020).

Figure 4.2:

The outline of the Eocene Aquifer with its regional location.

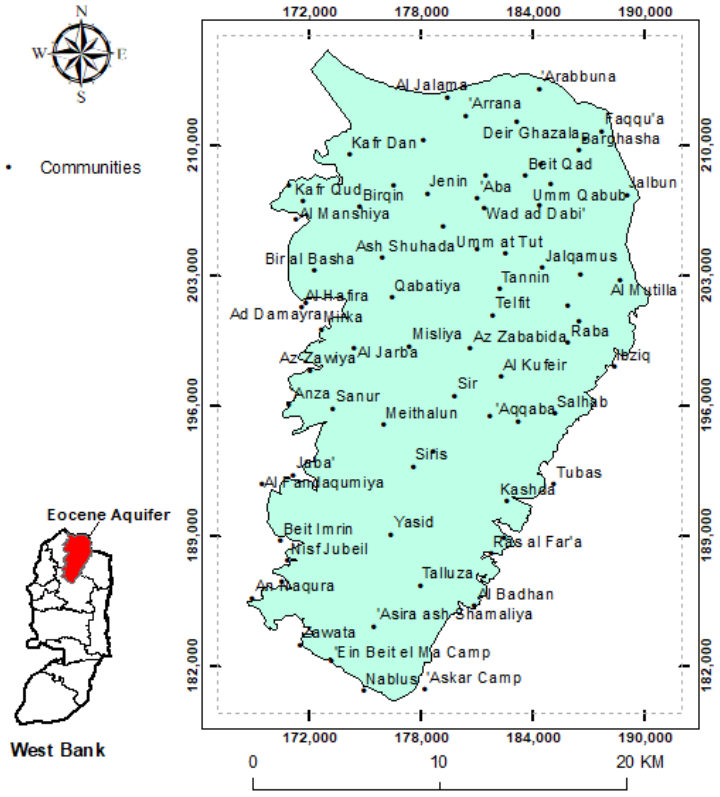

Figure 4.3:

The districts located within the Eocene Aquifer.

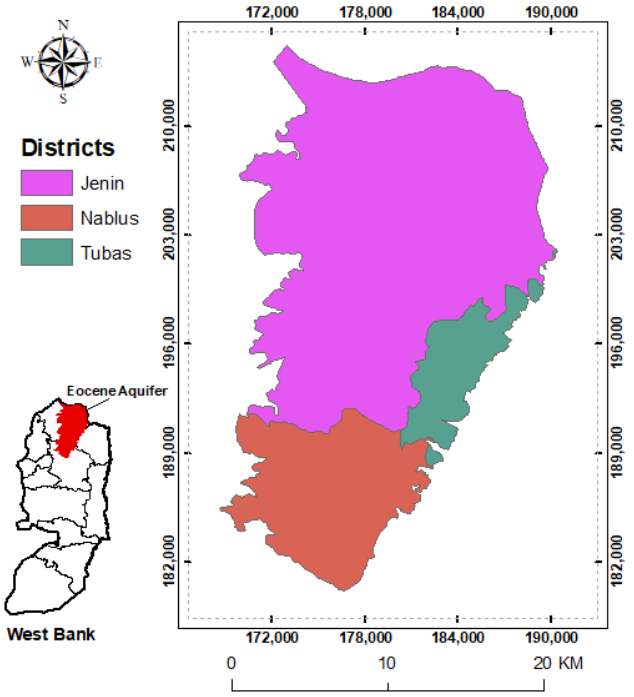

Figure 4.4:

The extends of Eocene Aquifer beyond the boundaries of the West Bank.

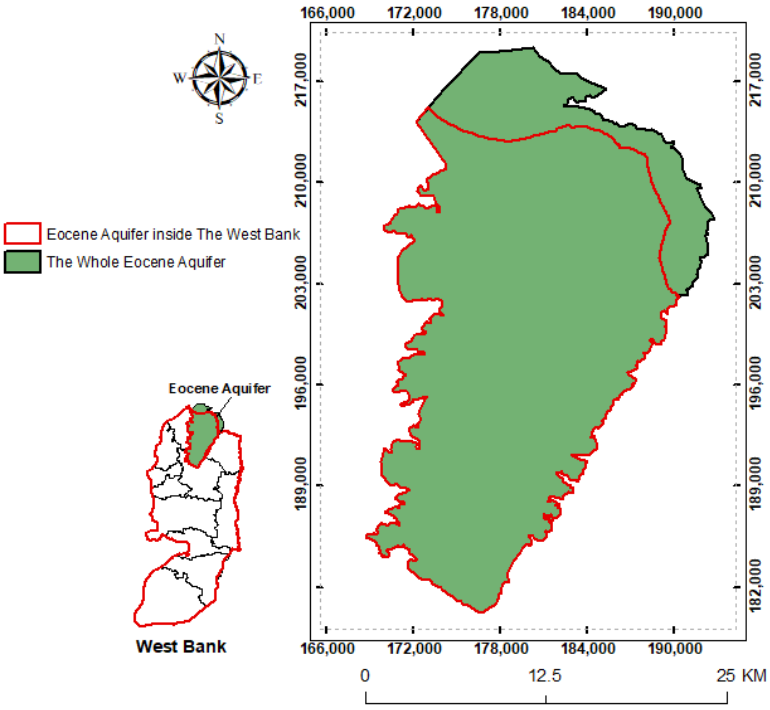

4.2 Climate

The climate of the study area is classified as hot and dry in summer, cool and humid in winter (UNEP, 2003). The minimum and maximum temperatures in winter are 7 °C and 15 °C respectively, and in summer the minimum and maximum temperatures are 20 °C and 33 °C, respectively. Towards the west, the potential evaporation rate decreases. The potential evaporation rate ranges between 1,850 mm and 2,100 mm. As for the humidity, the annual mean is around 62% (Almasri et al., 2020). The aquifer yield depends highly on rainfall, where the average annual rainfall in the study area for 2020-year equal to 503.22 mm (19.81 in) and ranges between 411 mm (16.2 in) and 777 mm (30.6 in). The rainy season in the study area extends from October to May, the maximum rainfall occurs in January, and the lowest temperature occurs in January and February (Kharmah, 2007). There are about 13 rain gauges located inside the study area (see figure 4.5).

Figure 4.5:

The distribution of rain gauges within the Eocene Aquifer.

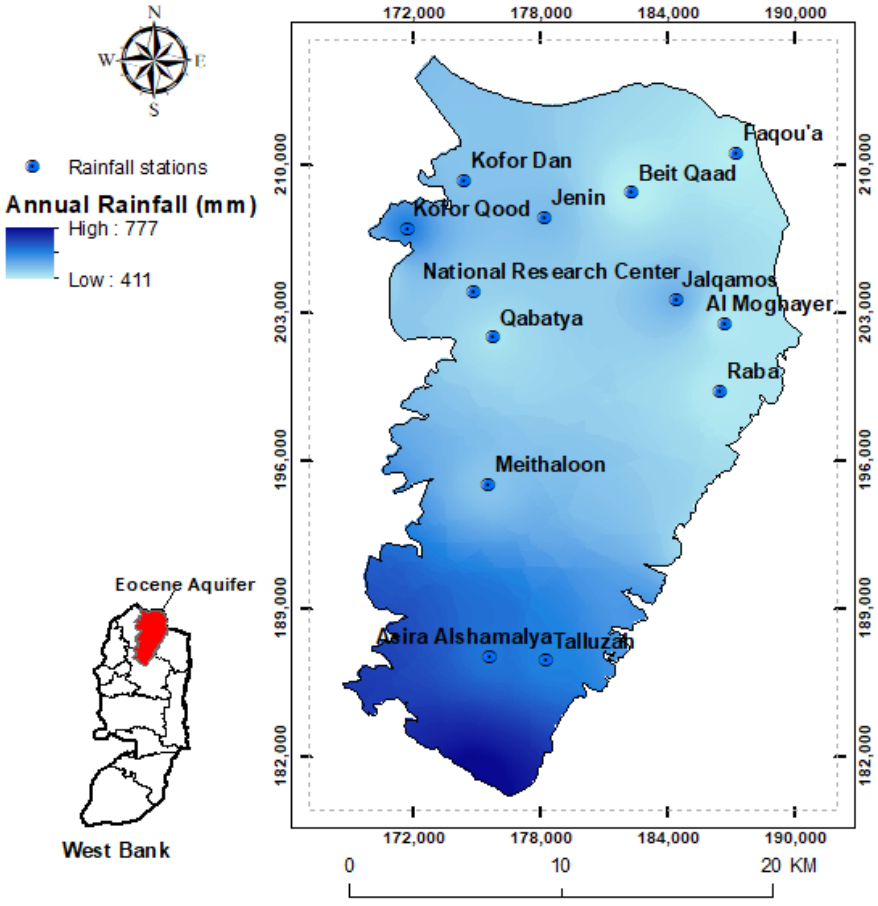

4.3 Topography

The elevations of the ground surface in the study area range from 75 m above sea level (AMSL) in the north and up to 925 m (AMSL) in the south (see figure 4.6). The study area is characterized by its containment of closed and semi-closed depressions such as the Arrabah Plain, Marj Sanur, and Marj Ibn Amer. The topography of the Jenin District is divided into three regions of the western and eastern slopes and the mountain crests, where the eastern slopes that lie between the central highlands and the Jordan Valley are classified as steep slopes and contribute to the formation of wadies. The mountain crests separate the western and eastern slopes with a height ranging from 400 m (AMSL) to 500 m (AMSL). The western slopes are classified as gentle slopes, with elevations ranging between 100 m (AMSL) and 400 m (AMSL) (ARIJ, 1996).

Figure 4.6:

Topography of the Eocene Aquifer.

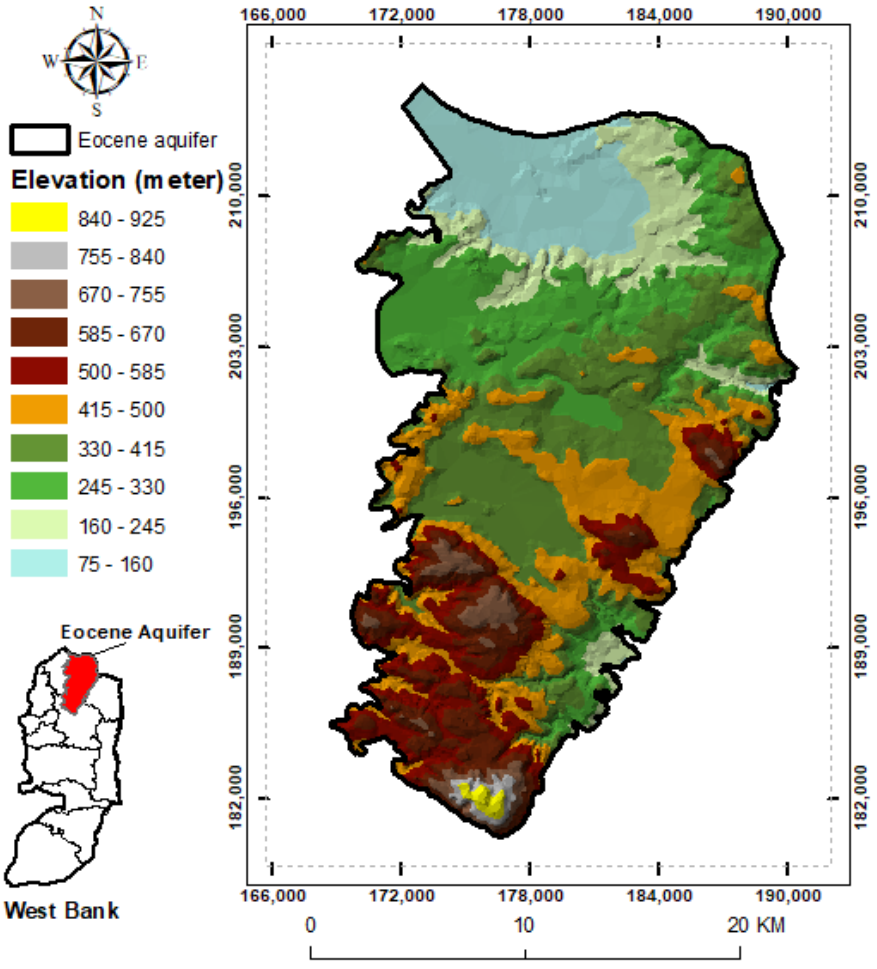

4.4 Soil texture

The study area is characterized by its fertile agricultural lands (Kharmah, 2007) and the soil in the study area is divided in terms of texture into two types (see figure 4.7): (1) clay, which constitutes the largest percentage of the study area as they constitute about 91.31%, (2) clay loam, which constitutes a percentage of 8.69%. Clay and clay loamy soils have a low infiltration rate of < 1.2 inches per day compared to other soil textures. This reflects the decreasing the amount of recharge in the areas containing these soils. In terms of water holding capacity, clay and clay loam soils have a water holding capacity of 3.6 and 3 in/ft, respectively. Since the clay soil has a higher AWC than clay loam soil, this reflects a higher maximum soil-water storage and less groundwater recharge than clay loam soil.

Figure 4.7:

Soil texture in the Eocene Aquifer.

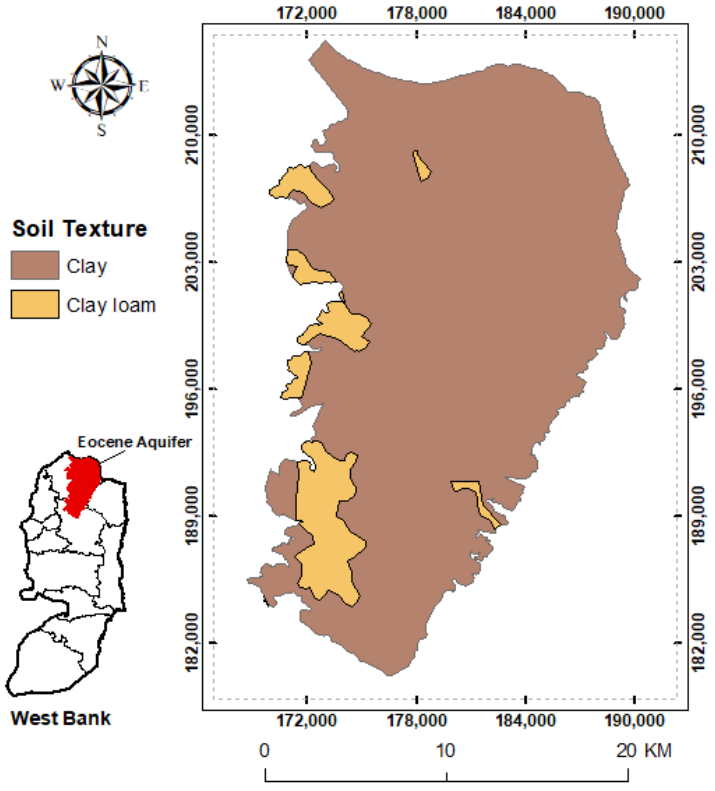

4.5 Water resources

In the Eocene Aquifer, water is used to secure irrigation and domestic needs. There are about 120 wells and 14 springs (see figure 4.8); 67 of wells are agricultural wells, six domestic wells, and others are dry or abandoned wells (Almasri et al., 2020).

Figure 4.8:

The distribution of wells within the Eocene Aquifer.

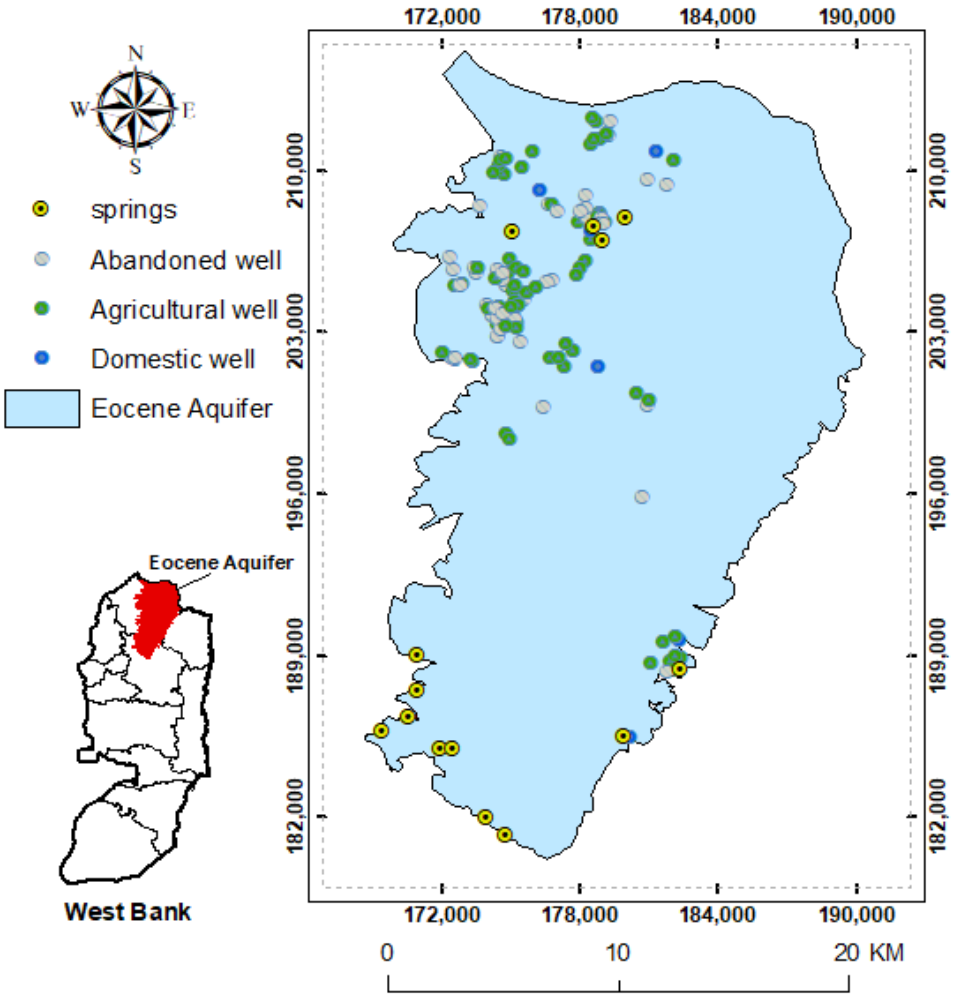

4.6 Land use

Land use patterns are shaped by a variety of climatic and topographical conditions, availability of natural resources, and political factors. As these factors affect the distribution of urban and agricultural areas, roads, and other land uses (ARIJ, 2002). Land use is one of the most influencing factors affecting spatial estimates of the groundwater recharge. The characteristics of the land use types differ from each other in many parameters, such as CN, slope, interception value, and soil water content (Barua et al., 2021). These parameters have a noticeable effect on the amount of recharge. Each type of land use has its own CN that expresses pervious and impervious surfaces. Whereas, residential areas that contain a large proportion of impervious surfaces have a high CN value indicating high potential surface runoff, low infiltration rate, and low potential recharge. The low CN value indicates the absence of impervious surfaces, and this causes

a decrease in the potential surface runoff and an increase in the infiltration rate, and thus the amount of recharge will be higher than the case of the high CN value (Song et al., 2021).

The amount of recharge is affected by the slope of the area, where the steep slope causes an increase in the potential surface runoff which leads to a decrease in the infiltration rate and thus reduce the potential recharge. While flat and slight slope lands contribute to an increase in the amount of recharge because the potential surface runoff is low and the infiltration rate is high. Some natural grasslands are mostly located in flat areas and this causes high amounts of recharge in these areas and this reflects the effect of land use on the amount of potential recharge (Hsieh et al., 2021).

The amount of recharge is affected by the interception value that results from the opposition of trees and plants to rainfall. The interception value in areas containing dense trees and forests is higher than in the case of areas containing natural grass. When the interception value increases, the amount of water exposed to the ground surface decreases. Thus, the rate of infiltration decreases and this causes a decrease in potential recharge (Ashaolu et al., 2020).

Soil water content has an effect on the amount of recharge. In irrigated areas, the soil water content is high, and thus this contributes to accelerating the arrival of the soil to saturation conditions and the occurrence of recharge. The non-irrigated areas need more time for recharge to occur and for the soil to reach saturation condition. Therefore, the irrigated areas have a higher recharge amount compared to the non-irrigated areas (Xiang et al., 2020).

The Eocene Aquifer contains 20 different types of land use (see figure 4.9). Table 4.1 summarizes the land use classifications and their areal distributions in the Eocene Aquifer.

Figure 4.9:

The Land use types in the Eocene Aquifer.

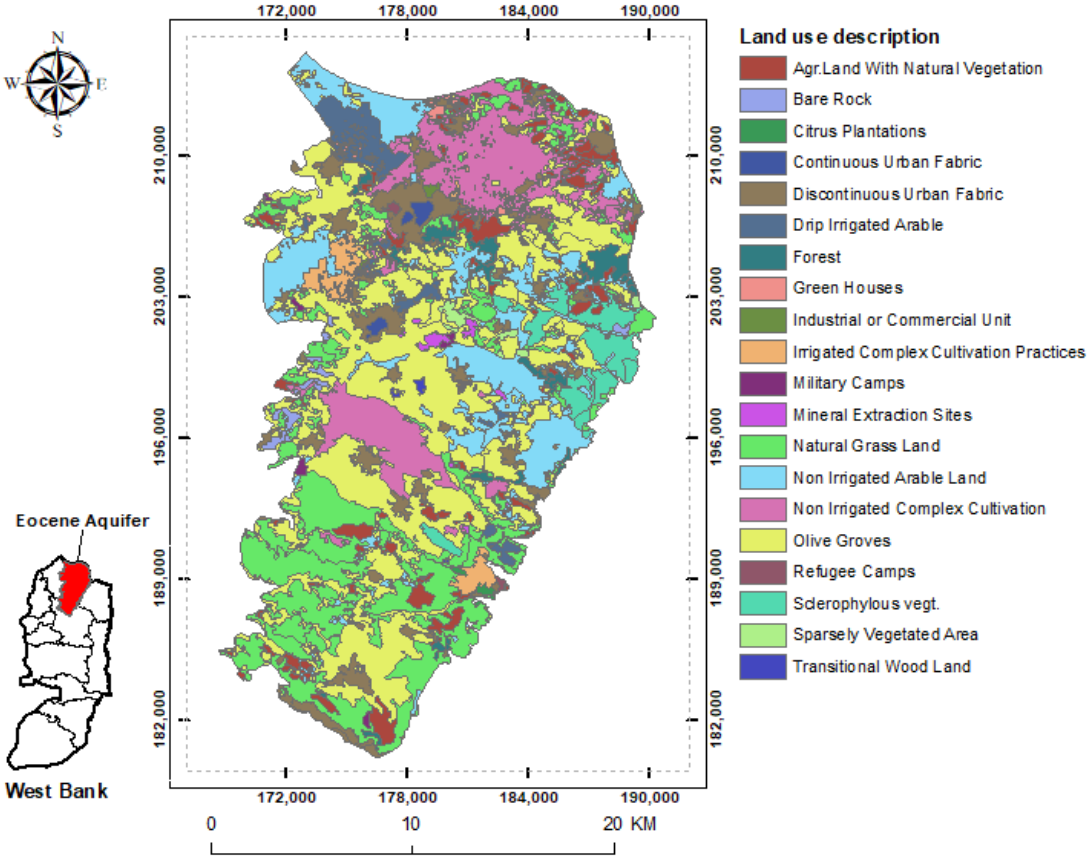

Table 4.1

The land use classifications and their areal distributions in the Eocene Aquifer.

Land Use Type	Area (km^2)	Percentage of Area
Olive groves	139	30.30%
Natural grassland	87	19.00%
Non-irrigated arable land	55.64	12.13%
Non-irrigated complex cultivation	54.88	12.00%
Discontinuous urban fabric	34.9	7.61%
Agricultural land with natural vegetation	23.5	5.11%
Sclerophyllous vegetation	16.91	3.68%
Drip irrigated arable	13	2.83%
Forest	10.4	2.26%
Irrigated complex cultivation practices	7.84	1.71%
Greenhouses	3.4	0.75%
Bare rock	2.83	0.62%
Sparsely vegetated area	2.16	0.47%
Continuous urban fabric	1.77	0.38%
Mineral extraction sites	1.74	0.38%
Military camps	1.15	0.25%

Citrus plantations	0.67	0.15%
Refugee camps	0.51	0.11%
Industrial or commercial unit	0.49	0.11%
Transitional woodland	0.49	0.11%

The land use in the Eocene Aquifer was divided into the following categories:

1. Agricultural land with natural vegetation: it forms agricultural lands that contain natural plants that grow without human assistance and obtain their needs from the natural environment (Josh, 2015). It constitutes about 5.11% of the Eocene Aquifer.
2. Bare rock areas: the areas where bedrock is visible on the ground surface and the soil layer in it is either absent or very thin and does not contain vegetation cover (Kosztra et al., 2017). It constitutes about 0.62% of the Eocene Aquifer.
3. Citrus plantations areas: the areas that contain citrus trees of various types such as lemon, orange, grapefruit, and pomelo (Rumiani et al., 2021). It constitutes about 0.15% of the Eocene Aquifer.
4. Continuous urban fabric areas: it forms the areas where transportation networks and urban structures predominate. As more than 80% of its area covered with impervious surfaces such as roads and buildings (Kosztra et al., 2017). It constitutes about 0.38% of the Eocene Aquifer.
5. Discontinuous urban fabric areas: it forms the areas where transportation networks and urban structures associated with vegetated areas. The area of impervious surfaces ranges from 30 to 80% of land coverage (Kosztra et al., 2017). It constitutes about 7.61% of the Eocene Aquifer.
6. Drip irrigated arable: the agricultural areas that contain crops are irrigated permanently or periodically using a drip irrigation system. It does not include intermittently irrigated agricultural areas. The crops in these areas can only be grown with artificial water supplies (Kosztra et al., 2017). It constitutes about 2.83% of the Eocene Aquifer.
7. Forest areas: it represents areas that contain forests that consist of coniferous and woodland trees. The height of trees in these areas usually more than 5 meters, with an interception ratio of at least 30% (Kosztra et al., 2017). It constitutes about 2.26% of the Eocene Aquifer.
8. Greenhouse's areas: it represents areas that contain greenhouses that are used to grow various types of plants such as vegetables, flowers, and fruits. The Plants in these areas depend for irrigation on artificial water sources and not on direct irrigation from

rainfall, where it blocks the rainfall from reaching it because it is closed (Mendoza-Fernández, 2021). It is considered an impervious surface. It constitutes about 0.75% of the Eocene Aquifer.

9. Industrial or commercial unit areas: it constitutes areas in which industrial and commercial use is active or public service facilities. Most of the area is occupied by buildings, industrial and commercial facilities, and impervious surfaces, and it may also contain plants (grass) (Kosztra et al., 2017). It constitutes about 0.11% of the Eocene Aquifer.
10. Irrigated complex cultivation practices areas: it represents a group of cultivated areas with different types of crops such as permanent, annual crops and pastures which depends on artificial irrigation and not on rain-fed irrigation (Kosztra et al., 2017). It constitutes about 1.71% of the Eocene Aquifer.
11. Military camps areas: it represents land that has military uses, such as training in military matters. It constitutes about 0.25% of the Eocene Aquifer.
12. Mineral extraction sites: it refers to the sites where the various construction materials such as quarries and sand pits are extracted. (Kosztra et al., 2017). It constitutes about 0.38% of the Eocene Aquifer.
13. Natural grassland: it represents the areas where grasses are predominant and that are not subject to human influence or are under moderate human influence. It is located mostly in flat areas and with a slight slope and often includes rocky areas (Kosztra et al., 2017). It constitutes about 19.00% of the Eocene Aquifer.
14. Non-irrigated arable land areas: it represents areas with non-permanent rainfed crops that are harvested annually. The production of these crops depends on rain-fed irrigation, not artificial irrigation (Kosztra et al., 2017). It constitutes about 12.13% of the Eocene Aquifer.
15. Non-irrigated complex cultivation areas: it represents a group of cultivated areas with different types of crops such as permanent and annual crops and pastures which depends on rain-fed irrigation (Kosztra et al., 2017). It constitutes about 12.00% of the Eocene Aquifer.
16. Olive groves areas: it represents the areas planted with olive trees (Kosztra et al., 2017). It constitutes the highest land use areas of the study area, as it constitutes about 30.30% of the Eocene Aquifer.

17. Refugee camps areas: it represents the areas established by the United Nations Relief and Works Agency (UNRWA). It is a densely populated residential area, with buildings significantly close to each other. This leads to constitutes a large percentage of impervious surfaces (UNRWA, 2019). It constitutes about 0.11% of the Eocene Aquifer.
18. Sclerophyllous vegetation areas: it represents the areas that contain the Sclerophyll plants, which is a dense plant that grows in locations with relatively high rainfall (Parsons and Cameron, 1974; Kosztra et al., 2017). It constitutes about 3.68% of the Eocene Aquifer.
19. Sparsely vegetated areas: it represents the areas that contain sparse vegetation that covers about 10 to 50% of the surface area and consists of semi-rough herbaceous species, as for the remaining area it is a naturally barren land. It constitutes about 0.47% of the Eocene Aquifer.
20. Transitional woodland areas: it represents the areas with dense transitional herbaceous vegetation are formed as a result of several activities such as forest regeneration after various damages, or forest degradation due to natural or human factors (such as pollution or drought) (Kosztra et al., 2017). It constitutes about 0.11% of the Eocene Aquifer.

4.7 Hydrogeology

The lithology and thickness of the Eocene Aquifer vary widely in the western and central parts. In the eastern part, it is mostly karstic reef limestone and soft chalk dominates. The primary hydrostratigraphic formations of the Eocene Aquifer (see figure 4.10) was arranged and summarized (from the oldest to the youngest) as follows (ARIJ, 2002): (a) limestone, dolomite and marl (Cenomanian to Turonian), (b) chalk and chert of Senonian age, (c) chalk, limestone and chert of Eocene age and (d) alluvium of Pleistocene. The importance of hydrogeological cross-sections is to understand and visualize hydostratigraphy of the groundwater aquifer. It is used to study and evaluate the characteristic of faulting, folding, and aquifer thicknesses. The hydrogeological cross-sections contribute to groundwater modeling because it facilitates the evaluation of the ways in which subsurface geometry affects the groundwater flow within aquifers, where contributes to its accurate representation in groundwater flow models and gives realistic

results (MEG, 1999). The hydrogeological cross-section that describes the Eocene Aquifer is shown in Figure 4.11.

Figure 4.10

Hydrostratigraphic Section of the West Bank (HWE, 2008).

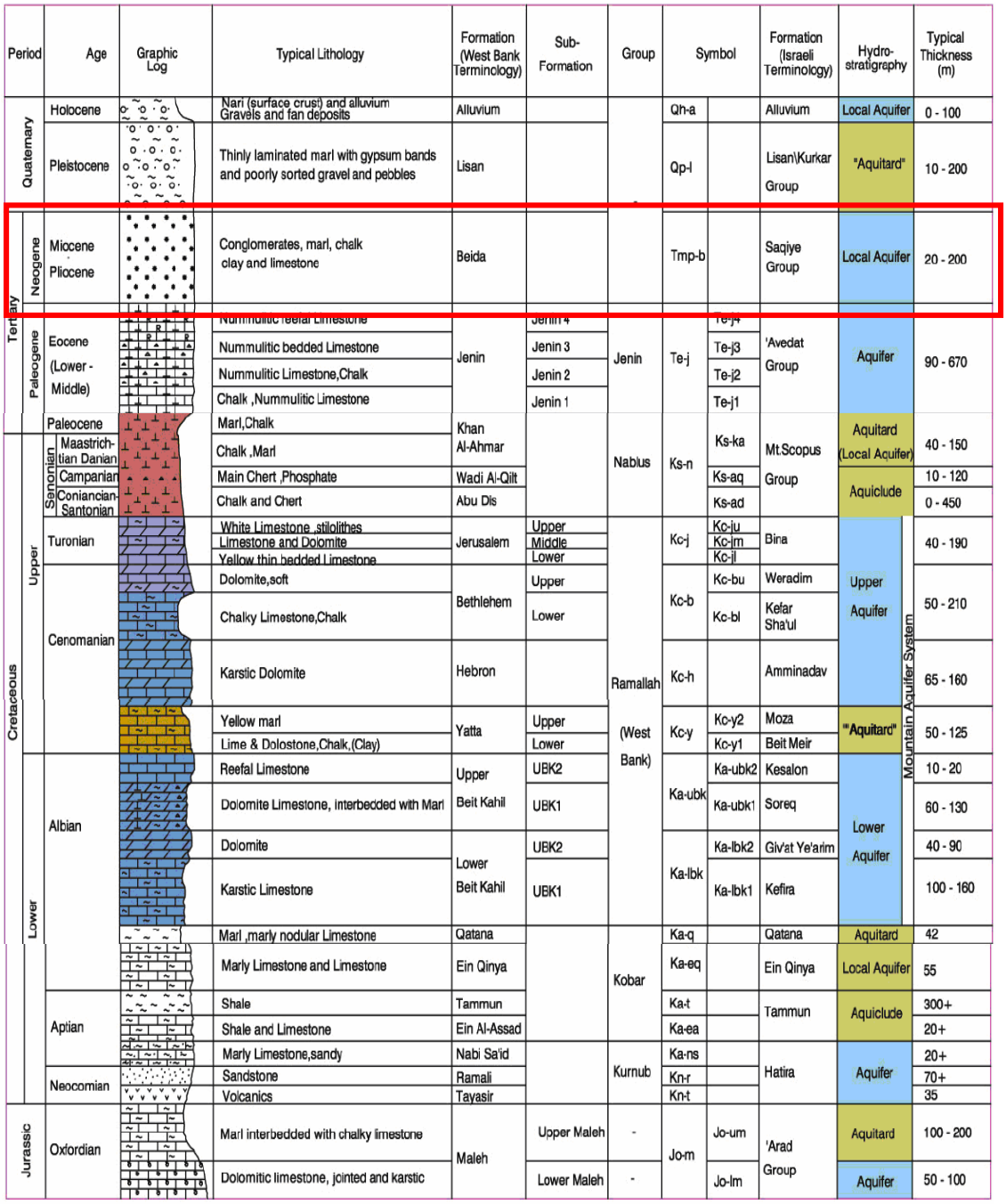

Figure 4.11:

Northern west bank hydrogeological cross section (BGS, 2005).

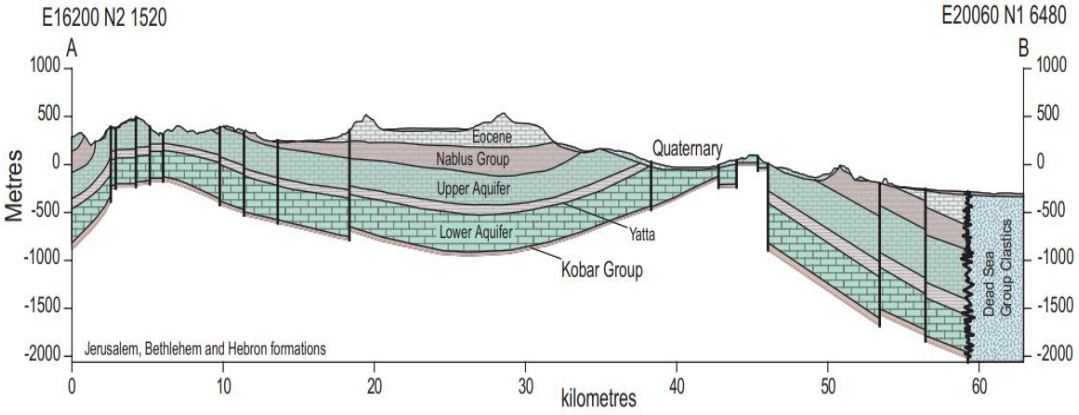

Chapter Five

Recharge Estimation of the Eocene Aquifer

5.1 SWB model domain

The SWB model was used to estimate the spatial and temporal variations in groundwater recharge for 2020[5]-year for the Eocene Aquifer located in the northern part of the West Bank, Palestine. The SWB code imposes restrictions on the shape of the study area to be either rectangular or square to avoid any missing data. This shape is expressed as the SWB model domain, and due to the rectangular shape that the Eocene Aquifer shape tends to, a rectangular outline was made that contains all the Eocene Aquifer to avoid an error in the running of the model. Figure 5.1 shows the rectangular shape of the study area was chosen based on the restrictions imposed by the SWB code. Later to review the results, extraction will be made using a clip tool (GIS tool) for the boundaries of the Eocene Aquifer with an area of 458.6 km^2, to separate the Eocene Aquifer boundaries from the SWB model domain. The model domain includes an area of about 904.3 km^2 with a 30 m×30 m uniform grid cells size (see figure 5.2) for a total of 1,004,504 cells. The grid cell size was chosen based on the smallest size of the land use features, in order for the SWB code to enter all land uses in the calculations and to give realistic results. The study area consists of 818 columns and 1228 rows.

[5] A year period starts on January 1, 2020 and ending on December 31, 2020.

Figure 5.1:

The outline of the study area imposed by the SWB code.

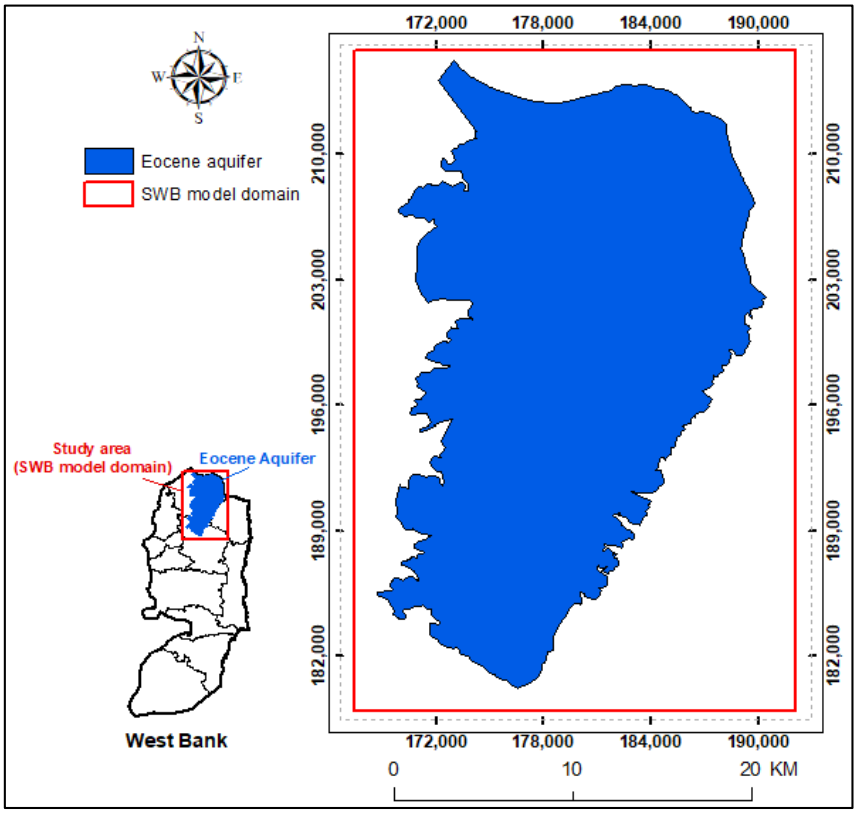

Figure 5.2:

Raster polygon features with a 30 m×30 m uniform grid cells size.

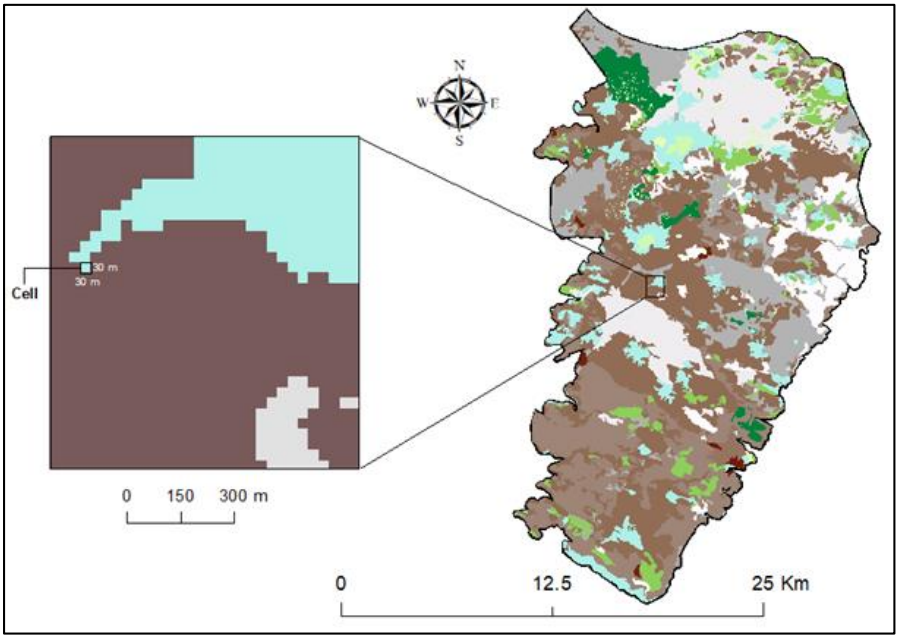

5.2 SWB model inputs

This section describes all the input data required by the SWB code in order to run the SWB model. These include climate data, hydrological soil group, available water capacity, land use, flow direction, and tables files. The following provides an explanation of all the inputs required by the SWB code:

5.2.1 Climate data

Daily temperature and precipitation data are essential inputs for estimating the amount of groundwater recharge in the SWB model. Three daily climate data are required and are considered the minimum climate data needed to run the model: the daily minimum temperature, the daily maximum temperature, and the daily precipitation.

The daily climate data for 2020-year were obtained from the Palestinian Meteorological Department (PMD). The daily rainfall data were obtained for 42 rain gauges and the daily minimum and maximum temperature data for four meteorological stations for 2020-year. These rainfall and meteorological stations are distributed inside, outside, and on the borders of the Eocene Aquifer.

The year of study (2020) was chosen because it is a year with available daily data for all stations in the study area and it does not contain any missing data. There are about 42 rain gauges whose daily data were entered into the calculations, of which about 13 are located within the Eocene Aquifer and about 29 are located on the borders and outside the study area (see figure 5.3). As for the meteorological stations, there are about four stations were used, only one station located within the Eocene Aquifer area and about three stations on the borders and outside the study area (see figure 5.4).

The obtained rainfall and temperature data represent point readings for the location of each station, but the SWB code requires readings for each grid cell within the model domain in order to treat it as continuous surfaces. Therefore, the inverse distance weighting (IDW) method was used to make interpolation between all the rain gauges and the meteorological stations separately and to obtain the values of minimum, maximum temperatures, and rainfall for each grid cell within the model domain.

Figure 5.3:

The distribution of rain gauges used in developing the SWB model.

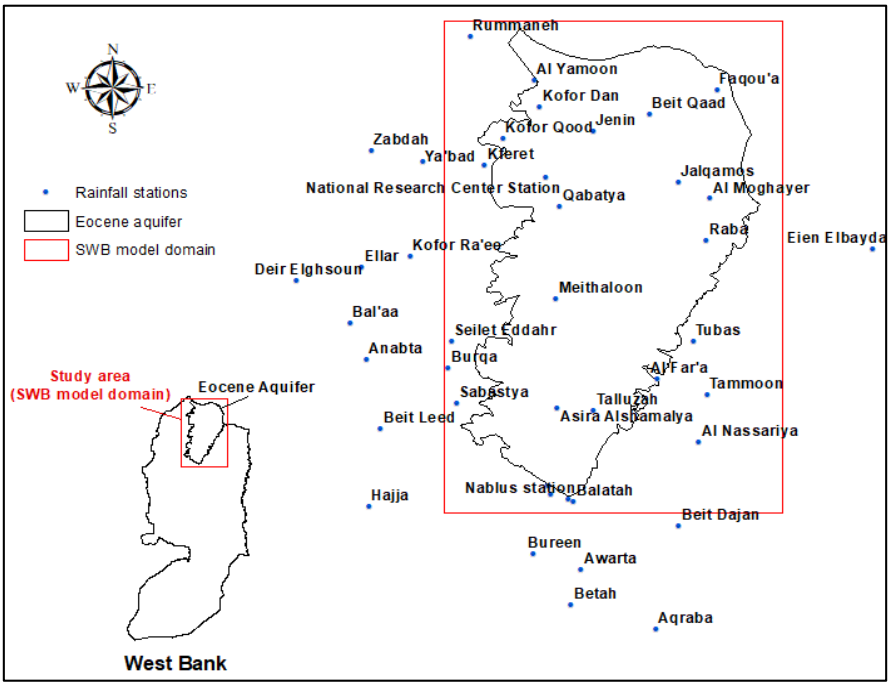

Figure 5.4:

The distribution of meteorological stations used in developing the SWB model.

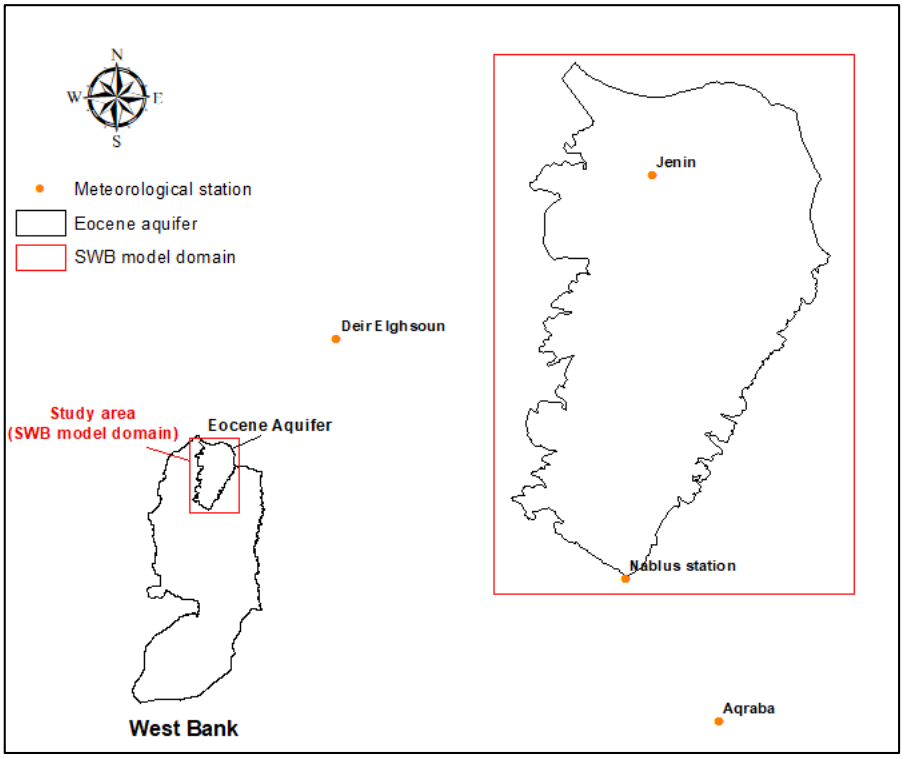

The ModelBuilder tool (GIS tool) (see figure 5.5) was used to process climate data by making an interpolation (IDW method) for all days of the study year and converting it from the raster file with 30-m spatial resolution to the ASCII grid file (using the raster to ASCII tool in GIS) that the code reads (see figure 1,2, and 3 in Appendix A).

The daily mean temperature for the 2020-year for the study area (SWB model domain) was ranging from 12.6 °C (54.2 °F) to 14.5 °C (58 °F) (see figure 4 in Appendix A) and the annual mean precipitation for the 2020-year for the study area was ranging from 378 mm (14.9 in) to 795 mm (31.3 in) (see figure 5 in Appendix A). The daily precipitation values were assigned in inches (in) and the temperature values in Fahrenheit (°F) units based on code restrictions.

Figure 5.5:

The description of ModelBuilder used to process climatic data.

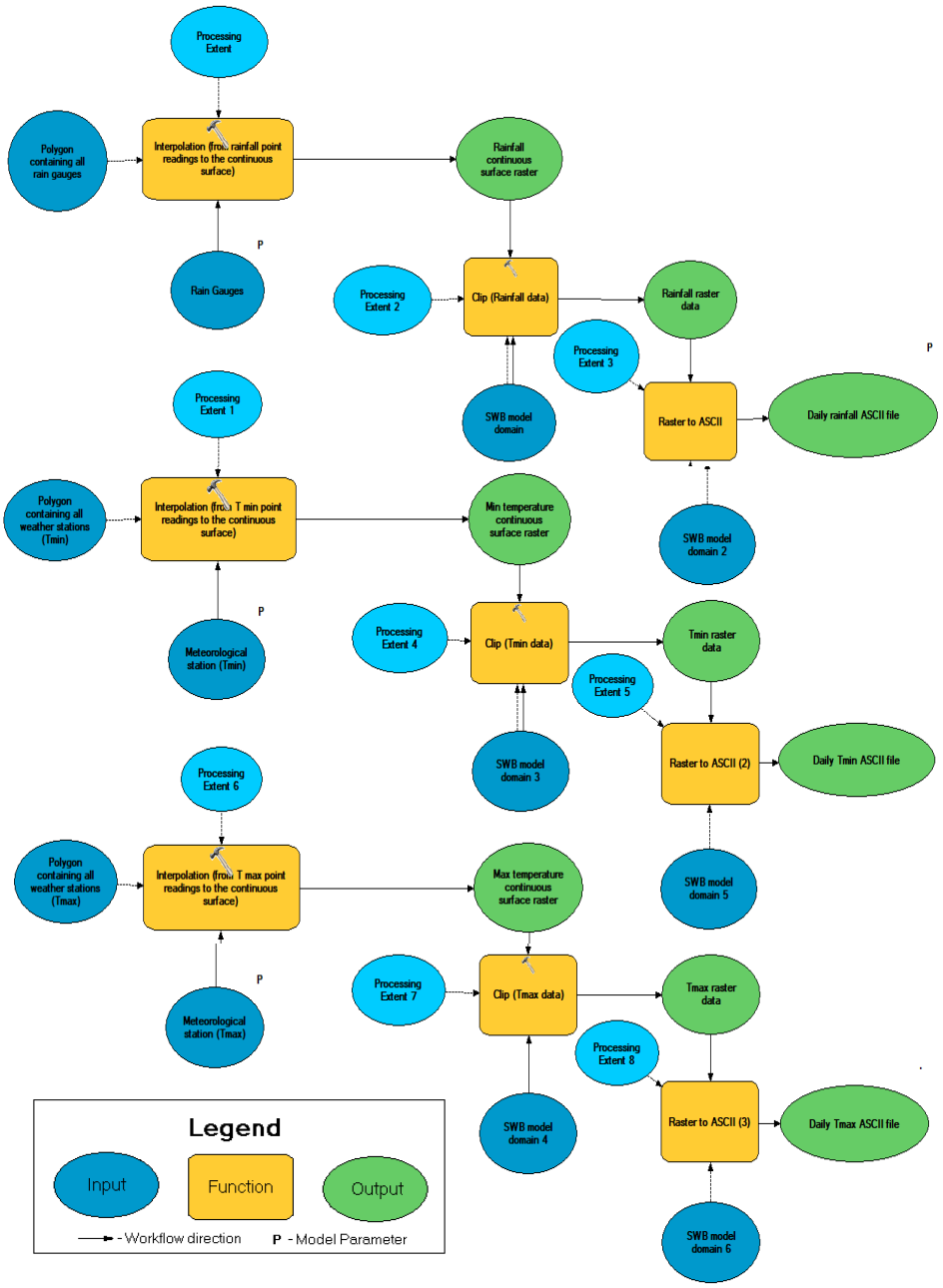

5.2.2 Hydrological soil group

Soil texture is an important and required feature to estimate the amount of groundwater recharge (Kakish and Katimbo, 2017). The USDA-NRCS classifies multiple soils into four classes based on infiltration capacity called hydrological soil group (HSG). The four classes are A, B, C, and D, where A has the highest infiltration capacity at > 183 mm/day (> 7.2 in/day) and the lowest potential surface runoff, while D has the lowest infiltration capacity at < 30.5 mm/day (< 1.2 in/day) and the highest potential surface runoff.

The soil data were obtained from the Palestinian Water Authority (PWA). The available data is in a GIS shapefile and was processed using ArcMap. Each soil texture was assigned a number from 1 to 4 in the Attribute table according to the USDA-NRCS soil classification. The number 1 refers to the HSG A, while the number 4 refers to the HSG D. The study area contains two soil textures: clay and clay loam according to the USDA-NRCS classification, all the study area has the same HSG D (4) (see figure 6 in Appendix A). By using ArcMap, the feature shapefile was converted to raster file with 30-m spatial resolution (using the feature to raster tool in GIS) and then to ASCII grid file (see figure 7 in Appendix A), which the code reads.

5.2.3 Available water capacity

The AWC is an essential input to estimate the recharge amount. It expresses the amount of water holding capacity in inches per foot of soil thickness which is necessary to calculate a value of MSWC (Westenbroek et al. 2010) (see equation 3.2). The AWC values were obtained from tables used by SWB code based on previous studies (Dripps, 2003; Thornthwaite and Mather, 1957). The AWC values were assigned to each soil texture within the study area using table 3.2. Whereas, the value of AWC for clay loam and clay soil is 3 and 3.6 in/ft, respectively. The available soil data obtained from the PWA were processed in the form of a shapefile using ArcMap. The SWB code required the AWC in the unit of inches per foot. The AWC for the study area was ranging from 3 to 3.6 in/ft (see figure 8 in Appendix A). The AWC values for each soil texture were entered into the attribute table and converted to a raster file with a 30-m spatial resolution and then to an ASCII grid file that the code reads (see figure 9 in Appendix A).

5.2.4 Land use

The SWB code uses the land use data to calculate spatial variations in the amount of groundwater recharge. Land use data for the study area were obtained from the PWA as shapefile features. The area of the Eocene Aquifer contains 20 types of land use (see figure 4.6), while within the SWB model domain there are 22 types of land use (see figure 10 in Appendix A); because the SWB model requires that the outline of the study area be a rectangular shape containing all the study area (the Eocene Aquifer).

The land use data obtained from the PWA were processed in the form of a shapefile using ArcMap. An integer number (land use code) for each land use type was assigned into the attribute table and converted from a feature file to a raster file with 30-m uniform spatial

resolution and then to an ASCII grid file that the code reads (see figure 11 in Appendix A). The study area (SWB model domain) contains 22 types of land uses. The main three land use types for the study area (SWB model domain) are Olive groves (25.26%), natural grassland (19.53%), and non-irrigated arable land (10.61%) (see table 5.1). One of the areas located outside the boundary of the West Bank, Palestine, and it represents the northern and northern-eastern part of the SWB model domain. The presence of this area outside the West Bank caused missing data for it. Therefore, the type of land use for this area was assumed and it was called the assumed northern area. This assumed area does not affect the model results because it is lower in elevation than the Eocene Aquifer, and this excludes the occurrence of inflow (surface runoff) to the study area.

Table 5.1:

The land use classification in the study area (SWB model domain).

Land Use Type	Area (km^2)	Percentage of Area
Olive groves	228.46	25.26%
Natural grassland	176.62	19.53%
Non-irrigated arable land	95.9	10.61%
The assumed northern area	82.2	9.09%
Discontinuous urban fabric	78.44	8.67%
Non-irrigated complex cultivation	64.95	7.18%
Sclerophyllous vegetation	53.85	5.95%
Agricultural land with natural vegetation	44.54	4.93%
Drip irrigated arable	24.88	2.75%
Forest	13.62	1.51%
Irrigated complex cultivation practices	13.39	1.48%
Greenhouses	5.67	0.63%
Bare rock	5.5	0.61%
Citrus plantations	4	0.44%
Mineral extraction sites	2.46	0.27%
Sparsely vegetated area	2.22	0.25%
Military camps	1.89	0.21%
Continuous urban fabric	1.77	0.20%
Refugee camps	1.23	0.14%
Transitional woodland	1.1	0.12%
Colonies	1.08	0.12%
Industrial or commercial unit	0.49	0.05%

5.2.5 Flow direction

The flow direction is one of the basic inputs of the SWB model, as the model uses it to calculate the inflow and the outflow (Westenbroek et al. 2010). The flow direction determines how to route overland flow between cells and helps to create a surface water

balance so that the SWB code can estimate the amount of water that collects on each grid cell.

The contour maps of the study area were obtained from the PWA. By using GIS software, the contour map was processed by converting it to triangular irregular networks (TIN) (create TIN tool in GIS) (see figure 12 in Appendix A), converting the resulting TIN to digital elevation model (DEM) (TIN to raster tool in GIS), resampled with 30-m uniform spatial resolution (raster processing resample tool in GIS), fill the DEM (hydrology fill tool in GIS) (see figure 13 in Appendix A), converting the resulting fill raster file to flow direction raster (hydrology flow direction tool in GIS) (see figure 14 in Appendix A), and then converting the resulted flow direction file to an ASCII grid file that the code reads (see figure 15 in Appendix A).

5.2.6 Tables files

Two lookup tables were used by SWB code to complete the water balance calculations for each grid cell within the model domain (Westenbroek et al. 2010). The first table is called the soil-water-retention table which is derived from the soil moisture curve (see figure 16 in Appendix A), taken from the modified version of the Thornthwaite-Mather method tables (Thornthwaite and Mather, 1957). The SWB code uses a soil-water-retention table to estimate the change in soil moisture during periods of unsatisfied potential evapotranspiration. It uses the values of APWL with the values of MSWC to calculate the value of soil moisture retained (SMR) for each grid cell in the model domain. The soil-water-retention table is attached with the SWB code package in the form of a gridded file (ASCII file format) and does not require modification or processing by the user (Westenbroek et al. 2010).

The second table represents the land use lookup table (see table 1 in Appendix E). The land use lookup table is one of the essential inputs for the SWB code as it contributes to estimating the amount of groundwater recharge because it contains the land use code (integer), CN, root depth (in), maximum recharge rate (maximum infiltration rate) (in/day), and interception value (in) for each land use type in the study area (SWB model domain). The study area contained about 22 types of land use. The land use lookup table was developed by using an Excel file and all previous parameters were entered for each land use type. The land use code has been assigned to the table for each land use type.

Whereas, the land use code value is the same as the value that was assigned in the land use attribute table in GIS when the ASCII file for land use was created. The CN was obtained for each land use type based on HSG (D) from the tables (TR-55 and SCS) that were developed by the USDA (USDA, 1986; USDA, 2004). The CN values were assigned after adjustment based on the percentage of impervious areas according to the equation 5.1 for connected impervious areas and equation 5.2 for unconnected impervious areas.

$$CN_c = CN_p + (\frac{P_{imp}}{100})(98 - CN_p) \quad (5.1)$$

$$CN_c = CN_p + (\frac{P_{imp}}{100})(98 - CN_p)(1 - 0.05R) \quad (5.2)$$

Where;

CN_c = composite curve number;

CN_p= pervious curve number;

P_{imp}= percent of imperviousness;

R= ratio of unconnected impervious area to total impervious area.

High-resolution areal maps were used to find the equivalent land use description for the study area in the USDA tables for the curve number (see table 2 in Appendix E).

The values for root depth were obtained from the modified version of the Thornthwaite-Mather method tables (Thornthwaite and Mather, 1957). The root depth was assigned for each land use type based on the HSG (D) located in the study area.

The values of the maximum recharge rate were obtained from USDA-NRCS (see table 3.2). The maximum recharge rate was about 1.2 in/day for the whole study area; because it depends on the HSG, which was the same for all the study areas (HSG D).

The interception values for each season (growing and dormant) and for each land use type were obtained from LIU and DE SMEDT (2004) and then assigned in the land use lookup table.

The land use lookup table was converted from Excel file into a text file that the code can read. The interaction between SWB code and input data shown in figure 5.6.

The final step is running the SWB model as shown in the SWB model tutorial (see Appendix F).

The results of the SWB model showed that the SWB code is powerful in estimating the spatially and temporally variations in recharge amount, the model contributed to a good description and understanding of the water budget in the aquifer, the model showed the effect of the land surface slope and curve number values on the amount of recharge, and the SWB model divided the aquifer into zones based on recharge rates.

Figure 5.6:

The interaction between SWB code and input data.

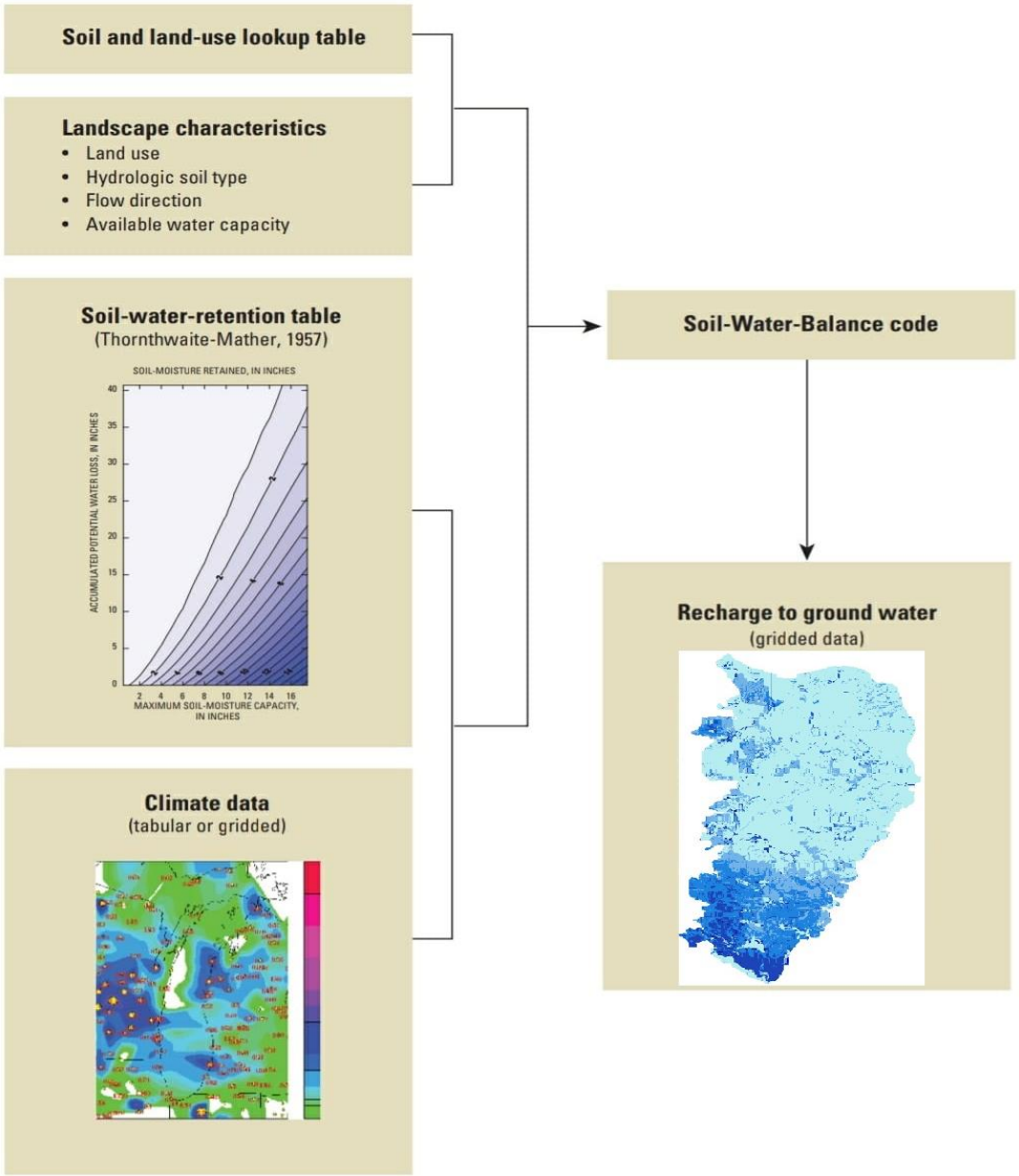

5.3 Model Verification

It is the process of checking that the model was built in the correct manner, in conformity with the assumptions and specifications on which the model was based on. The main objective of the verification process is to check the quality of the results (Banks et al., 2010; Carson, 2002). Many different processes and techniques can be used for the purpose of verifying the model, which includes examining the outputs of the model in order to verify the model, to verify the reasonableness of the results, examining the model by a competent expert person, and using related previous models (Banks et al., 2010). The verification process should improve the credibility of the model and increase confidence in it (Carson, 2002).

Model verification is an important and essential step in hydrological modeling studies, as it contributes significantly to increasing confidence in the model results (Anderson et al. 2015). The process of verification of groundwater models is important and essential in order to evaluate the performance of the models (Day, 2019). In the case of the SWB model, there is no agreed verification method, but the user is allowed to choose the verification method he deems appropriate based on the available data and the characteristics of the aquifer (Smith and Westenbroek, 2015).

There are many methods that can be used to estimate the amount of groundwater recharge, which can be used to verify the SWB models to increase the confidence in the model results (Day, 2019), and these methods are:

i. The Water Budget Method

   It is one of the most common methods for estimating the amount of groundwater recharge. This method uses mass balance equations to study the movement and quantity of water inside and outside the aquifer (Healy et al. 2007). In general, water budget methods are applicable to estimations of diffuse and concentrated recharge (Healy and Scanlon, 2010). Diffuse recharge is defined as the movement of water through an unsaturated zone to the groundwater table and is prevalent in humid climates. As for the concentrated recharge, it occurs when the water does not contribute uniformly to the recharge, as it is concentrated in small areas forming ponds of water that infiltrate to the ground surface, exceeding the field capacity of

the soil and infiltrate to the groundwater table and it is prevalent in arid areas (Day, 2019).

Hatfield et al. (1999) estimated the recharge of groundwater for Walnut Creek watershed in the U.S., using the water budget method. They proved that this method does not give results based on spatial and temporal variations in the amount of recharge and does not take into consideration in its calculations the characteristics of watersheds such as surface geology and land use. This affects the accuracy of the results because groundwater and pollutant transport models depend mainly on the availability of spatially and temporally variations of recharge estimates (Lewis and Walker, 2002).

ii. The Baseflow Separation Method

In watersheds where the water level is higher than the streams (gaining stream), the water balance approach can be used to estimate the amount of baseflow, which is commonly assumed to be equal to the amount of groundwater recharge (Cherkauer and Ansari, 2005). Baseflow occurs when water infiltrates to the ground surface and recharges the aquifer by raising the water table and eventually flows into streams (Healy and Scanlon, 2002). The baseflow discharge is equivalent to groundwater recharge (Schicht and Walton, 1961; Day, 2019) (see equation 5.3).

$$R = Q_{off} - Q_{on} + Q_{BF} + ET + \Delta S \quad (5.3)$$

Where;

R is recharge;

Q_{off} is groundwater off the watershed;

Q_{on} is groundwater onto the watershed;

Q_{BF} is baseflow discharge;

ET is evapotranspiration from groundwater;

ΔS is the change in groundwater storage.

The baseflow was used to estimate the amount of groundwater recharge in several previous environmental studies (Lorenz and Delin, 2007; Day, 2019). The baseflow method requires that the study area contain streams with a sufficient number of

readings to reflect spatial and temporal variations in groundwater recharge (Day, 2019).

iii. The Lysimeter Method

It is one of the physical methods used to estimate the amount of groundwater recharge of the unsaturated zone and it depends on the water budget methods. This method provides point estimates for the quantities of recharge. In order for the method to give realistic results that vary spatially and temporally, a large number of lysimeter devices must be available and distributed over the study area (Healy and Scanlon, 2010). It is one of the most commonly used physical methods for estimating the amount of recharge. In this method, weighing and pan lysimeters are used, which are placed below the soil-root zone to measure the drainage rates of the water passing through it (Day, 2019). The lysimeter method provides good local recharge estimates, but if used on a large scale, it is expensive, difficult to construct, and requires high periodic maintenance (Scanlon et al., 2002).

iv. The Chemical Tracer Method

Chemical tracers are used to study and estimate the amount of groundwater recharge and the quality and source of water (Healy and Scanlon, 2010). Chemical tracers are divided into three categories: natural environmental tracers, historical tracers, and applied tracers (Scanlon et al., 2002). Natural tracers include chloride (Cl), tritium (^{3}H), and chlorine-36 (^{36}Cl). These tracers are called natural because they are produced naturally within the earth's atmosphere (Healy and Scanlon 2010). As for historical traces, they are the result of human activity (Cook and Böhlke, 2000). Among these historical tracers that are used for groundwater studies are ^{36}Cl and ^{3}H (Phillips et al., 1988). As for applied tracer's dyes are used, which are the most common types for scientific research purposes (Helmke et al., 2005). In the chemical tracer's method, tracers are added to the soil column and the aquifer water concentrations are measured to know the recharge rates. However, the chemical tracer method is not practical in spatially and temporally variations recharge estimations (Helmke et al., 2005; Day, 2015).

All methods vary between each other in terms of application, ease of use, and availability of the necessary data. All previous methods are not suitable for use in

this research because some of them do not give spatially and temporally variable results for the amount of recharge and do not take into consideration in their calculations the land use types such as the water budget method, some of them require the availability of a sufficient number of data for the study area such as baseflow separation method that requires a sufficient number of streams readings, and the study area (Eocene Aquifer) does not contain streams. Some methods give accurate and realistic results at a local scale, but if they are used on a large scale, they are expensive, difficult to construct, and require high periodic maintenance, such as the Lysimeter method, which requires the presence of large numbers of lysimeter devices in order to give accurate results for the groundwater recharge based on spatially and temporally variations on a large scale. Some methods are impractical in estimating the amount of recharge that varies in space and time, such as the Chemical tracer method.

v. The Water Table Fluctuation Method (WTF)

The most widely used methods for estimating groundwater recharge rates are the ones that depend on groundwater levels, due to the availability of groundwater level data, simplicity and the ease of estimating the spatially and temporally variable recharge quantity using this method (Healy and Cook, 2002). The WTF method is one of the common methods for estimating the amount of groundwater recharge of unconfined aquifers. This method can be applied to any well that taps the groundwater level, and the groundwater level data for it is abundantly available (USGS, 2017). In addition, this method does not require any assumptions for the movement of water through the unsaturated zone (USGS, 2017). The WTF method depends in its calculations on the measurement of spatial and temporal variations of groundwater levels. This method is also called water table rise (WTR). This method assumes that the rise in the groundwater level is caused by the recharge that recharges the water level in the aquifers (Healy and Scanlon, 2010; Day, 2019). While the decline in the groundwater level, it is caused by pumping from the aquifer (USGS, 2018). The WTF method assumes that the water in the soil column is equal to the difference in the height of the water in the column multiplied by the specified yield (Healy and Scanlon, 2010). The specific yield is equal to the volume of water taken

into or released from storage per unit change in head per unit area (USGS, 2017). Recharge in this method is calculated using equation 5.4.

$$R = S_y \frac{dh}{dt} = S_y \frac{\Delta h}{\Delta t} \quad (5.4)$$

Where;

R is recharge;

S_y is specific yield;

h is water table height;

t is time.

To calculate the recharge amount, Δh is set which is equal to the difference between the rise peak and the low point of the extrapolated antecedent recession curve at the peak time. The antecedent recession curve represents the effect that the well hydrograph would have followed in the absence of rainfall that causes the water level to rise in the aquifers (see figure 5.7)

Figure 5.7:

Determination of water table rise (USGS, 2017).

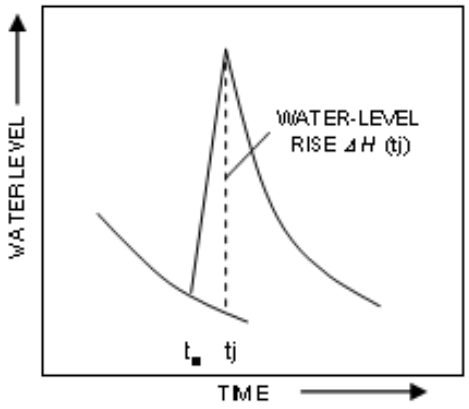

The WTF method is considered one of the most effective methods due to its high accuracy, low cost, and ease of use (Xu and Beekman, 2003). In this research, this method was used because it is a simple and direct method that gives realistic results for the quantities of recharge based on spatial and temporal variations in addition to the availability of the necessary data for it. Due to the absence of previous studies specialized in estimating the amount of groundwater recharge for the study area (Eocene Aquifer), the SWB model was verified for the study area using the WTF method. The amount of

groundwater recharge was calculated by this method using groundwater level data and the specific yield of wells obtained from PWA. The data was obtained for nine wells that are distributed within the study area (see figure 1 in Appendix B). The graphs from 2 to 10 in Appendix B shows the fluctuation of the groundwater level of these wells during the period 2014-2017. The graphical extrapolation method (see figure 5.8) was used to calculate the value of Δh for each year and the resulting values were used to calculate the recharge (USGS, 2017). Table 5.2 shows the results of groundwater recharge using the WTF method.

Figure 5.8:

Graphical extrapolation method to the water table fluctuation method for estimating recharge (USGS, 2017).

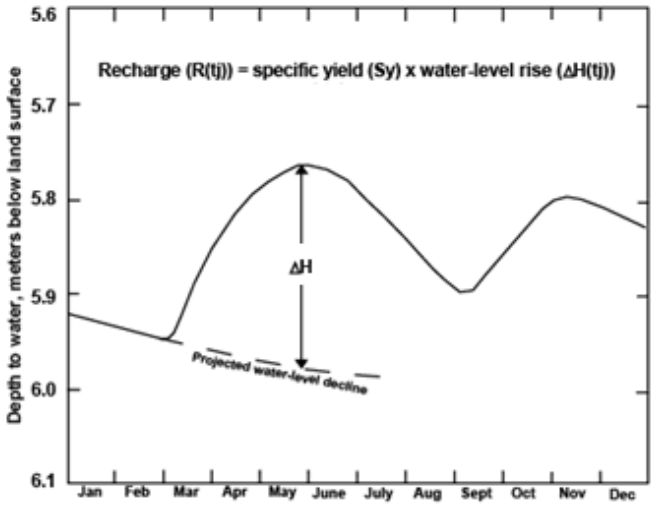

Table 5.2:

Groundwater recharge for the Eocene Aquifer from WTF method.

Well	Δh/Δt (m/year)	Specific Yield	Groundwater Recharge (mm/year)
17-21/009	17.966	0.001	18
17-21/014	17	0.001	17
17-20/009J	7.86	0.003	2.36
17-20/014A	10.02	0.01	100.2
17-21/015	3.204	0.003	9.612
17-20/036J	30.5	0.003	91.5
17-20/014Q	35.92	0.003	107.76
17-20/021J	7.54	0.003	22.62
17-21/022	2.923	0.0003	0.88

Using the IDW method from GIS tools, the recharge values based on each well resulting from the WTF method were represented and the mean potential recharge value was calculated, which was 50.73 mm/year (2 in/year) for the entire study area, while the results of the SWB model showed that the mean potential recharge was equal to 50.25 mm/year (1.97 in/year). These values showed that there is no significant difference between the simulated recharge resulting from the SWB model and the observed recharge resulting from the WTF method. However, the SWB model was adjusted to find the closest match between recharge values and to get more realistic results. This is almost very close to the calibration concept. The curve number values were manually adjusted by -2%, -1%, and -0.5% (see table 3 in Appendix E), and the SWB model was re-run after the adjustment. The recharge rate was analyzed for all the adjustments in the curve number values, where it was shown that the version adjusted by -0.5% produced the closest fit with the recharge rate generated by the WTF method. The mean recharge becomes equal to 50.70 mm/year (1.996 inches/year). After choosing the closest version model to represent the current study, the performance of the model was evaluated by calculating the relative error and the goodness of fit between the recharge rates generated by SWB model and the WTF method. The relative error was compared using equation 5.5 (Smith and Westenbroek, 2015).

$$Relative\ error = \frac{|SWB\ Recharge - WTF\ Recharge|}{WTF\ Recharge} \tag{5.5}$$

The RE value was equal to 0.06 %.

As for the goodness of fit between the recharge rates resulting from the SWB model and the WTF method, it was calculated using three methods. These methods included: 1) the root mean square error (RMSE), 2) the absolute mean error (AME), and 3) the Nash-Sutcliffe model efficiency coefficient (NSE). The recharge values obtained from the SWB model were represented as the simulated or predicted values, while the recharge values obtained from the WTF method were represented as the observed or realistic values. The AME method is the difference between the observed and simulated recharge according to equation 5.6 (Smith and Westenbroek, 2015).

$$AME = \frac{1}{n} \sum_{i-1}^{n} |P_i - O_i| \quad (5.6)$$

Where;

n is the number of years of groundwater level data at each well;

P_i is the predicted value and;

O_i is the observed value.

The AME value was equal to 11.6%.

The RMSE method which represents the square root of the deviation between the observed and simulated recharge values according to equation 5.7 (Smith and Westenbroek, 2015).

$$RMSE = \sqrt{\frac{1}{n} \sum_{i-1}^{n} (P_i - O_i)^2} \quad (5.7)$$

The RMSE value was equal to 0.0105 which is close to zero.

The Nash Sutcliffe model efficiency method (see equation 5.8) is used for hydrological models where it is defined as one minus the sum of the absolute squared difference between the simulated values and the observed values that were normalized by the variance in the observed mean values of the amount of recharge during the study period (Nash et al. 1970; Krause et al. 2005).

$$NSE = 1 - \frac{\frac{1}{n} \sum_{i-1}^{n} (O_i - P_i)^2}{\frac{1}{n} \sum_{i-1}^{n} (O_i - \bar{O})^2} \quad (5.8)$$

Where;

O_i is the observed value;

P_i is the predicted value and;

$\bar{O}$ is the mean of the observed values.

For the values of NSE, the model is completely identical between the observed and simulated potential recharge values if the value of NSE is one. A zero value of NSE indicates that the SWB model has the same predictive skill as the mean of the observed values. While the negative values indicate that the observed and simulated recharge values have a high variance (Nash et al. 1970; Day, 2019). The value of NSE in this study

was equal to 0.66, which means that the simulated recharge values resulted from the SWB model are close to be completely identical for the observed recharge values resulted from WTF method.

vi. The Water Demand Calculation Method (WDC)

Water demand is defined as the amount or volume of water that the user will require to satisfy his needs. It depends on water quality, area size, climate, population, land use, standards of living, water price, and industrial and commercial activities in the area (EEA, 1999; Poudel, 2020).

In this method, the water demand in the area supplied by water from the Eocene Aquifer is calculated for the same study period and a comparison is made between the amount of water demand and the amount of groundwater recharge. If the amount of water demand is higher than the amount of recharge, this indicates a water deficit in the aquifer by the amount of the difference between the water demand and the recharge. This causes a decrease in the groundwater level with time. If the amount of the water demand is less than the amount of recharge, this indicates that the water situation in the aquifer is good and the groundwater level is increasing with time (Shrestha et al., 2016).

The water deficit in the aquifer is defined as the difference between the amount of recharge and the amount of water supply that meets the water demand (Jalota et al., 2018). The Eocene Aquifer contains many unlicensed wells that do not have readings. This led to a lack of data for the amount of water pumped from the aquifer (water supply). In this research the amount of water supply is assumed to equal to the amount of water demand.

There are four main types of water demand, which are domestic water demand, livestock water demand, commercial and industrial water demand, and agricultural water demand.

In this research, the WDC method was used to verify the reliability of the model. This method was used for its ease and availability of data. The data needed for water demand calculation were obtained for the area of the Eocene Aquifer from PWA, MoA, MoA-Livestock Department, and Jenin Municipality.

In this part of the research, these main types of water demands were calculated. The agricultural water demand was calculated for the entire study area using the data obtained from MoA (see table 4 in Appendix E). The total annual amount of the agricultural water demand was about 22,678,300 m^3 (22.6 MCM), which constitutes the largest value of water demand in the study area. Figure 1 in Appendix C shows the agricultural water demand for the communities located within the Eocene Aquifer.

For the livestock water demand, it was calculated based on the data obtained from the MoA - Livestock Department (see tables 5, 6, and 7 in Appendix E), where livestock was divided in the process of calculating water demand according to water consumption. The water demand for sheeps, cows, and poultry was calculated for the study area. The total annual water demand for sheeps was about 377,330 m^3 (0.377 MCM), for cows was about 146,531 m^3 (0.146 MCM), and for poultry it was about 377,696 m^3 (0.377 MCM). Figures 2, 3, and 4 in Appendix C show the distribution of livestock water demand for the communities within the Eocene Aquifer. The total annual amount of livestock water demand was about 901,577 m^3 (0.9 MCM).

For domestic water demand, it was calculated based on data obtained from PWA and from the Palestinian Central Bureau of Statistics (PCBS). The domestic water demand (see table 8 in Appendix E) was about 7,198,618 m^3/y (7.19 MCM).

For the industrial and commercial water demand, the total annual amount of the industrial and commercial water demand was obtained from the Water and Sanitation Department in Jenin Municipality. All industrial and commercial places are concentrated in the study area in Jenin District. The total annual industrial and commercial water demand was about 518,662 m^3 (0.518 MCM).

The annual quantity of water purchased from the Mekorut company was obtained, which is estimated at about 3,000,000 m^3 (3 MCM) for the study area. As a result of these calculations, the total annual amount of water demand for the communities of the Eocene Aquifer is about 28,297,137 m^3 (28.29 MCM) (see table 5.3).

Table 5.3:

Summary of the water demand calculations for the communities of the Eocene Aquifer.

Types of Water Demand	Annual Water Demand (m^3)
Domestic	7,198,618
Agricultural	22,678,300
Livestock	901,557
Industrial and commercial	518,662
Mekorut	- 3,000,000
Sum	**28,297,137**

From the wells data obtained from PWA (see figures from 11 to 19 in Appendix B), it can be noted that the depth to water table has been increasing with time which means that the groundwater level in the Eocene Aquifer has been decreasing with time. This happened due to the increase in water demand resulting from the increase in the population, intensive agriculture, and decrease of recharge quantity. The amount of groundwater recharge of the Eocene Aquifer is less than the water demand. This leads to a decrease in the groundwater level with time (increasing the depth to water table). Table 5.4 shows the variations of the average depth to water table for the wells in the Eocene Aquifer. As can be noted that all wells have increased the average depth to water table with time, and this indicates a decrease in the groundwater level with time for the Eocene Aquifer.

Table 5.4:

The variations of the average depth to water table for the wells in the Eocene Aquifer.

Well	Depth to water table average (m)	Depth to water table average (m)
	2000-2006	2009-2017
17-21/014	25	85.5
17-20/009J	10.5	13.6
17-20/014A	62	69.2
17-21/009	38	110.67
17-21/015	51.7	61
17-20/036J	57	77
17-20/014Q	35	96
17-20/021J	19	21
17-21/022	43	55

The research showed that the annual recharge amount of the Eocene Aquifer is about 23.25 MCM, while the total annual water demand for the communities of the Eocene

Aquifer is about 28.29 MCM. This means that there is a water deficit in the Eocene Aquifer, estimated at about 5.04 MCM. This is the main reason for the decrease in the groundwater level with time within the aquifer.

The results of the SWB model showed that the amount of groundwater recharge to the Eocene Aquifer is less than the amount of water demand, and this means that the level of groundwater in the aquifer is gradually decreasing with time, which was proven by the water level readings in the aquifer wells. It can be noticed that there is a conformity between the results of the SWB model and the results of the WDC method. This indicates that the SWB model was reasonably built and gives realistic and logical results.

5.4 Sensitivity Analysis

The simplest method of sensitivity analysis is to compare changes in parameter values against their effects on groundwater recharge by using a graphical representation (Tubeileh et al., 2006). Some spatially well-distributed cells were selected over the study area and the recharge was recorded for each parameter in each trial (see table 5.5).

Table 5.5:

Land use type and the location of the selected cells.

Cell Number	Land Use Type
(1075, 1952)	Olive groves
(1114, 1514)	Natural grassland
(1057, 1567)	Discontinuous urban fabric
(1020, 1502)	Drip irrigated arable
(926, 1118)	Natural grassland
(817, 1448)	Agricultural land with natural vegetation
(769, 1562)	Natural grassland

Sensitivity analysis was performed for curve number, maximum infiltration rate, root zone depth, and interception to select the most sensitive parameter. The sensitivity analysis for this model focused on the curve number because it was found that the model is very sensitive to it as there is a high uncertainty in its values and distribution (see figures 5.9, 5.10, 5.11 and 5.12).

Figure 5.9:

Model sensitivity to the curve number for the Eocene Aquifer.

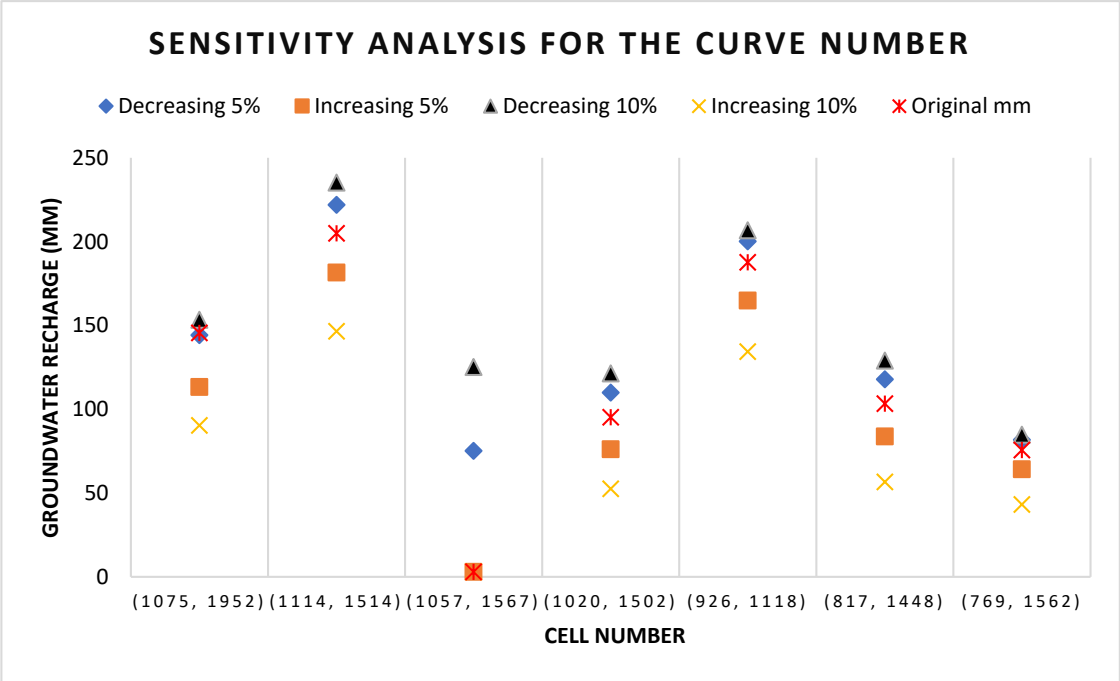

Figure 5.10:

Model sensitivity to the maximum infiltration rate for the Eocene Aquifer.

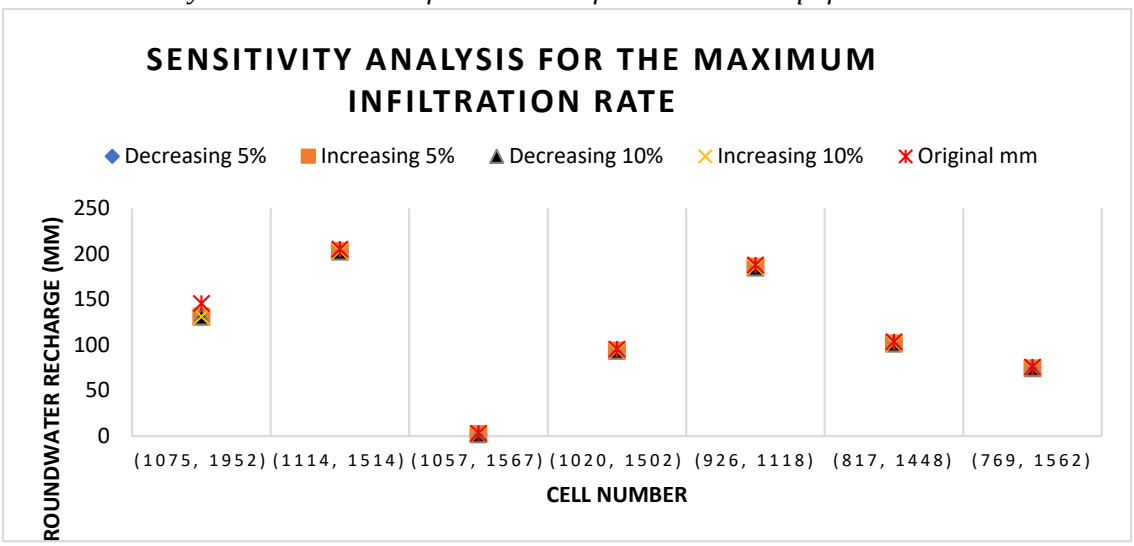

Figure 5.11:

Model sensitivity to the root zone depth for the Eocene Aquifer.

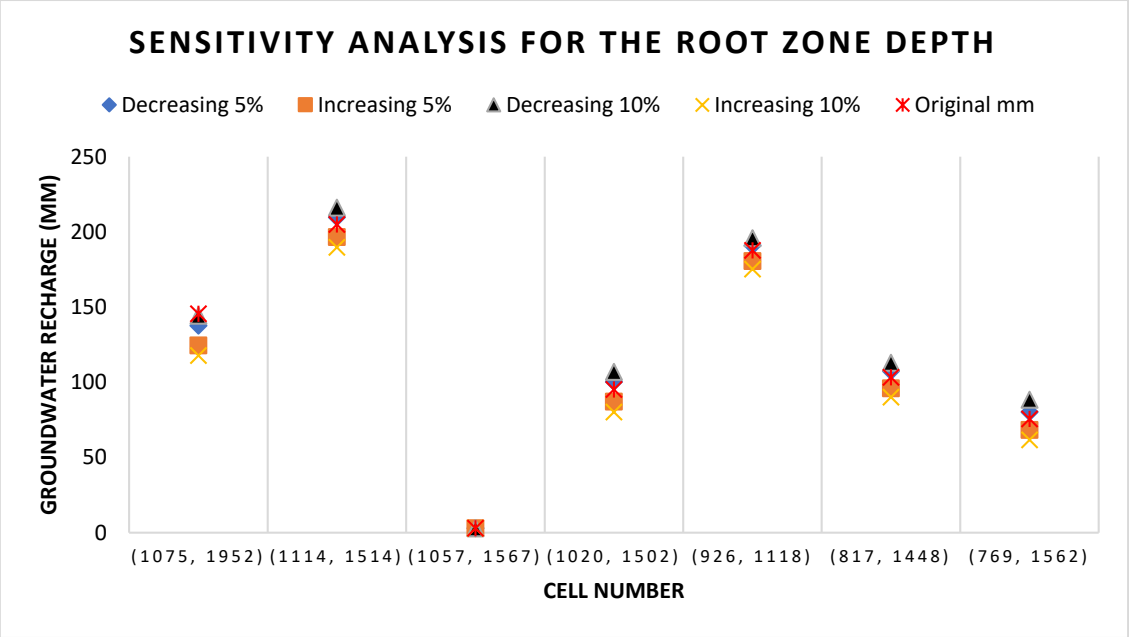

Figure 5.12:

Model sensitivity to the interception for the Eocene Aquifer.

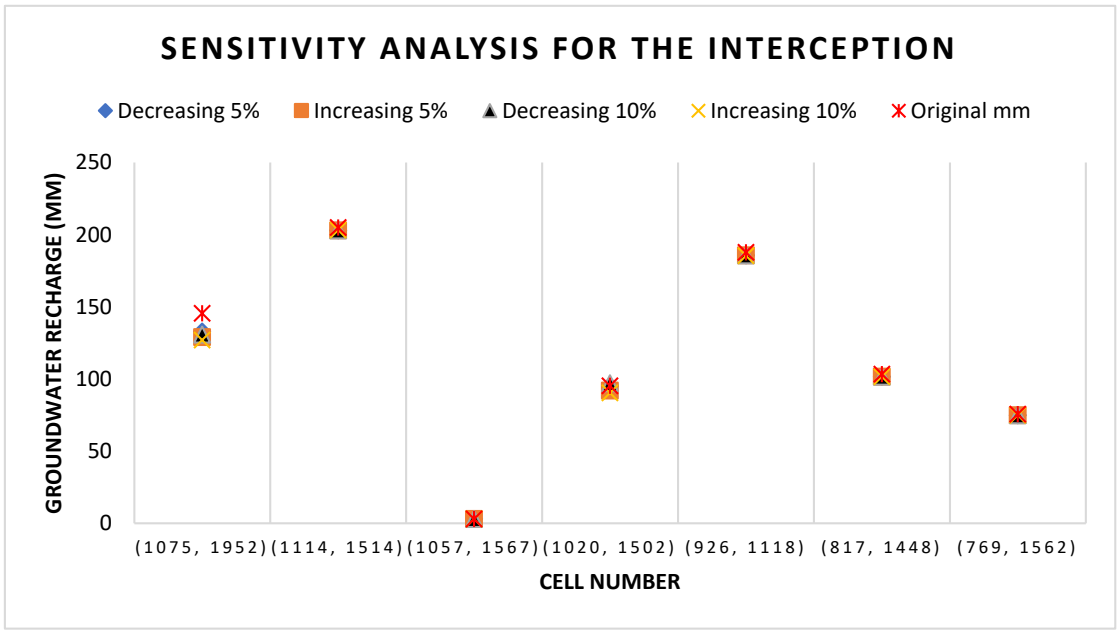

To check the sensitivity of the recharge to the curve number, a sensitivity analysis was performed. Sensitivity analysis examines how the percentage change in the curve number affects the percentage change resulting in the recharge. In this analysis, other parameters such as maximum infiltration rate, root zone depth, and interception were not studied because they have a little effect on recharge compared to the effect of the curve number. The curve number values were adjusted for all land uses. They were adjusted by ± 5%

and ± 10%, and then the model was re-run after each adjustment. By using equation 5.9 (the formula for the relative sensitivity of the original and adjusted annual average recharge value) (Smith and Westenbroek, 2015), the results can be analyzed as follows:

$$Relative\ Percent\ Sensitivity\ (RPS) = \frac{Percent\ change\ in\ SWB\ model\ results}{Percent\ change\ in\ parameter\ (CN)} \times 100 \quad (5.9)$$

Sensitivity analysis was necessary to understand how the recharge rate is affected by the change in the curve number values. The land uses in the study area are considered highly sensitive to the recharge rate, especially when the curve number values decrease by 5%, the value of RPS reached the highest value of about 293.43% (see table 9 in Appendix E). The value of 293.43% means that 5% of the RPS represents the percentage of change that occurred for the recharge values when adjusting the curve number values by -5% (decreasing the curve number values by 5% causes an increase in the recharge value by 5% of the RPS value). The value of the recharge rate before adjustment was equal to 50.70 mm/year (1.996 in/year), where the value of the recharge rate after decreasing the curve number values by 5% became about 58.53 mm/year (2.3 in/year). As for the lowest value of RPS, it was equal to -108.27%, when the curve number values were increased by 5% and the value of the recharge rate was equal to 53.37 mm/year (2.1 in/year). The results show that the curve number values have a significant influence on the results of the SWB model. An increase in the value of the curve number leads to a decrease in the recharge rate and vice versa; because the increase in the curve number reflects the presence of impervious areas that reduce the infiltration rate and thus reduce the amount of recharge. This part of the research showed that groundwater recharge is highly sensitive to small variations in the curve number values. Thus, in order to increase the accuracy of recharge rate estimates, care should be taken when selecting the curve number values.

5.5 SWB model results

5.5.1 Potential Groundwater Recharge

The SWB model succeeded in estimating the quantity of the spatial and temporal variations of groundwater recharge for the Eocene Aquifer during the study period (2020).

The SWB model showed that the recharge rate was 50.70 mm/year (1.996 in/year), which equals to 23,252,650 m^3 (23.25 MCM/year). Figure 5.13 shows the spatial and temporal distributions of the recharge amount in the Eocene Aquifer. The highest rates of recharge are distributed in the study area, where they occur in the northern part of Nablus District (the southern part of the Eocene Aquifer), the southwestern part of Tubas District (the southeastern part of the Eocene Aquifer), and in the western part of Jenin District (the northwest part of the Eocene Aquifer). Nablus District constitutes 54.53% of the recharge amount of the Eocene Aquifer, and it is estimated at about 135.82 mm/year (5.35 in/year), which is equal to 12.68 MCM/year. Jenin District constitutes 39.71% of the recharge amount of the aquifer, and it is estimated at about 28.26 mm/year (1.11 in/year), which is equal to 9.23 MCM/year. While Tubas District constitutes the lowest percentage, which is 5.76% of the recharge amount, and it is estimated at about 34.66 mm/year (1.36 in/year), which is equal to 1.34 MCM/year. The different results of groundwater recharge variation (spatially and temporally) for the Eocene Aquifer are illustrated in the following sections.

Figure 5.13:

The spatial distribution of the total recharge for year 2020 in the Eocene Aquifer.

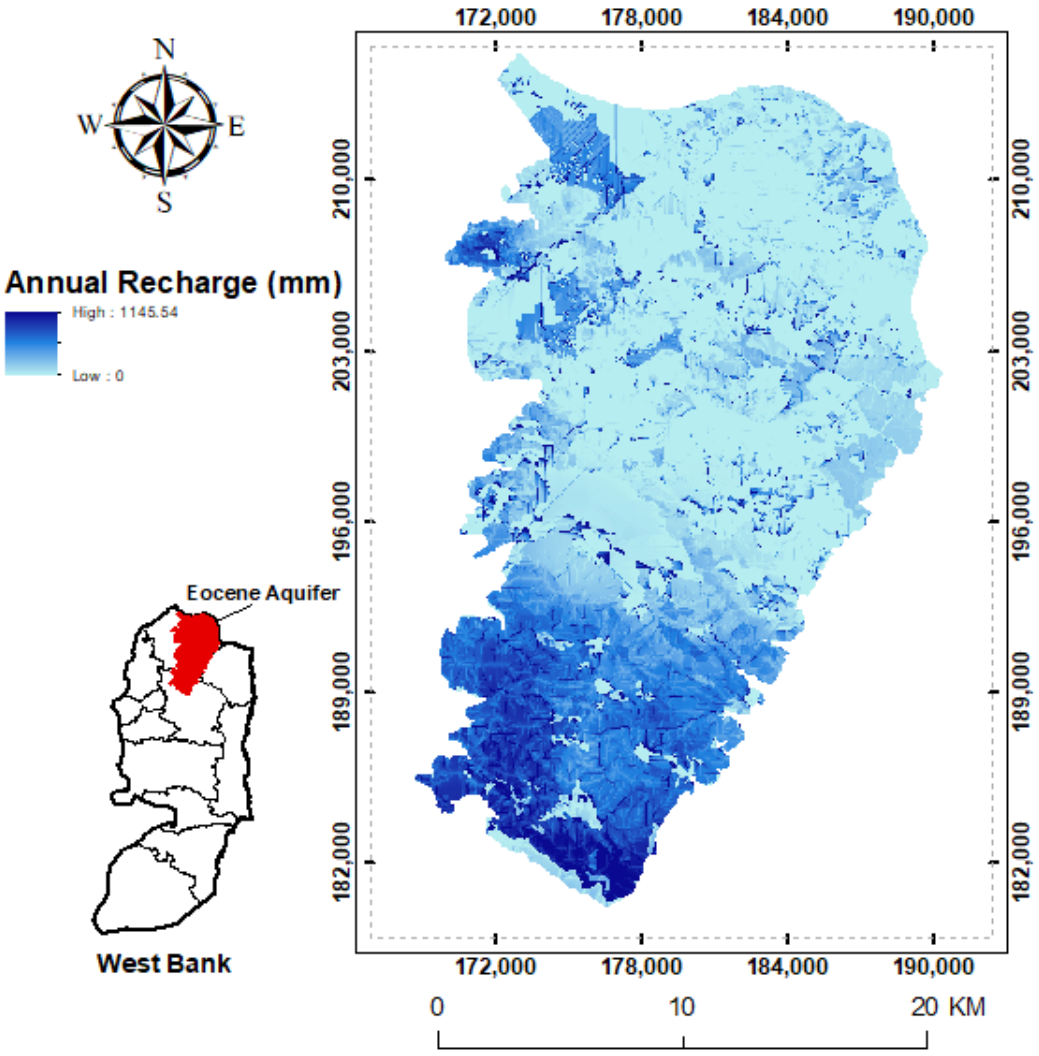

5.6.2 Spatial Distribution of Groundwater Recharge

The spatial distribution of annual groundwater recharge for the Eocene Aquifer for the year 2020 is illustrated in the figure 5.13.

Figure 5.13 helps to deduce and distinguish areas with high and low recharge. For example, the eastern parts of the Eocene Aquifer witness low recharge values due to low rainfall and high evaporation, while the southern parts witness high recharge values due to the abundance of rainfall and low evaporation compared to the eastern areas.

5.5.3 Temporal Distribution of Groundwater Recharge

The temporal variations of groundwater recharge for the Eocene Aquifer from January to December are as illustrated in figures from 1 to 12 in Appendix D.

Figure 5.14 shows that recharge occurs in the months of January, February, March, November, and December. The highest amount of recharge occurs in the months of January, February, and March, while the lowest recharge occurs in November and December. As for the months of April, May, June, July, August, September, and October, no recharge occurs, and this corresponds to the temporal variation of rainfall as shown in figures 5.15 and 5.16. It can be noted that the first three months (January, February, and March) constitute the highest recharge rates due to the high amounts of rainfall and low temperatures in those months. Figure 5.16 indicates that the recharge rates in November and December are very low with the presence of high rainfall, this case is due to the low soil moisture content and the AWC is almost zero in that period, so most of the water that infiltrated to the soil was stored in the soil column.

Figure 5.14:

The temporal distribution of groundwater recharge from January to December for 2020.

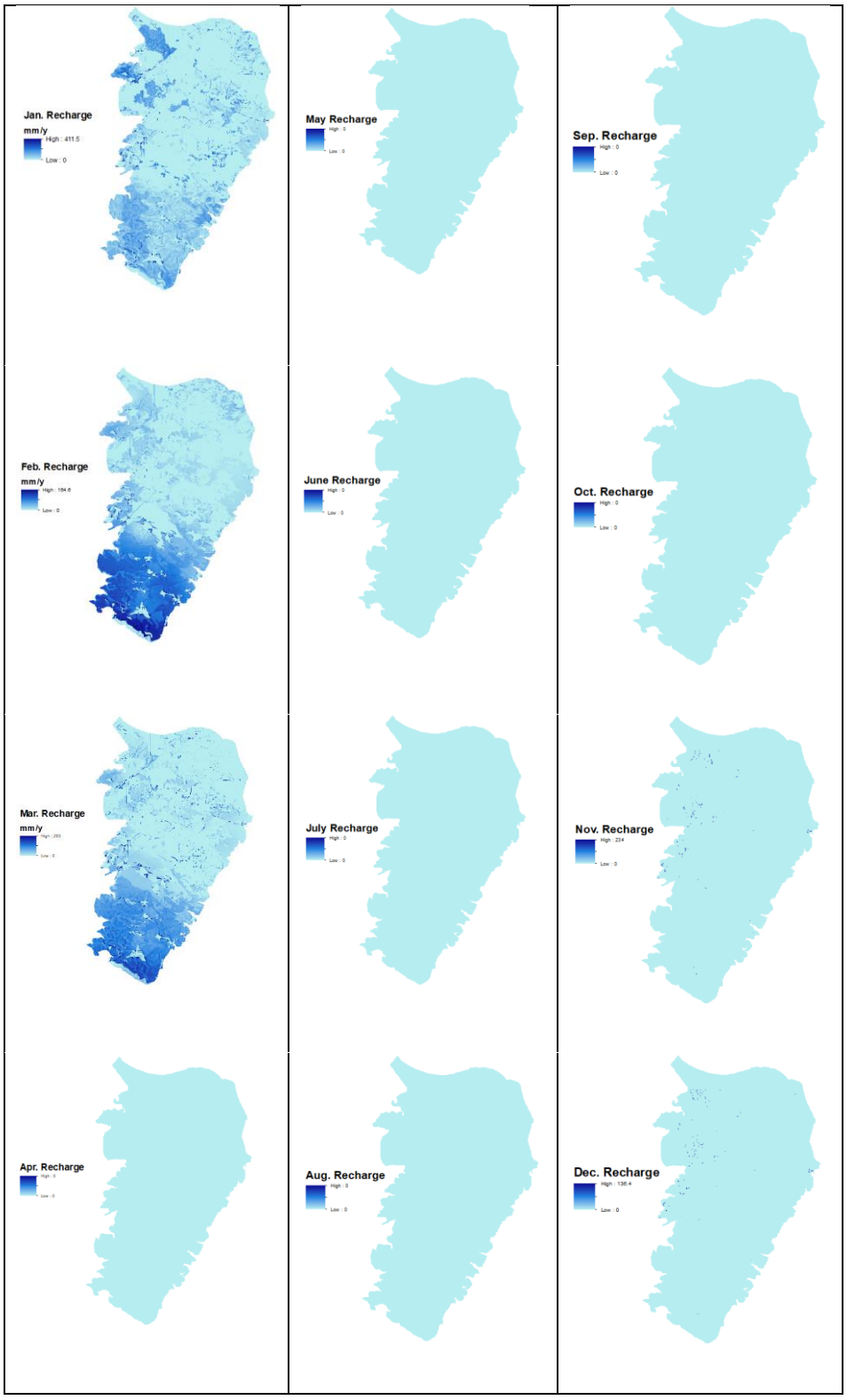

Figure 5.15:

The temporal distribution for rainfall from January to December for 2020.

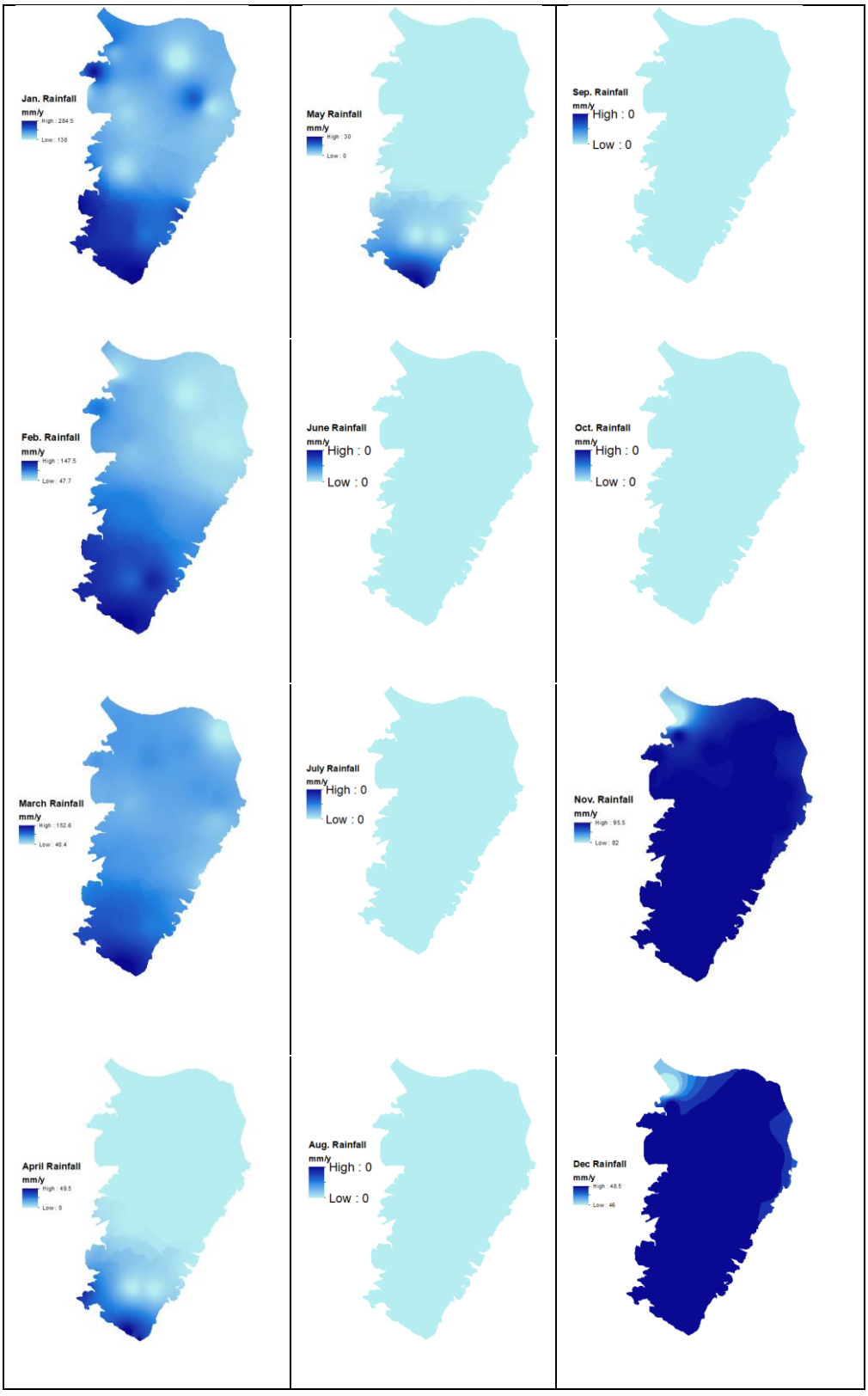

Figure 5.16:

The total monthly rainfall and the total monthly recharge for year 2020 for the Eocene Aquifer.

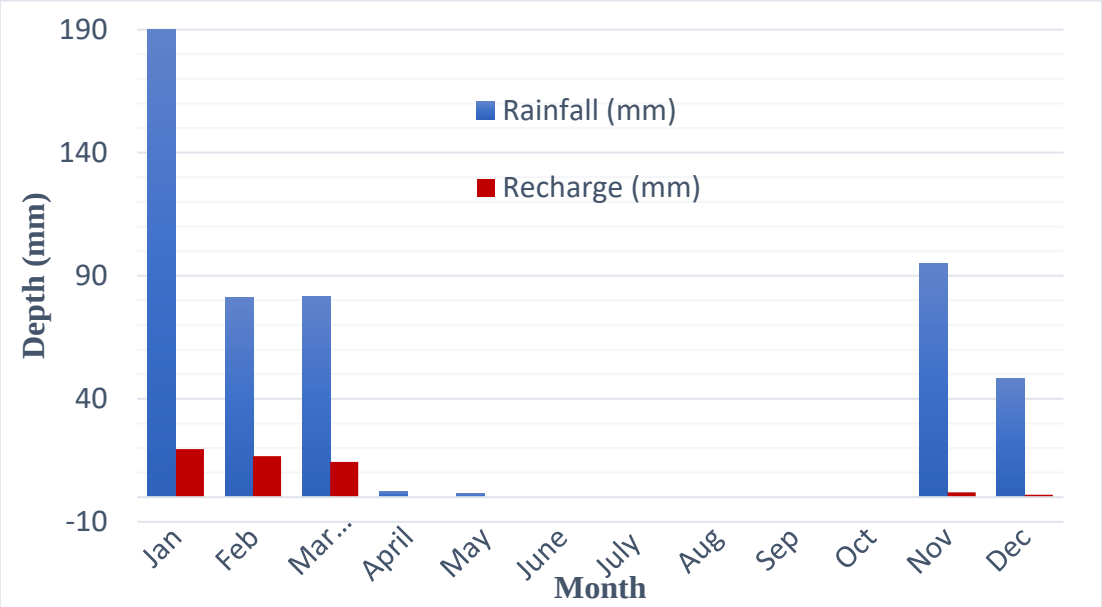

5.5.4 Potential Groundwater Recharge Zones

The Eocene Aquifer was divided into 5 zones based on groundwater recharge rates (see figure 5.18). The aquifer was divided into Very Low, Low, Moderate, High, and Very High zones. This division is based on the amount of recharge, as the result of SWB model showed that the annual recharge rates for these zones ranged from 0 to 40.4 mm for Very Low zone, from 40.4 to 103.3 mm for Low zone, from 103.3 to 170.7 for Moderate zone, from 170.7 to 310 mm for High zone and from 310 to 1145.5 mm for Very High zone.

Figure 5.18:

The groundwater recharge zones.

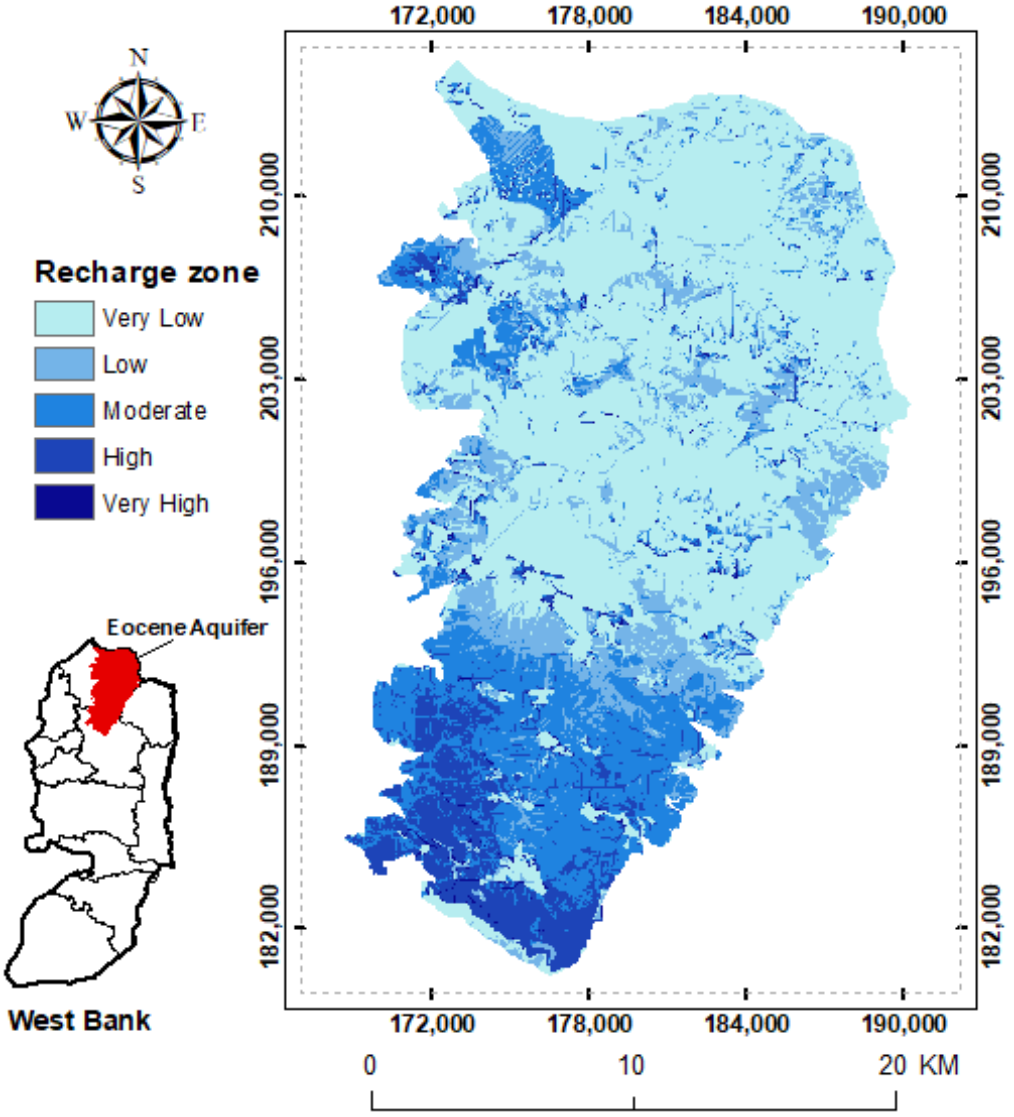

5.5.5 Relationship to Climate

In most cases, preliminary estimates of groundwater recharge are made using rainfall amounts, where recharge is estimated as a percentage of rainfall. The average rainfall for the Eocene Aquifer during the study period was 503.22 mm (19.81 in), while the groundwater recharge rate was equal to 50.70 mm (1.996 in). This showed that the recharge rate was about 10.07% of the rainfall.

Figure 13 in Appendix D, which presents the relationship between recharge and rainfall, shows that there is a correlation with an R^2= 0.70. Equation 5.10 resulted from the relationship between rainfall and recharge for the Eocene Aquifer area.

$$Recharge = (0.56 \times Rainfall) - 200 \quad (5.10)$$

Where;
Recharge is in mm;
Rainfall is in mm.

This equation is similar to the empirical equations used in local studies. This equation takes into account the amounts of rainfall only, while there are many other parameters that have an effect on the amount of recharge. The resulting recharge rate from equation 5.10 for the entire Eocene Aquifer area was about 81.8 mm/year (3.22 in/year) and the total annual recharge amount was about 37.51 MCM. While the groundwater recharge rate based on the SWB model is 50.70 mm/year (1.966 in/year) and the total annual recharge of the entire Eocene Aquifer during the study period is 23.25 MCM. From the previous results of recharge amount, it can be concluded that the amount of recharge does not depend only on rainfall, and it is not permissible to estimate the amount of recharge only based on rainfall, but there are many basic parameters that affect the amount of recharge such as land use types, evapotranspiration, interception, HSG, change in soil moisture, and AWC.

It can be noted from Figure 13 in Appendix D that there are three points whose recharge values are almost zero, with the presence of rainfall values. This indicates that these points are located in impervious areas. Figure 14 in Appendix D shows the relationship between recharge and rainfall when the effect of these three points is neglected. It can be noted that when the effects of the points are neglected, the resulting equation differs and gives higher recharge values for the same study area.

Equation 5.11 resulted from the relationship between rainfall and recharge, with neglected zero recharge points for the Eocene Aquifer area.

$$Recharge = (0.52 \times Rainfall) - 170 \quad (5.11)$$

Where;
Recharge is in mm;
Rainfall is in mm.

The resulting recharge rate from equation 5.11 for the entire Eocene Aquifer area was about 91.67 mm/year (3.61 in/year) and the total annual recharge amount was about 42.04 MCM. Through the results of the equations (5.10 and 5.11), it can be noted that neglecting the effect of recharge values for impervious surfaces causes an increase in the total recharge values. This explains the high recharge values resulting from local studies that depend on empirical equations and that depend only on the amount of rainfall. While the SWB code estimates the amount of recharge based on spatial and temporal distributions, daily rainfall values, change in soil moisture, HSG, AWC, root zone depth, evapotranspiration, and land use types.

5.5.6 Relationship to Land Use

Groundwater recharge depends on land uses in the study area (see table 10 in Appendix E). The top four land use types in terms of area are olive groves, which constitute the largest land use area in the Eocene Aquifer, estimated at about 30.3% of the aquifer area, natural grassland, non-irrigated arable land, and non-irrigated complex cultivation. These types of land use constituted a percentage of the area of the Eocene Aquifer 19, 12.13, and 12%, respectively. The recharge depth for olive groves was about 50.87 mm (2 in), for natural grassland about 116.53 mm (4.59 in), for non-irrigated arable land about 2.46 mm (0.097 in), and for non-irrigated complex cultivation about 4.77 mm (0.187 in) (see figure 15 in Appendix D). As for the top four types in terms of the highest percentage of recharge for land uses, they are natural grassland, olive groves, agricultural land with natural vegetation, and drip irrigated arable (see figure 16 in Appendix D). These types of land use constituted a percentage of the amount of groundwater recharge 43.5, 30.4, 10.2, and 5.8%, respectively. It can be noted that the recharge percentage that resulted from natural grassland is higher than the recharge percentage that resulted from olive groves which have the largest area in the study area, the reason for this is due to the spatial and temporal distribution of rainfall, interception, HSG, and the nature of the topography.

5.5.7 Relationship to Curve Number

The curve number is the most influential parameter on the groundwater recharge value (see figure 5.9). The curve number is an indicator of surface runoff. Curve number values range from 0 to 100, where 0 indicating no surface runoff (pervious surface), and 100 indicating the highest value of surface runoff (impervious surface). The top four curve

number values in terms of area are 78.6, which constitute the largest curve number area in the Eocene Aquifer, estimated at about 30.3% of the aquifer area, 93.53, 80.6, and 95.52 (see figure 5.19). These curve number values constituted a percentage of the area of the Eocene Aquifer 24, 19.12, and 8.21%, respectively. The recharge depth for the CN equals 78.6 was about 50.87 mm (2 in), for the CN value equals 93.53 was about 3.60 mm (0.142 in), for the CN value equals the 80.6 was about 116.11 mm (4.57 in), and for the CN value equals 95.52 was about 2.05 mm (0.08 in). The top four CN values in terms of the highest percentage of recharge are 80.6, 78.6, 79.6, and 88.55. These values of curve number constituted a percentage of the amount of groundwater recharge 43.8, 30.41, 10.17, and 9.48%, respectively. It can be noted that the recharge percentage that resulted from curve number value 80.6 is higher than the recharge percentage that resulted from curve number value 78.6, the reason for this is due to the spatial and temporal distribution of rainfall, interception, and the nature of the topography.

Figure 5.19:

The distribution of curve number values inside the Eocene Aquifer.

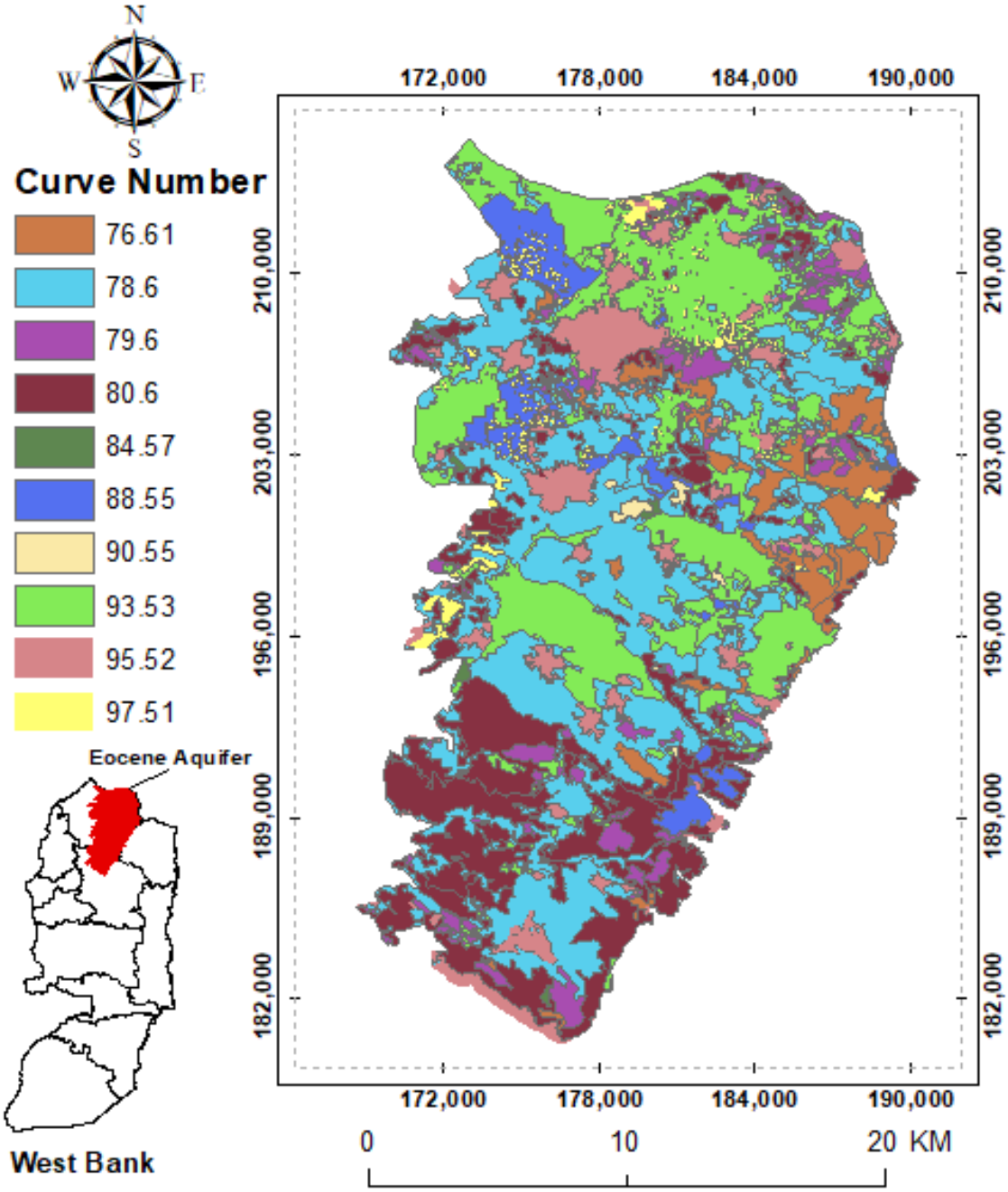

Chapter Six

Conclusions and Recommendations

6.1 Conclusions

The following are the research main conclusions:

1. The process of estimating the amount of groundwater recharge of the Eocene Aquifer is important and essential in order to obtain a good description and understanding of the water budget in the aquifer and to achieve a balance between recharge and total pumping (the management aspect);
2. The SWB code is effective in estimating the spatially and temporally variable recharge quantity;
3. The highest recharge rates occur in the southern and northwestern parts of the Eocene Aquifer. The lowest rates of recharge are distributed in the center and north of the aquifer. The largest annual recharge occurs in Nablus District, estimated at about 12.68 MCM, followed by Jenin District, which is estimated at about 9.23 MCM, while the lowest annual recharge occurs in Tubas District, estimated at about 1.34 MCM. This corresponds to the spatial distribution of rainfall and the land use types in the study area;
4. The results of this study showed that the recharge values for the Eocene Aquifer are completely different from the values obtained from previous local studies for the same study area, which uses empirical equations that depend on the amount of rainfall only.
5. It was apparent from this work that the amount of recharge does not depend only on rainfall. It is totally wrong to estimate the amount of recharge based on rainfall only amount as there are many parameters that affect the amount of recharge such as land use types, evapotranspiration, interception, and HSG;
6. The topographical nature has a noticeable influence on determining the groundwater recharge value. This in turn affects the groundwater level, the increase in the slope leads to an increase in the amount of runoff and a decrease in the amount of infiltration, which leads to a decrease in the amount of recharge;
7. The performance of the SWB model was evaluated after the verification process using RE and goodness of fit (RMSE, AME, and NSE) between the simulated

recharge values generated by SWB model and the observed recharge values resulting from the WTF method. The results showed that the observed and simulated recharge values were very close;

8. Sensitivity analysis is necessary to understand how the recharge is affected by the change in curve number values. The research showed that land use types are highly sensitive to recharge rates when curve number values are adjusted by small variations. Therefore, care must be taken when choosing the values of the curve number values because they have a significant impact on groundwater recharge;
9. The groundwater recharge rate based on the SWB model is 50.7 mm/year (1.966 in/year) and the total annual recharge for the entire Eocene Aquifer during the study period is 23.25 MCM. The recharge rate is about 10.07% of the rainfall;
10. The research showed that the total annual amount of water demand for the communities of the Eocene Aquifer is about 28.29 MCM. The results support the on-going decrease in the groundwater level in the Eocene Aquifer. This is due to the annual water deficit, which was estimated at about 5.04 MCM compared to recharge;

6.2 Recommendations

The following recommendations address future work that can take into consideration the following issues:

1. Simulate how groundwater recharge is affected by the change in rainfall due to climate change since rainfall is the main climatic factor of the recharge process.
2. Increasing the study period for the Eocene Aquifer area to obtain comprehensive and long-term recharge values.
3. Applying the SWB model to all aquifers in Palestine to obtain realistic recharge values in order to maintain the water resources.
4. Develop a groundwater management plan for the area of the Eocene Aquifer based on the results of the SWB model, in order to manage and maintain renewable and sustainable water resources in this aquifer.
5. Develop a contaminant fate and transport model for the area of the Eocene Aquifer in order to assess the quality of groundwater and protect it from pollution.
6. Develop plans and methods to increase the groundwater level in the Eocene Aquifer; in order to save the water situation in the aquifer and to overcome the water deficit.

7. Paying attention to the environmental situation of land use types with highly recharge in the Eocene Aquifer area, which are: natural grassland, olive groves, agricultural land with natural vegetation. These land use types constitute about 84.1% of the recharge rate of the Eocene aquifer area. It is also necessary to place warning and awareness signs in these areas.
8. Increasing interest in groundwater monitoring wells especially in the southern part of the Eocene Aquifer area, by increasing the number of monitoring wells to obtain accurate results for the amount of recharge using the WTF method.
9. Study the groundwater quality in areas that are considered of high recharge. This helps in developing precautionary plans to protect the aquifer from pollution, and to understand the negative impact of the transformation of these areas into residential areas on the water situation in the aquifer.
10. Compare the results of ArcHydro tools with the results of Hydrology Flow tools in the GIS to process data and use the most accurate results.
11. Compare the effect of the change in different interpolation methods on the results of the SWB model and adopt the most reasonable method.

List of Abbreviations

Abbreviation	Meaning
SWB	**Soil Water Balance**
USGS	United State, Geological Survey
PWA	Palestinian Water Authority
PMD	Palestinian Meteorological Department
MoA	Ministry of Agriculture (MoA)
ASCII	American Standard Code for Information Interchange
WTF	Water Table Fluctuation
WDC	Water Demand Calculation
MAPR	Mean Annual Potential Recharge
BFS	Baseflow Separation
BALSEQ	Sequential Water Balance
CRD	Cumulative Rainfall Departure
GWM	Groundwater Management
RMSE	Root Mean Square Error
SMD	Soil Moisture Deficit
GUI	Graphical User Interface
GIS	Geographic Information System
HSG	Hydrological Soil Group
AWC	Available Water Capacity
DEM	Digital Elevation Model
USDA	U.S. Department of Agriculture
NRCS	Natural Resource Conservation Service
MSWC	Maximum Soil Water Capacity
CN	Curve Number
ARC	Antecedent Runoff Condition
ET	Evapotranspiration
PET	Potential Evapotranspiration
AET	Actual Evapotranspiration
ISM	Initial Soil Moisture
APWL	Accumulated Potential Water Loss

FSM	Final Soil Moisture
AMSL	Above Mean Sea Level
MCM	Million Cubic Meters
UNRWA	United Nations Relief and Works Agency
IDW	Inverse Distance Weighting
TIN	Triangular Irregular Networks
SMR	Soil Moisture Retained
SCS	Soil Conservation Service
WTR	Water Table Rise
AME	Absolute Mean Error
NSE	Nash-Sutcliffe Model Efficiency Coefficient
PCBS	Palestinian Central Bureau of Statistics

References

Adane, Z. A., Nasta, P., Zlotnik, V., & Wedin, D. (2018). Impact of grassland conversion to forest on groundwater recharge in the Nebraska Sand Hills. *Journal of Hydrology: Regional Studies, 15*, 171-183.

Adhikari, A. (2020, February 22). *The Rising Nepal*. Retrieved from Groundwater Recharge Begins From Gongabu: https://risingnepaldaily.com/main-news/groundwater-recharge-begins-from-gongabu

Aliewi, A. (2007). *WATER RESOURCES IN PALESTINE*. Ramallah-Palestine: House of Water and Environment. Retrieved from goo.gl/x5dwpT

Almasri, M. N., Judeh, T. G., Shadeed, S. M. (2020). Identification of the Nitrogen Sources in the Eocene Aquifer Area (Palestine). *Water, 12*, 1121.

Anderson, M. P., Woessner, W. W., & Hunt, R. J. (2015). *Applied Groundwater Modeling (Second Edition).*

Applied Research Institute-Jerusalem (ARIJ). (1995). *Environmental Profile for the West Bank.* Jerusalem: Applied Research Institute.

Applied Research Institute-Jerusalem (ARIJ). (1996). Environmental Profile of the West Bank. *Applied Research Institute, Volume 7.*

Applied Research Institute-Jerusalem (ARIJ). (2002). *Atlas of Palestine (West Bank and Gaza) 2nd ed.* Jerusalem, Palestine: Applied Research Institute.

Asbah, S. (2004). *Monthly Recharge Estimation for the Auja-Tamseeh Catchment of the Catchment of the Western Basin Aquifers-System, Palestine.* Birzeit, Palestine: Birzeit University.

Ashaolu, E. D., Olorunfemi, J. F., Ifabiyi, I. P., Abdollahi, K., & Batelaan, O. (2020). Spatial and temporal recharge estimation of the basement complex in Nigeria, West Africa. *Journal of Hydrology: Regional Studies*, *27*, 100658.

Baalousha, H. (2005). *Using CRD Method for quantification of groundwater recharge in the Gaza Strip, Palestine.* Aachen, Germany: Aachen University of Technology (RWTH).

Banks, J., Carson, J., Nicol, D., and Nelson, B. (2010). *Discrete-event System Simulation.* Prentice Hall.

Barua, S., Cartwright, I., Dresel, P. E., & Daly, E. (2021). Using multiple methods to investigate the effects of land-use changes on groundwater recharge in a semi-arid area. *Hydrology and Earth System Sciences, 25*(1), 89-104.

BGS. (2005). *A new Map for the West Bank.* British Geological Survey.

Cambraia Neto, A.J., Rodrigues, L.N. (2020). Evaluation of groundwater recharge estimation methods in a watershed in the Brazilian Savannah. *Environmental Earth Sciences, 79,* 140.

Carson, J. (2002). MODEL VERIFICATION AND VALIDATION. *Proceedings of the 2002 Winter Simulation Conference*, 52-58.

Cherkauer D.S., and Ansari, S.A. (2005). estimating ground water recharge from topography,hydrogeology, and land cover. *Ground Water, 43*(1), 102-112.

Cook, P. G. and Böhlke, J.K. . (2000). Determining timescales for groundwater flow and solute transport In Environmental Tracers in Subsurface Hydrology, ed. P. G. Cook and A. L. *Herczeg. Boston: Kluwer Academic Publishers*, 1–30.

Cronshey, R., McCuen, R., Miller, N., Rawls, W., Robbins, S., and Woodward, D. (1986). *Urban hydrology for small watersheds - TR-55 (2nd ed.).* Washington, D.C: U.S. Department of Agriculture, Soil Conservation Service.

Crosbie, R. S., McCallum, J. L., Walker, G. R., Chiew, F.H.S. (2010). Modelling climate-change impacts on groundwater recharge in the Murray-Darling Basin, Australia. *Hydrogeology Journal, 18*(7), 1639-1656.

Day, E. S. (2019). *Application of the USGS soil-water-balance (SWB) model to estimate spatial and temporal aspects of groundwater recharge in north-central Iowa*. Lowa State: Lowa State University. Retrieved from https://lib.dr.iastate.edu/etd/17664

DE Silva, C. H., & Rushton, K. R. (2007). Groundwater recharge estimation using improved soil moisture balance methodology for a tropical climate with distinct dry seasons. *Hydrological Sciences Journal, 52*(5), 1051-1067. Retrieved from https://www.tandfonline.com/doi/pdf/10.1623/hysj.52.5.1051

Dingman, S.L. (2015). *Physical Hydrology.* S. Lawrence Dingman.

Döll, P.,& Fiedler, K. (2008). Global-scale modeling of groundwater recharge. *Hydrology and Earth System Sciences Discussions, 12*(3), 863-885. Retrieved from https://hal.archives-ouvertes.fr/hal-00305174

Dripps, W., Bradbury, K. (2007). A simple daily soil–water balance model for estimating the spatial and temporal distribution of groundwater recharge in temperate humid areas. *Hydrogeology Journal, 15*, 433-444.

Dripps, W.R. (2003). *The spatial and temporal variability of groundwater recharge within the Trout Lake basin of northern Wisconsin.* Madison, Wis.: University of Wisconsin, Ph.D. dissertation.

Fetter, C.W. (2001). *Applied hydrogeology + Visual Modflow.* Flownet and Aqtesolv student version software on CD-ROM: Prentice Hall, Upper Saddle River.

Freeze, R.A., & Cherry, J.A. (1979). *Groundwater.* New Jerssy: Prentice-Hall, Englewood Cliffs.

Groundwater Foundation. (2005). *Groundwater Foundation*. Retrieved from What is Groundwater?: https://www.groundwater.org/get-informed/basics/whatis.html

Hargreaves, G.H., and Samani, Z.A. (1985). Reference crop evapotranspiration from temperature. *Applied Engineering in Agriculture, 1*(2), 96–99.

Harlow, J., & Hagedorn, B. (2018). SWB Modeling of Groundwater Recharge on Catalina Island, California, during a Period of Severe Drought. *Water*, *11*, 58. Retrieved from https://doi.org/10.3390/w11010058

Hart, D. J., Schoephoester, P. R., & Bradbury, K. R. (2012). *Groundwater Recharge in Dane County, Wisconsin: Estimating Recharge Using a GIS-Based Water-Balance Model.* Dane County, Wisconsin: Wisconsin Geological and Natural History Survey.

Hartmanna, A., Gleeson, T., Wada, Y., & Wagener, T. (2017). Enhanced groundwater recharge rates and altered recharge sensitivity to climate variability through subsurface heterogeneity. *Proceedings of the National Academy of Sciences of the United States of America (PNAS)*, *114*, 2842–2847.

Hatfield, J.L., Jaynes, D.B., Burkhart, M.R., Cambardella, C.A., Moorman,T.B., Prueger, J.H., & Smith, M.A. (1999). Water quality in Walnut Creek watershed: Setting and farming practices. *Journal of Environmental Quality*, *28*, 11-24.

Healy, R.W., and Cook P.G. (2002). Using groundwater levels to estimate recharge. *Hydrogeology Journal*, *10*, 91–109.

Helmke, M.F., Simpkins, W.W., and Horton, R. . (2005). Fracture-controlled nitrate and atrazine transport in four Iowa till units. *journal of environmental*, 227-236.

Hsieh, P. C., & Huang, T. T. (2021). Evaluation of hillslope storage with variable width under temporally varied rainfall recharge. *Hydrology and Earth System Sciences Discussions*, 1-38.

HWE. (2008). *Protecting Trans-boundary Groundwater Sources from Pollution: Research, Training and Guidelines for Palestinian and Israeli Municipalities.* Palestine: House of Water and Environment and Friends of the Earth- Middle East.

Jalota, S. K., Vashisht, B. B., Sharma, S., and Kaur, S. (2018). Chapter 3 - Climate Change Impact on Crop Productivity and Field Water Balance. In *Understanding*

Climate Change Impacts on Crop Productivity and Water Balance (pp. 87-148). Academic Press.

Jemal A. M. (2006). Assessment of artificial groundwater recharge. *MSc thesis, International Institute For Geo-Information Science And Earth Observation Enschede*, The Netherlands.

Jezdimirovic, J., Sencan, G., Hanak, E. (2019). *Groundwater Recharge.* California: The Public Policy Institute of California (PPIC). Retrieved from https://www.ppic.org/wp-content/uploads/groundwater-recharge.pdf

Jhariya, D. C., Kumar, T., Gobinath, M., Diwan, P., & Kishore, N. (2016). Assessment of groundwater potential zone using remote sensing, GIS and multi criteria decision analysis techniques. *Geological Society of India, 88*(4), 481-492.

Josh., J. (2015, Nov 23). *Geography/Natural Vegetation*. Retrieved from Jargran Josh: https://www.jagranjosh.com/general-knowledge/natural-vegetation-1448263595-1

Juaidi, A.,. (2008). GIS-Based Modeling of Groundwater Recharge for The West Bank. *An-Najah National University*.

Jyrkama, M.I. & Sykes, J.F. (2007). The impact of climate change on spatially varying groundwater recharge in the grand river watershed (Ontario). *Journal of Hydrology, 338*(3-4), 237-250.

Kakish, K., and Katimbo, A. (2017). *Evaluation of Groundwater Recharge Potential Using GIS – Case study at the Salmon River Watershed.* Canada: The University of British Columbia (UBC).

KHALAF, J. (2010). Spatial and Temporal Distribution of Groundwater Recharge in the West Bank Using Remote Sensing and GIS Techniques. *Durham theses, Durham University*. Retrieved from http://etheses.dur.ac.uk/442/

Kharmah, R. (2007). Optimal Management of Groundwater Pumping, The Case of the Eocene Aquifer, Palestine. *An-Najah National University*.

Komakech, H.C., & Bont, C.D. (2018). Differentiated Access: Challenges of Equitable and Sustainable Groundwater Exploitation in Tanzania. *Water Alternatives, 11*(3), 623-637.

Kosztra, B., Büttner, B., Hazeu, G., and Arnold, S. (2017). *Updated CLC illustrated nomenclature guidelines.* Austria: European Environment Agency.

Kotchoni, D. O. V., Vouillamoz, J. M., Lawson, F. M. A., Adjomayi, P., Boukari, M., & Taylor, R. G. (2018). Relationships between rainfall and groundwater recharge in seasonally humid Benin: a comparative analysis of long-term hydrographs in sedimentary and crystalline aquifers. *Hydrogeology Journal, 27*(2), 447–457. doi:10.1007/s10040-018-1806-2

Koussis, A. D., Georgopoulou, E., Kotronarou,A., Lalas, D. P., Restrepo,P., Destouni, G., Prieto, C., Rodriguez, J. J., Rodriguez-Mirasol, J., Cordero T., & Gomez-Gotor A. (2010). Cost-efficient management of coastal aquifers via recharge with treated wastewater and desalination of brackish groundwater: general framework. *Hydrological Sciences Journal*, 1217-1233.

Krause, P., Boyle, D.P., and Bäse, F. (2005). Comparison of different efficiency criteria for hydrological model assessement. *Advances in Geosciences 5*, 89-97. doi:https://www.adv-geosci.net/5/89/2005/adgeo-5-89-2005.pdf

Kumar, C. P. (2003). Estimation of Ground Water Recharge Using Soil Moisture Balance Approach. *Soil and Water Conservation, Soil Conservation Society of India, 2*, 53-58.

Lentswe, G.B., & Molwalefhe, L. (2020). Delineation of potential groundwater recharge zones using analytic hierarchy process-guided GIS in the semi-arid Motloutse watershed, eastern Botswana. *Hydrology: Regional Studies, 28*.

Lewis, F.M. and Walker, G.R. . (2002). Assessing the potential for significant and episodic recharge in southwestern Australia using rainfall data. *Hydrogeology Journal, 10*, 229-237.

LIU Y., DE SMEDT F. (2004). WetSpa Extension, A GIS-based Hydrologic Model for Flood Prediction and Watershed Management, latest update (February 2009). *Department of Hydrology and Hydraulic Engineering, Vrije Universiteit Brussel*, 126.

Lorenz, D.L., and Delin, G.N. . (2007). A regression model to estimate regional ground water recharge. *Ground Water, 45*(2), 196–208.

Lwasaki, Y., Nakamura, K., Horino, H., & Kawashima, S. (2014). Assessment of factors influencing groundwater-level change using groundwater flow simulation, considering vertical infiltration from rice-planted and crop-rotated paddy fields in Japan. *Hydrogeology Journal, 22*(8), 1841-1855.

Manna, F., Murray, S., Abbey, D., Martin, P., Cherry, J., & Parker, B. (2019). Spatial and temporal variability of groundwater recharge in a sandstone aquifer in a semiarid region. *Hydrology and Earth System Sciences (HESS), 23*(4), 2187–2205. Retrieved from https://doi.org/10.5194/hess-23-2187-2019

Melati, M. D., Fan, F. M., & Athayde, G. B. (2019). Groundwater recharge study based on hydrological data and hydrological modelling in a South American volcanic aquifer. *Comptes rendus - Geoscience, 351*(6), 441- 450.

Mendoza-Fernández, A. J., Peña-Fernández, A., Molina, L., and Aguilera, P. A. (2021). The Role of Technology in Greenhouse Agriculture: Towards a Sustainable Intensification in Campo de Dalías (Almería, Spain). *Agronomy, 11*(1), 101.

Metropolitan Council. (2014). *Twin Cities Metropolitan Area Regional Groundwater Flow Model, Version 3.0. Prepared by Barr Engineering.* Saint Paul, MN: Metropolitan Council. Retrieved from https://metrocouncil.org/METC/files/59/595b5c07-58f9-40b7-9d82-0475f8279f98.pdf

Meyland, S. J. (2011). Examining safe yield and sustainable yield for groundwater supplies and moving to managed yield as water resource limits become a reality. *WIT Transactions on Ecology and the Environment, 145*, 1743-1754.

Millennium Engineering Group (MEG). (1999). *Physical Setting and Reference Data Eastern and Northeastern Basins.*

Mishra, S.K., and V.P. Singh. (2003). Soil Conservation Service curve number (SCS-CN) methodology. *Kluwer Academic Publishers, Water Science Technology Library*, 536 p.

Mockus, V. (1964). Estimation of direct runoff from storm rainfall. In *chap. 10 of National engineering handbook, section 4, hydrology* (p. 30). U.S. Department of Agriculture. Soil Conservation Service.

Nash, J.E., and Sutcliffe, I.V. (1970). River flow forecasting through conceptual models, Part 1-A discussion of principles. *Jour. of Hydrology, 10*(3), 282-290.

Owor M., Taylor R.G., Tindimugaya C., & Mwesigwa D. (2009). Rainfall intensity and groundwater recharge: empirical evidence from the Upper Nile Basin. *Environmental Research Letters, 4*, 1748-1754.

Palestinian Water Authority (PWA). (2001b). *Data Review on the West Bank Aquifers. Working Report SUSMAQ-MOD # 02 V2.0. Sustainable Management of the West Bank and Gaza Aquifers.* Ramallah: Water Resources and Planning Department. Palestinian Water Authority.

Palestinian Water Authority (PWA). (2018). *Water Authority Strategic Plan.* Ramallah: Palestinian Water Authority.

Parsons, R. F. and Cameron, D. G. (1974). Maximum Plant Species Diversity in Terrestrial Communities. *The Association for Tropical Biology and Conservation, 6*(3), 202. doi:10.2307/2989653

Phillips, F., J. Mattick, T. Duval, D. Elmore, and Kubik, P. (1988). Chlorine 36 and tritium from nuclear weapons fallout as tracers for long-term liquid and vapor movement in desert soils. *Water Resources Research, 24*(11), 1877-1891.

Poudel, E. M. K. (2020, October 6). *Water Demand | Types Of Water Demand | Factors Affecting Water Demand*. Retrieved from Dream Civil: https://dreamcivil.com/types-of-water-

demand/?fbclid=Iwar14jdlmndwufnjzy9aap4xidgrmgwhaliy7b9Ymqf8g1SzGNDBkDMIfPi8

Rukundo, R., & Doˇgan, A. (2019). Dominant Influencing Factors of Groundwater Recharge Spatial Patterns in Ergene River Catchment, Turkey. *Water, 11*, 653.

Rumiani, M., Hamhehzarghani, H., Karegar, A., & Ghaderi, R. (2021). Optimization of citrus tree sampling pattern for estimating population of citrus nematode in the soil of infested orchards in Fars province, southern Iran. *Crop Protection*, 142.

Salim, N., & Wildi, W. (2003). *Water cycle, recharge estimation and its complexityin a semi-arid region, case study (West Bank –Palestine).* F.-A. Forel,Section of Earth Sciences, CH-1290. Versoix, Switzerland: University of Geneva.

Scanlon, B. R., Healy, R. W., Cook, P. G. (2002). Choosing appropriate techniques for quantifying groundwater recharge. *Hydrogeology Journal, 10*, 18–39.

Schicht, R.J., and Walton, W.C. . (1961). Hydrologic budgets for three small watersheds in Illinois. *State Water Survey Rep. Invest*, 40: 40.

Sharma, M. L. (1986). Measurement And Prediction Of Natural Groundwater Recharge — An Overview. *Journal of Hydrology (New Zealand), 25*(1), 49-56. Retrieved November 6, 2020, from http://www.jstor.org/stable/43944572

Shrestha, S., Pandey, V. P., Thatikonda, S., and Shivakoti, B. R. (2016). *Groundwater Environment in Asian Cities.* Elsevier Gezondheidszorg.

Simmers, I. (1990). Aridity, groundwater recharge and water resources management. *Verlag Heinz Heise, Hanover*.

Singh, S.K., Zeddies, M., Shankar, U., & Griffiths, G.A. (2018). Potential groundwater recharge zones within New Zealand. *Geoscience Frontiers, 10*(3), 1065-1072.

Smith, E. A., & Westenbroek, S. M. (2015). *Potential Groundwater Recharge for the State of Minnesota Using the Soil-Water-Balance Model, 1996–2010.* U.S. Geological Survey Scientific Investigations. Retrieved from http://dx.doi.org/10.3133/sir20155038

Smith, E.A., and Westenbroek, S.M. (2015). *Potential groundwater recharge for the State of Minnesota using the Soil-Water-Balance model, 1996–2010.* Virginia: U.S. Geological Survey Scientific Investigations Report 2015–5038. doi:http://dx.doi.org/10.3133/sir20155038

Song, W., Jiao, J., Du, P., & Liu, H. (2021). Optimizing the soil conservation service curve number model by accounting for rainfall characteristics: a case study of surface water sources in Beijing. *Environmental Monitoring and Assessment, 193*(3), 1-17.

SUSMAQ. (2004). *Conceptual, Steady-State and Transient-State Models of the Eocene Aquifer in the North-eastern Aquifer Basin.* Ramallah: Palestinian Water Authority.

Thapa, R., Gupta, S., Guin, S., & Kaur, H. (2017). Assessment of groundwater potential zones using multi-influencing factor (MIF) and GIS: a case study from Birbhum district, West Bengal. *Applied Water Science, 7*, 4117-4131.

The European Environment Agency (EEA). (1999). *Environment in the European Union at the turn of the century.* Environmental assessment report No 2.

The United States Department of Agriculture (USDA)-Natural Resources Conservation Service (NRCS). (2004). *Hydrologic Soil-Cover Complexes (SCS).* U.S: The United States Department of Agriculture (USDA).

The United States Department of Agriculture (USDA)-Natural Resources Conservation Service. (1986). *Urban Hydrology for Small Watersheds TR-55.* U.S: The United States Department of Agriculture (USDA).

Thornthwaite, C.W. (1948). An approach toward a rational classification of climate. *Geographical Review, 38,* 55-94.

Thornthwaite, C.W. and J.R. Mather. (1957). Instructions and tables for computing potential evapotranspiration and the water balance. *Centerton, New Jersey, Laboratory of Climatology, 10*(3), 185–311.

Tubeileh, H., Shaheen, H., & Aliewi, A. (2006). Modeling the Eocene Aquifer in Northern West Bank. *An-Najah University Journal for Research - A (Natural Sciences), 20*, 42-62.

U.S. Geological Survey (USGS). (2017, Jan 3). *Water-Table Fluctuation (WTF) Method*. Retrieved from U.S. Geological Survey (USGS): https://water.usgs.gov/ogw/gwrp/methods/wtf/estimating_graphical.html

UNEP. (2003). *Desk Study on the Environment in the Occupied Palestinian Territories.* United Nations Environment Programme (UNEP): Nairobi, Kenya.

University of Minnesota Extension. (2018). *University of Minnesota Extensionhttps://extension.umn.edu/soil-management-and-health/soil-compaction*. Retrieved from Soil compaction: https://extension.umn.edu/soil-management-and-health/soil-compaction

UNRWA. (2019). *UNRWA Annual Operational report 2019 for the Reporting period 01 January – 31 December 2019.* Palestine, Jerusalem: United Nations Relief and Works Agency (UNRWA).

USDA. (2011). *Soil Infiltration.* United States Department of Agriculture. Retrieved from https://www.nrcs.usda.gov/Internet/FSE_DOCUMENTS/nrcs142p2_053268.pdf

USGS. (2010, October 29). *Earthquake Glossary*. Retrieved from US Geological Survey: https://earthquake.usgs.gov/learn/glossary/?term=lithology

USGS. (2016). *Soil-Water-Balance (SWB) for estimating groundwater recharge.* U.S: U.S. Geological Survey.

USGS. (2018, October 9). *Aquifers and Groundwater*. Retrieved from Water Science School:https://www.usgs.gov/special-topic/water-science-school/science/aquifers-and-groundwater

USGS. (2019, April 2). *Infiltration and the Water Cycle*. Retrieved from Water Science School:https://www.usgs.gov/special-topic/water-science-

school/science/infiltration-and-water-cycle?qt-science_center_objects=0#qt-science_center_objects

Vandas S. J., Winter, T. C., & Battaglin, W. A. (2002). *Water and the Environment.* The American Geosciences Institute (AGI).

Westenbroek, S.M., Kelson, V.A., Dripps, W.R., Hunt, R.J., Bardbury, K.R. (2010). *SWB - A Modified Thornwaite-Mather Soil-Water-Balance Code for Estimating Groundwater Recharge.* U.S. Geological Survey Techniques and Methods 6-A31.

Woodward, D.E., Hawkins, R.H., Jiang, R., Hjelmfelt, A.T., Mullem, J.A., and Quan, Q.D. (2003). *Runoff curve number method Examination of the initial abstraction ratio.* Philadelphia: American Society of Civil Engineers: World Water and Environmental Resources Congress 2003, Conference Proceedings Paper, June 24–26.

Woodward, D.E., Hawkins. R.H., Hjelmfelt, A.T., Jr., Van Mullem, J.A., and Quan, Q.D. (2002). *Curve number method-Origins, applications and limitations.* U.S. Department of Agriculture. Natural Resources Conservation Service, Hydraulics and Hydrology Technical Reference. Retrieved from https://www.nrcs.usda.gov/wps/portal/nrcs/main/national/water/quality/

Xiang, W., Evaristo, J., & Li, Z. (2020). Recharge mechanisms of deep soil water revealed by water isotopes in deep loess deposits. *Geoderma, 369*, 114321.

Xu, Y., Beekman, H.E. (2003). Groundwater estimation in Southern Africa. *UNESCO ISHP*, 64.

Yang, J. L., & Zhang, G. L. (2011). Water infiltration in urban soils and its effects on the quantity and quality of runoff. *Journal of Soils and Sediments, 11*(5), 751-761.

Yeh, H. F., Cheng, Y. S., & Lee, C. H. (2016). Mapping groundwater recharge potential zone using a GIS approach in Hualian River, Taiwan. *Sustainable Environment Research, 26*(1), 33-43.

Yenehun, A., Walraevens, K., Batelaan, O. (2017). Spatial and temporal variability of groundwater recharge in Geba basin, Northern Ethiopia. *Journal of African Earth Sciences, 134*, 198-212.

Ziolkowska, J. R., Peterson, J. M. (2017). *Competition for Water Resources.* US and Europe: ELSEVIER.

Appendices

Appendix A. Swb Inputs

Figure A.1

Example of ASCII file for daily precipitation (in).

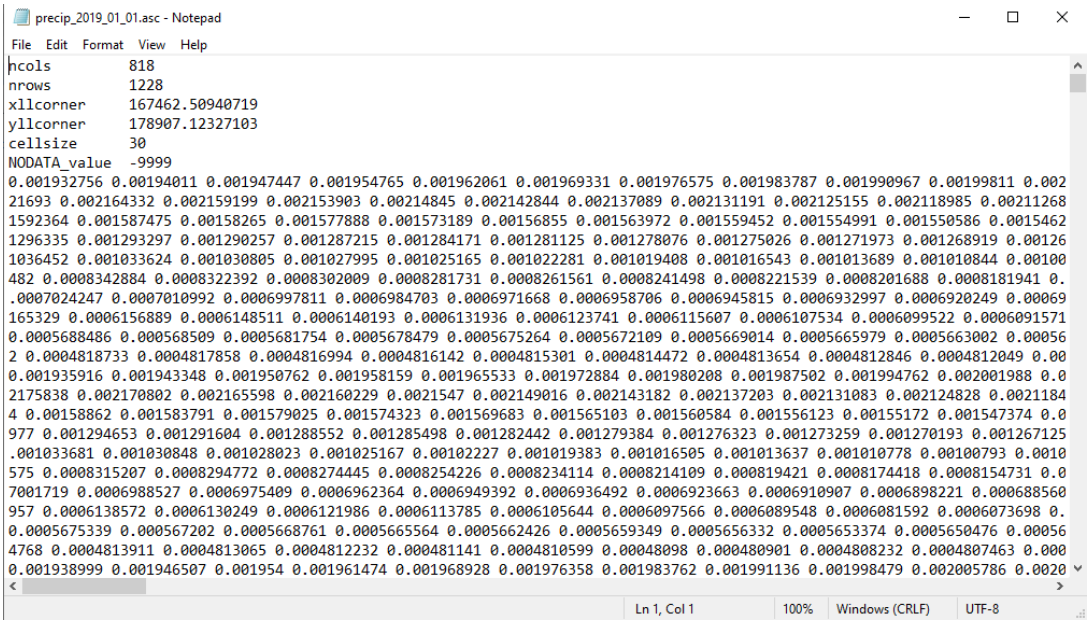

Figure A.2

Example of ASCII file for daily minimum temperature (°F).

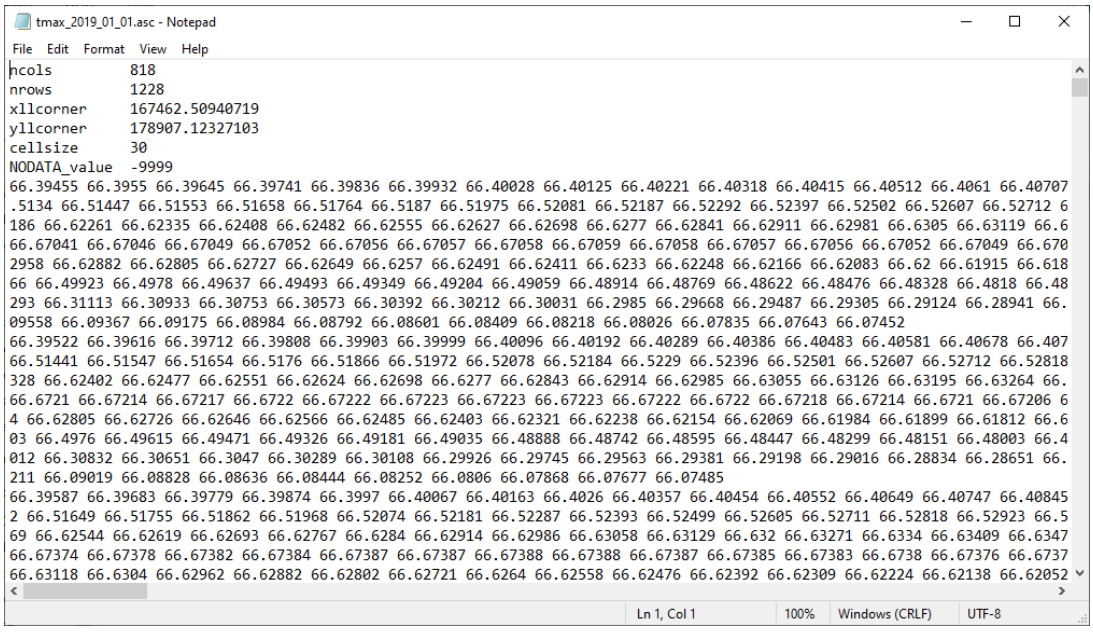

Figure A.3

Example of ASCII file for daily maximum temperature (°F).

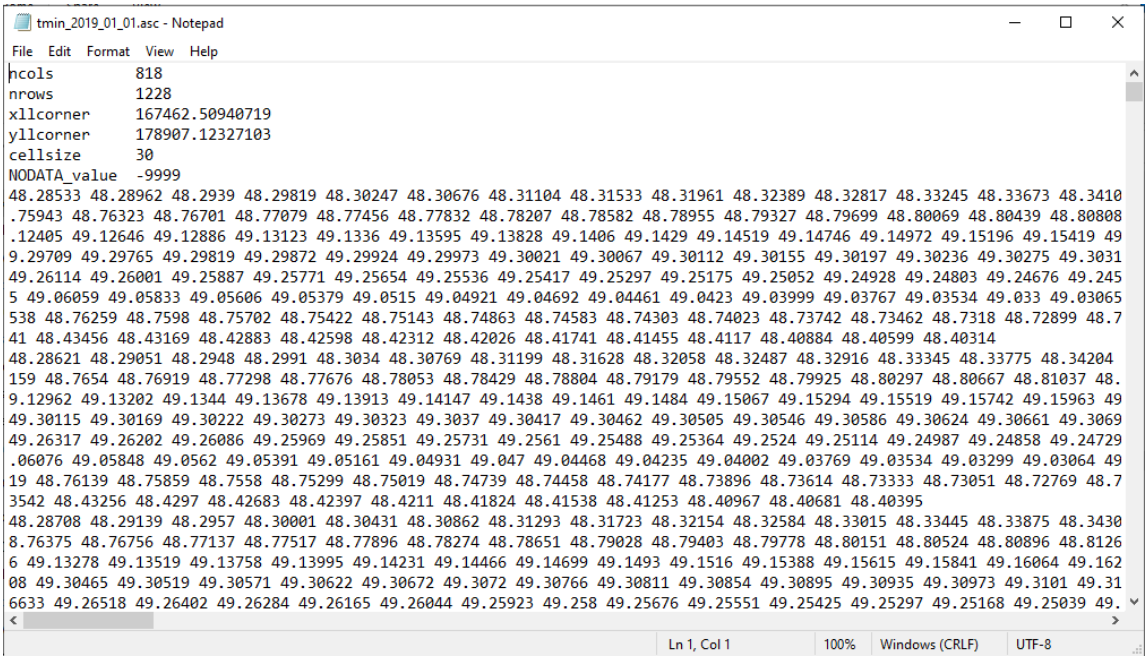

Figure A.4

The daily mean temperature for 2020 for the study area.

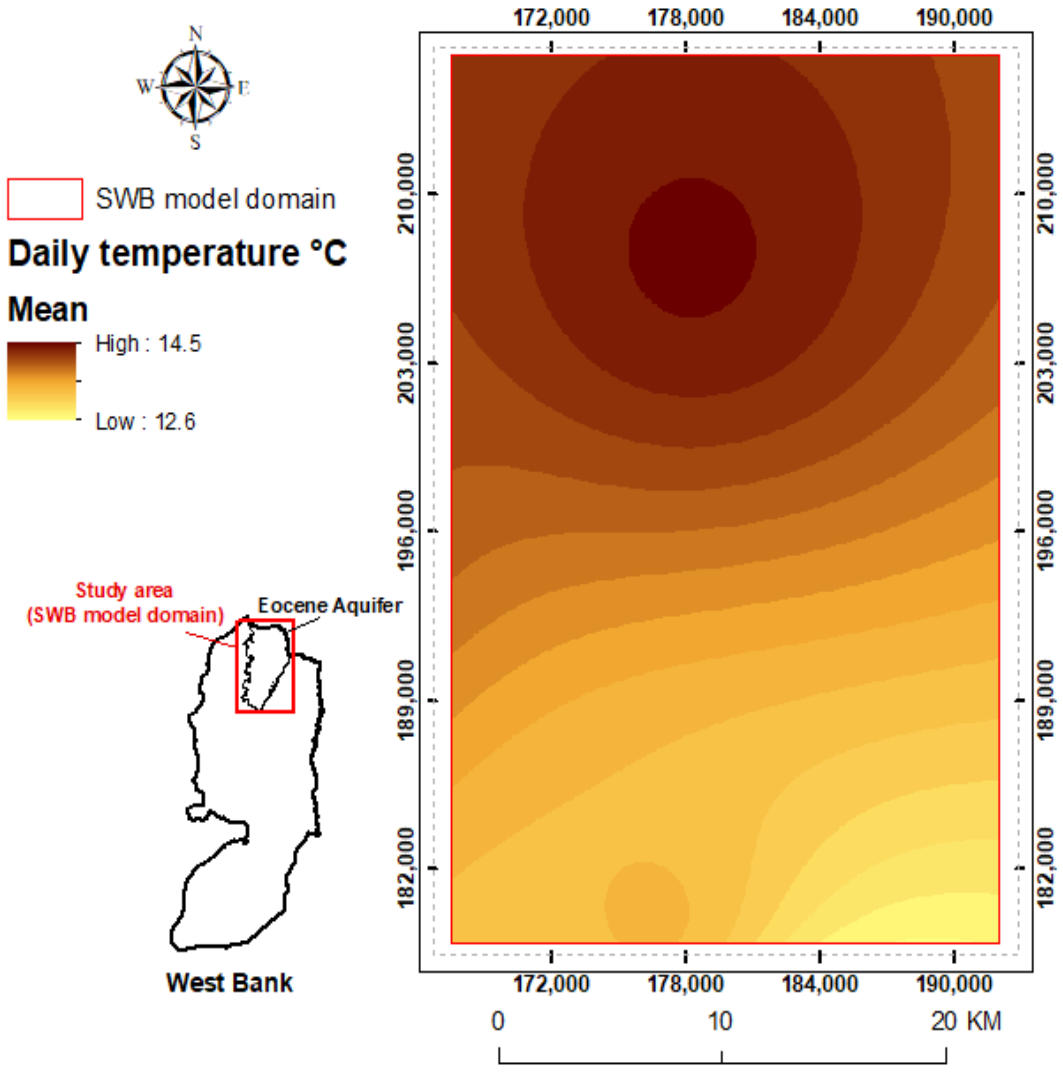

Figure A.5

The annual mean precipitation for 2020 for the study area.

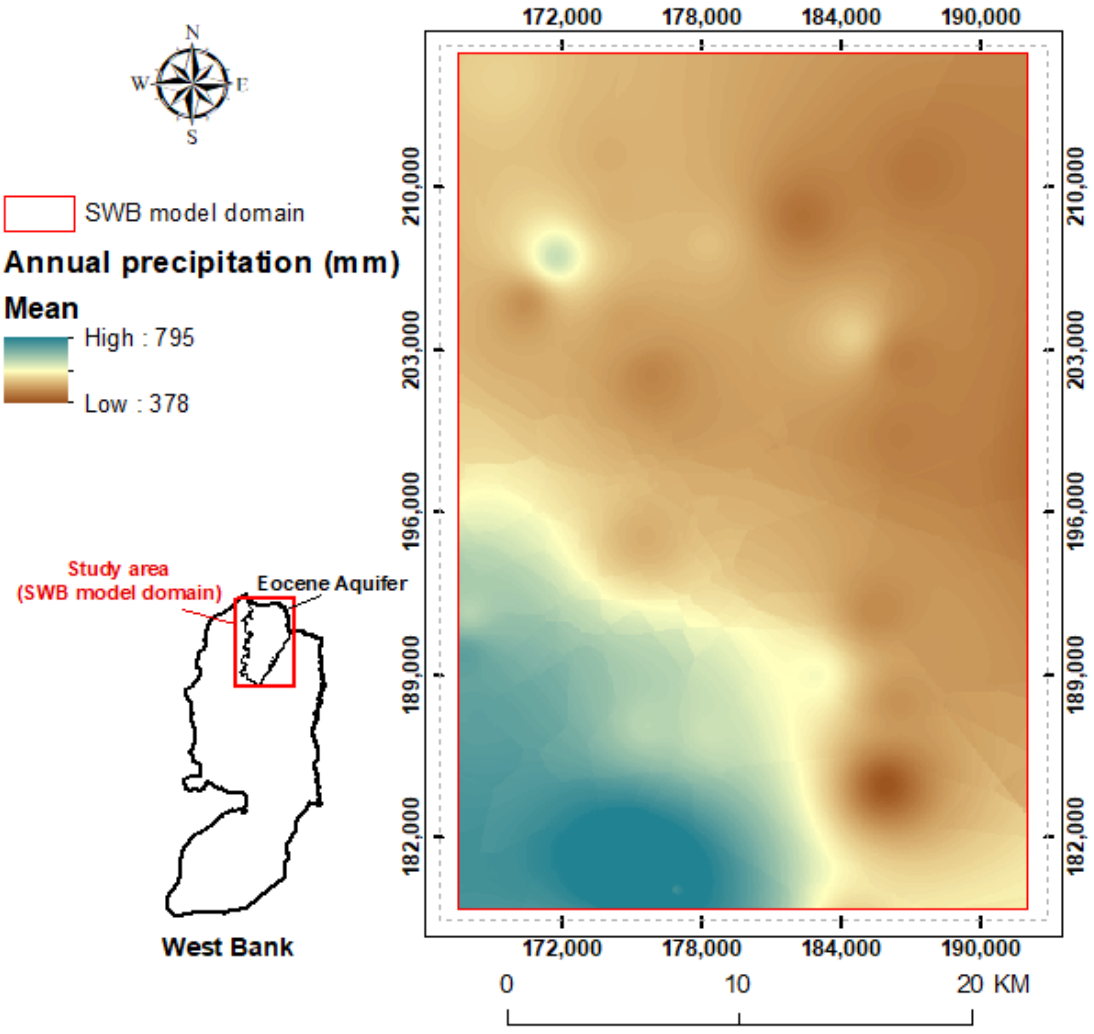

Figure A.6

Hydrological soil group for the study area.

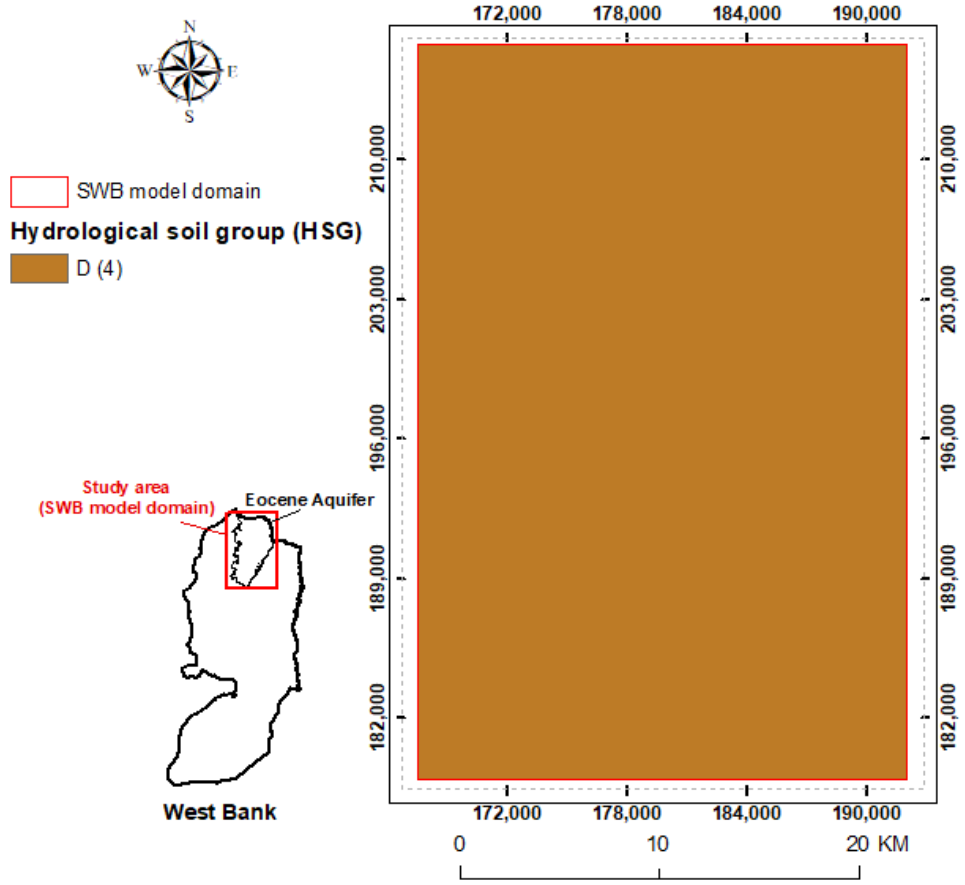

Figure A.7

The ASCII file for the hydrological soil group of the study area.

Figure A.8

Available water capacity for the soil of the study area.

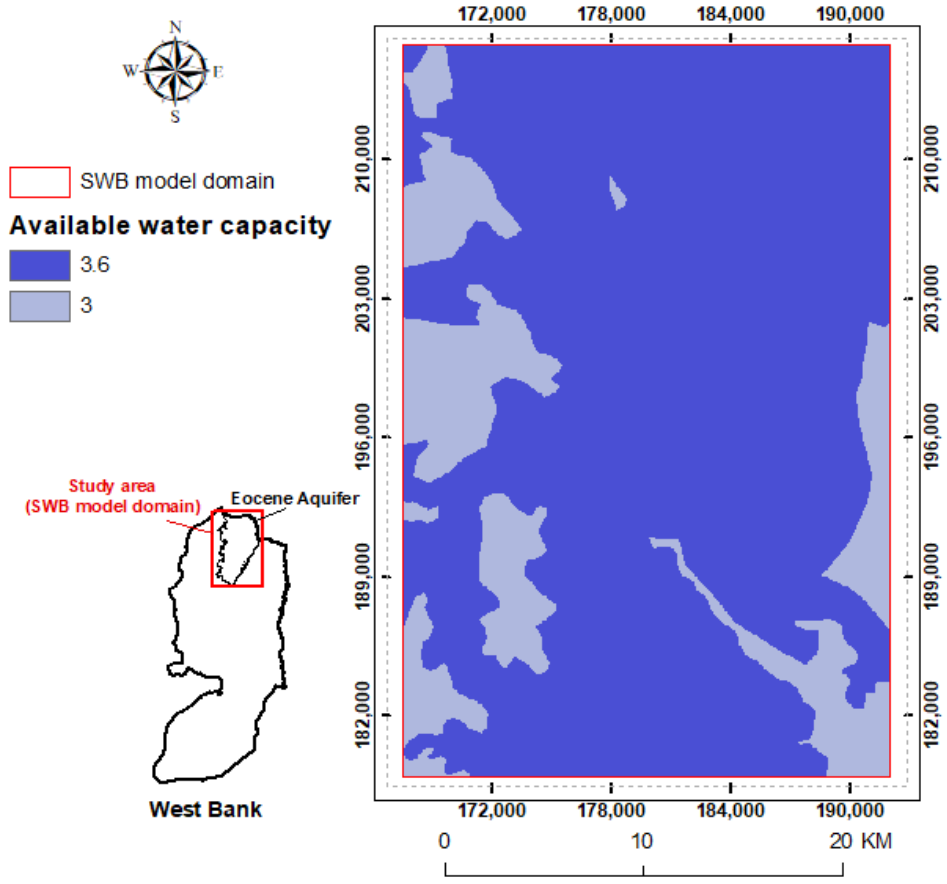

Figure A.9

The ASCII file for the soil available water capacity for the study area.

Figure A.10

Land use classification for the study area.

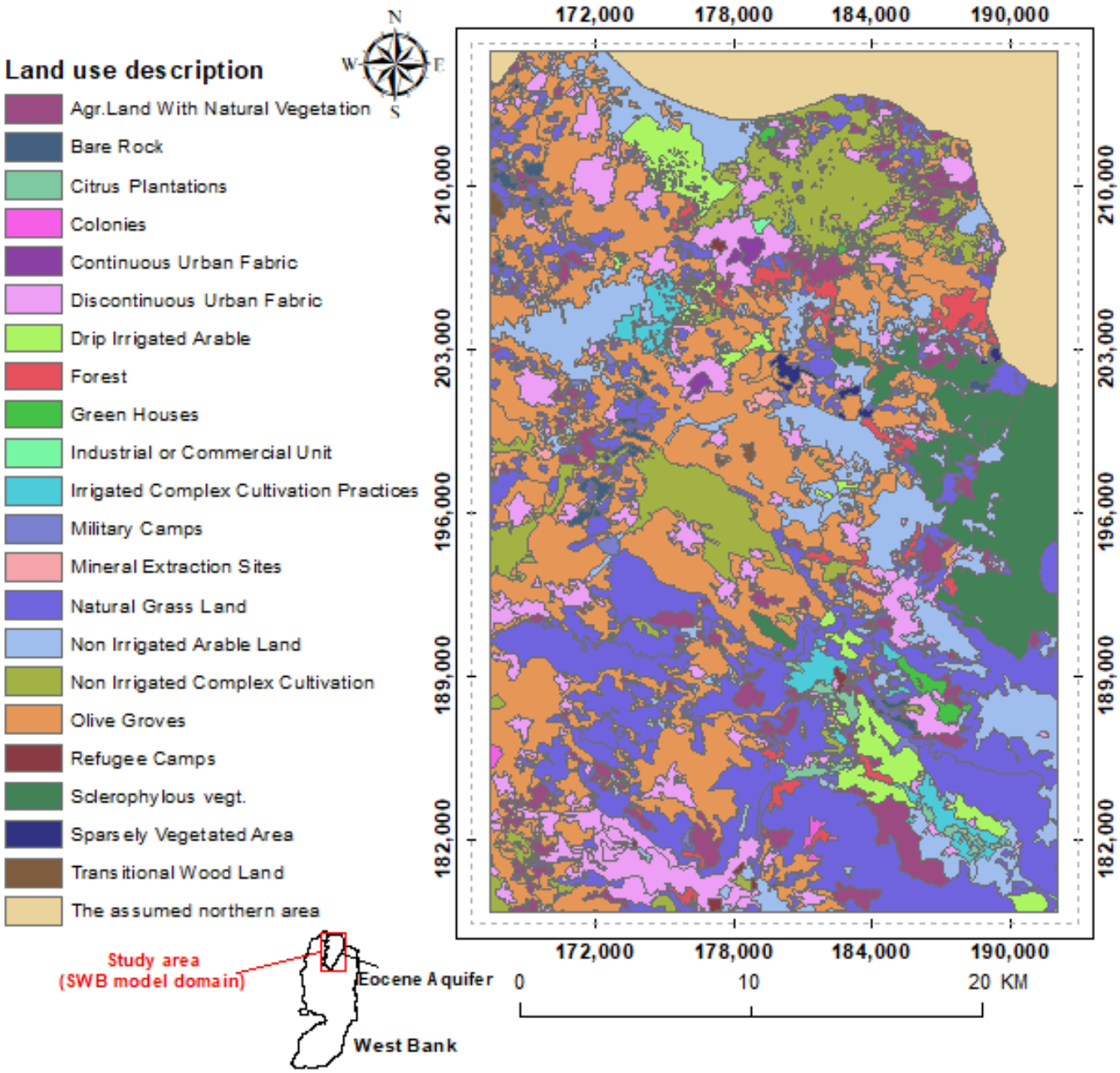

Figure A.11

The ASCII file for the land use codes for the study area.

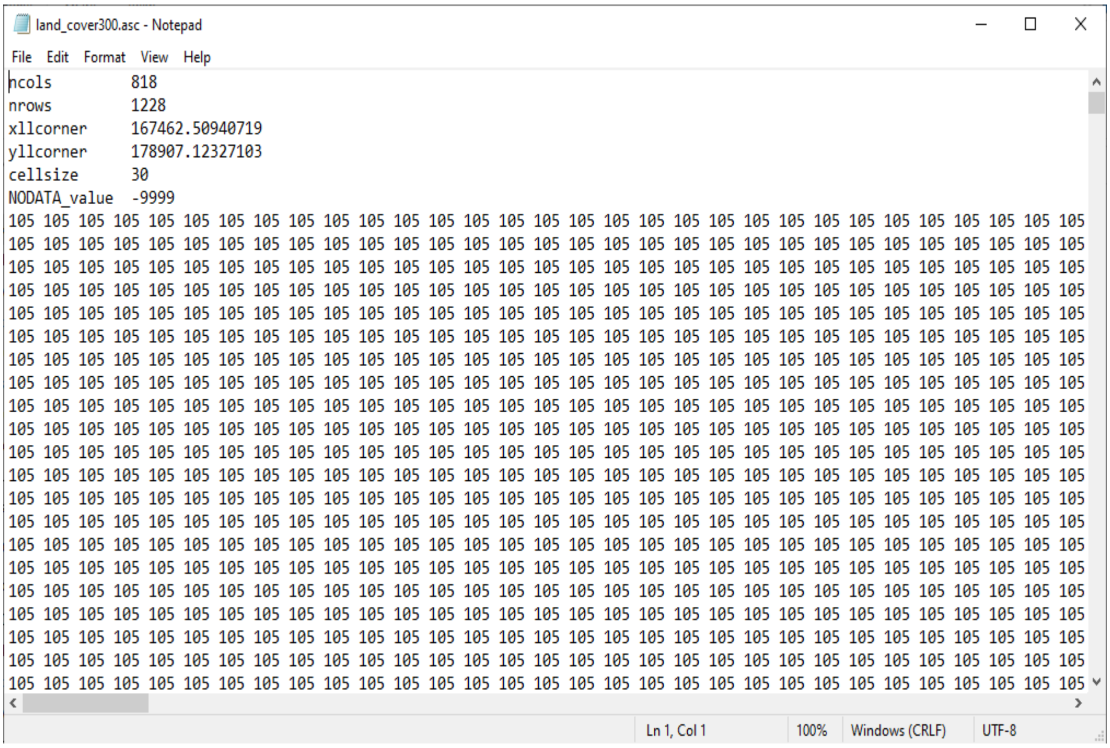

```
ncols         818
nrows         1228
xllcorner     167462.50940719
yllcorner     178907.12327103
cellsize      30
NODATA_value  -9999
105 105 105 105 105 105 105 105 105 105 105 105 105 105 105 105 105 105 105 105 105 105 105 105 105 105 105 105 105 105 105
105 105 105 105 105 105 105 105 105 105 105 105 105 105 105 105 105 105 105 105 105 105 105 105 105 105 105 105 105 105 105
105 105 105 105 105 105 105 105 105 105 105 105 105 105 105 105 105 105 105 105 105 105 105 105 105 105 105 105 105 105 105
105 105 105 105 105 105 105 105 105 105 105 105 105 105 105 105 105 105 105 105 105 105 105 105 105 105 105 105 105 105 105
105 105 105 105 105 105 105 105 105 105 105 105 105 105 105 105 105 105 105 105 105 105 105 105 105 105 105 105 105 105 105
105 105 105 105 105 105 105 105 105 105 105 105 105 105 105 105 105 105 105 105 105 105 105 105 105 105 105 105 105 105 105
105 105 105 105 105 105 105 105 105 105 105 105 105 105 105 105 105 105 105 105 105 105 105 105 105 105 105 105 105 105 105
105 105 105 105 105 105 105 105 105 105 105 105 105 105 105 105 105 105 105 105 105 105 105 105 105 105 105 105 105 105 105
105 105 105 105 105 105 105 105 105 105 105 105 105 105 105 105 105 105 105 105 105 105 105 105 105 105 105 105 105 105 105
105 105 105 105 105 105 105 105 105 105 105 105 105 105 105 105 105 105 105 105 105 105 105 105 105 105 105 105 105 105 105
105 105 105 105 105 105 105 105 105 105 105 105 105 105 105 105 105 105 105 105 105 105 105 105 105 105 105 105 105 105 105
105 105 105 105 105 105 105 105 105 105 105 105 105 105 105 105 105 105 105 105 105 105 105 105 105 105 105 105 105 105 105
105 105 105 105 105 105 105 105 105 105 105 105 105 105 105 105 105 105 105 105 105 105 105 105 105 105 105 105 105 105 105
105 105 105 105 105 105 105 105 105 105 105 105 105 105 105 105 105 105 105 105 105 105 105 105 105 105 105 105 105 105 105
105 105 105 105 105 105 105 105 105 105 105 105 105 105 105 105 105 105 105 105 105 105 105 105 105 105 105 105 105 105 105
105 105 105 105 105 105 105 105 105 105 105 105 105 105 105 105 105 105 105 105 105 105 105 105 105 105 105 105 105 105 105
105 105 105 105 105 105 105 105 105 105 105 105 105 105 105 105 105 105 105 105 105 105 105 105 105 105 105 105 105 105 105
105 105 105 105 105 105 105 105 105 105 105 105 105 105 105 105 105 105 105 105 105 105 105 105 105 105 105 105 105 105 105
105 105 105 105 105 105 105 105 105 105 105 105 105 105 105 105 105 105 105 105 105 105 105 105 105 105 105 105 105 105 105
105 105 105 105 105 105 105 105 105 105 105 105 105 105 105 105 105 105 105 105 105 105 105 105 105 105 105 105 105 105 105
105 105 105 105 105 105 105 105 105 105 105 105 105 105 105 105 105 105 105 105 105 105 105 105 105 105 105 105 105 105 105
```

Figure A.12

The TIN for the study area.

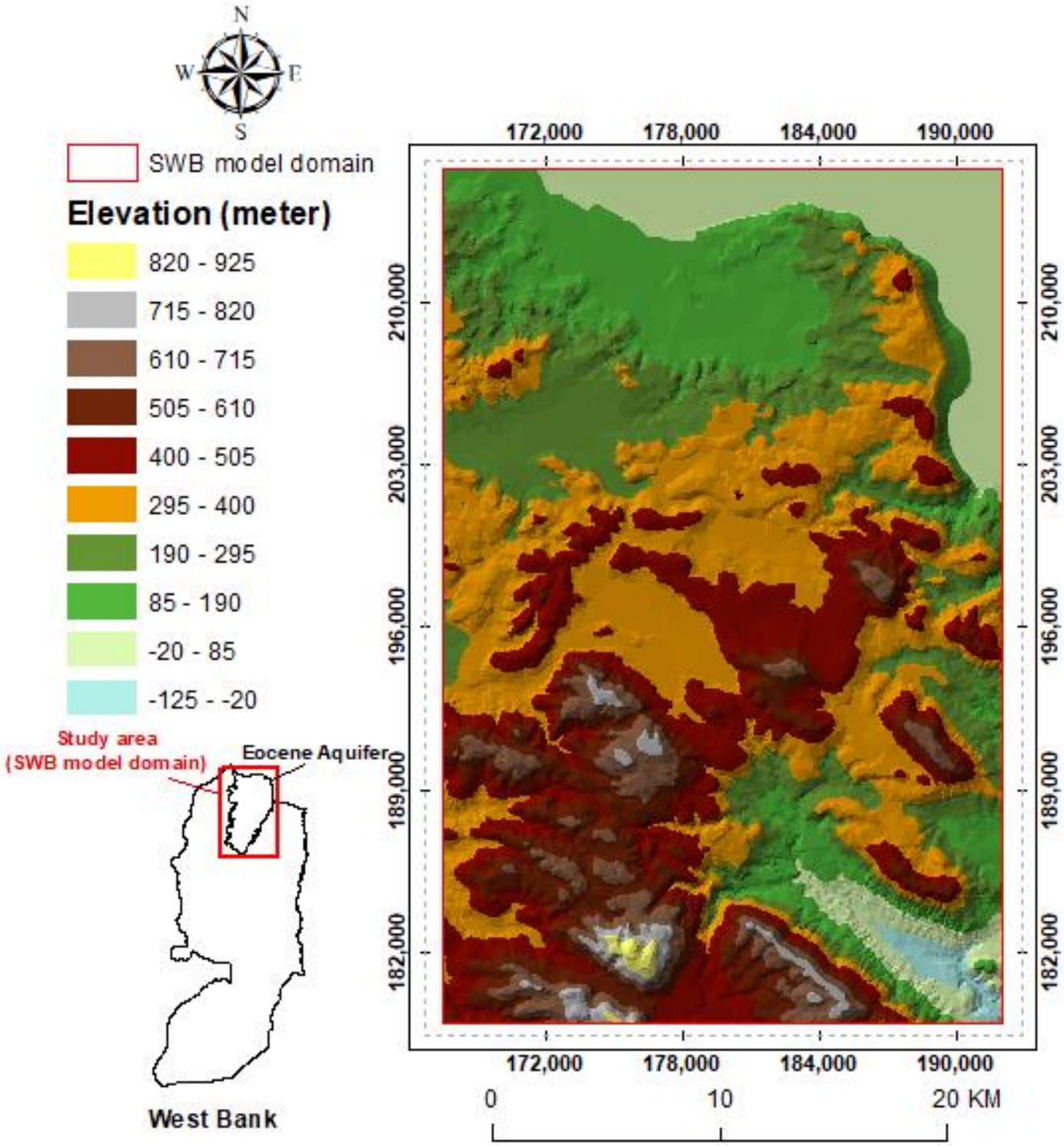

Figure A.13

The DEM for the study area.

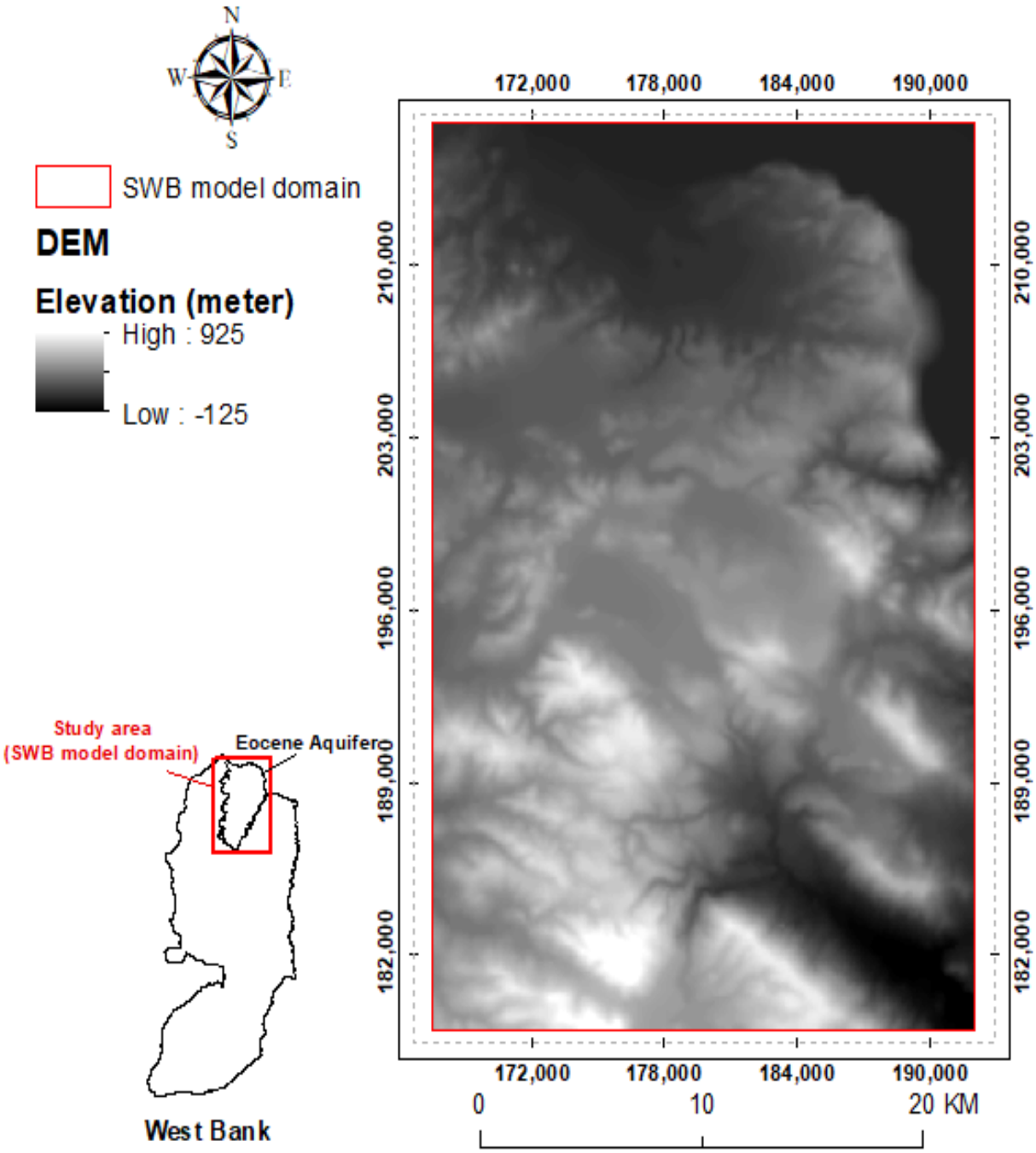

Figure A.14

The flow direction grid for the study area.

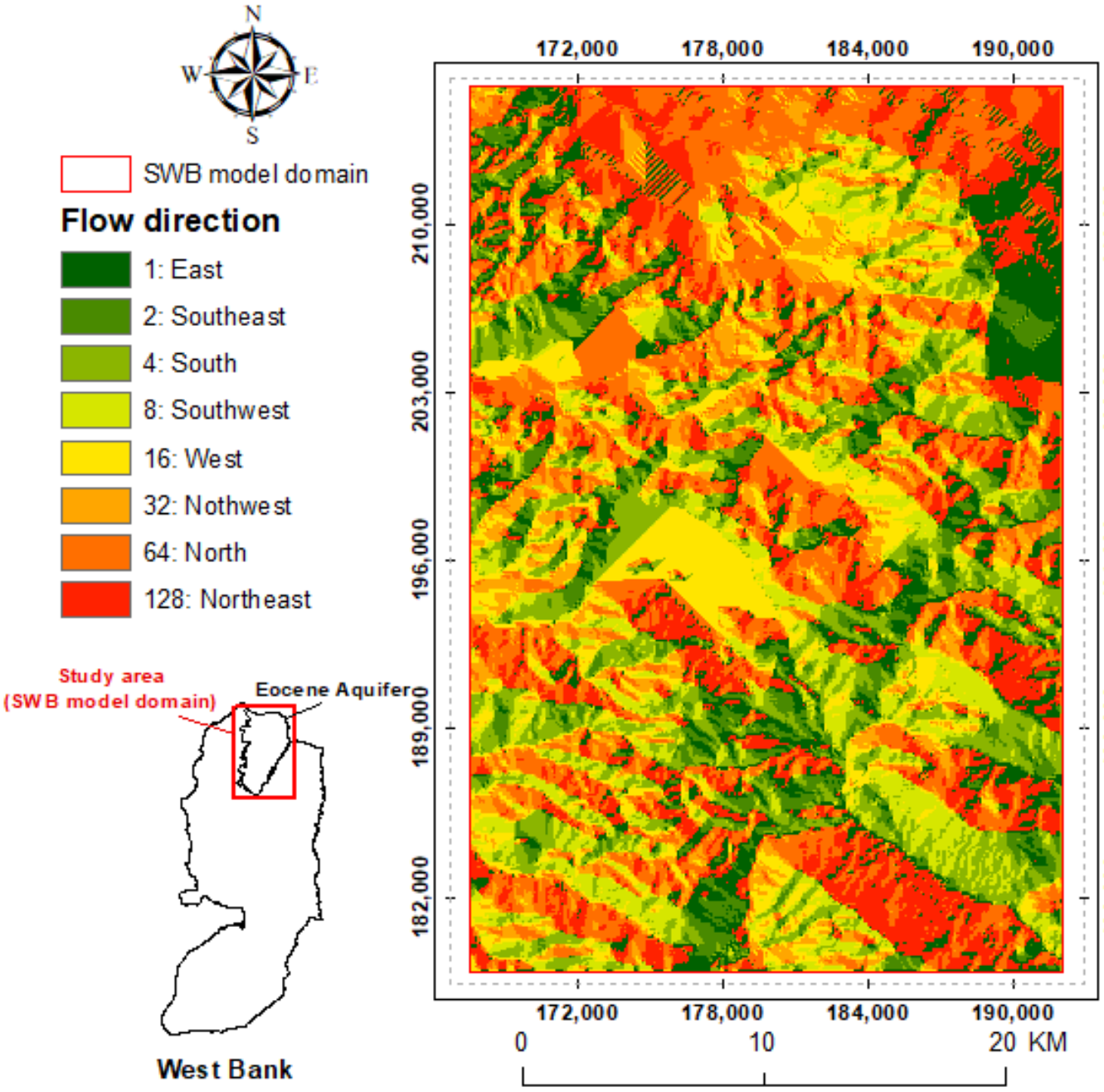

Figure A.15

The ASCII file of the flow direction for the study area.

Figure A.16

The soil moisture retention curve.

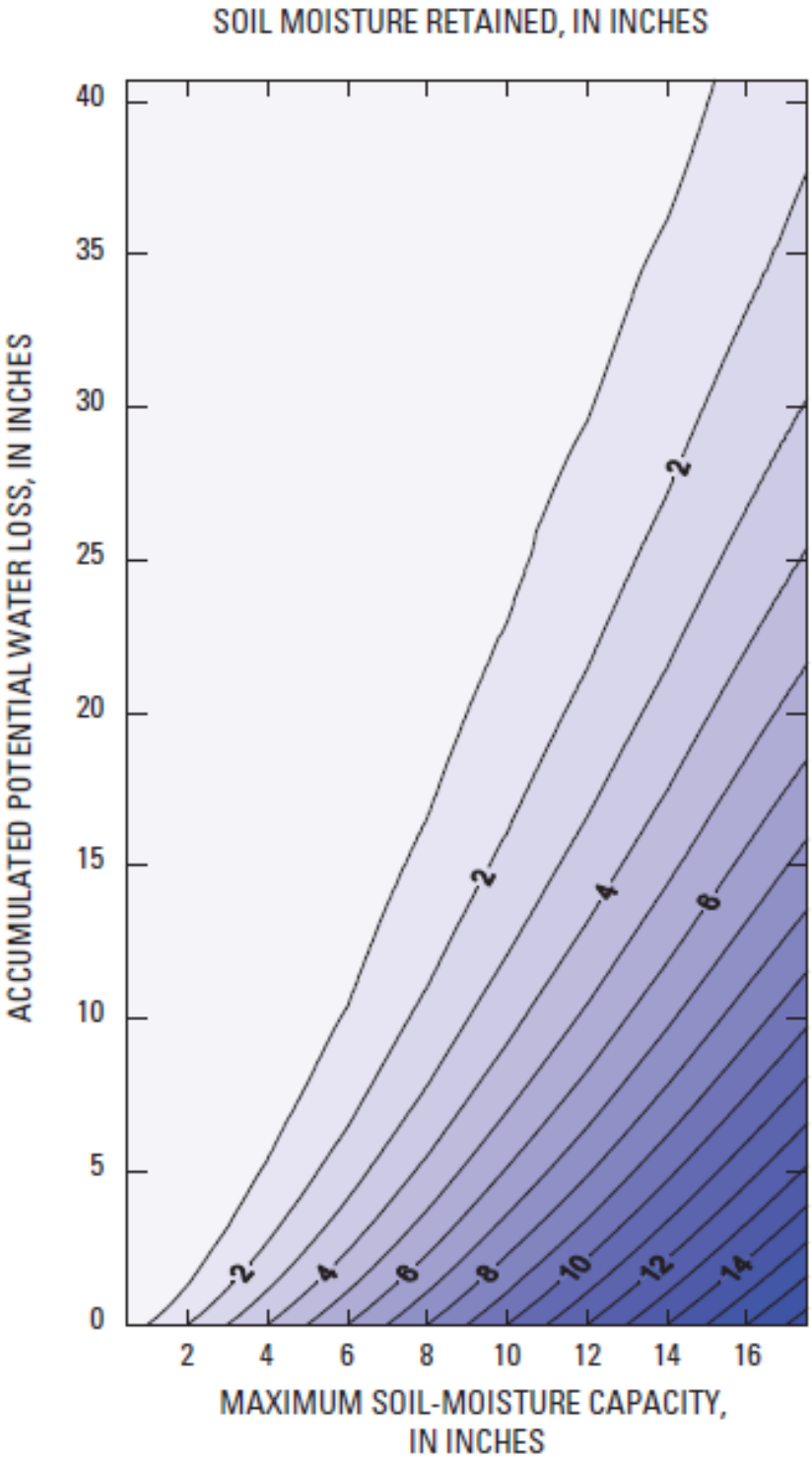

Appendix B. Wells Data

Figure B.1

The distribution of the wells used in the WTF method.

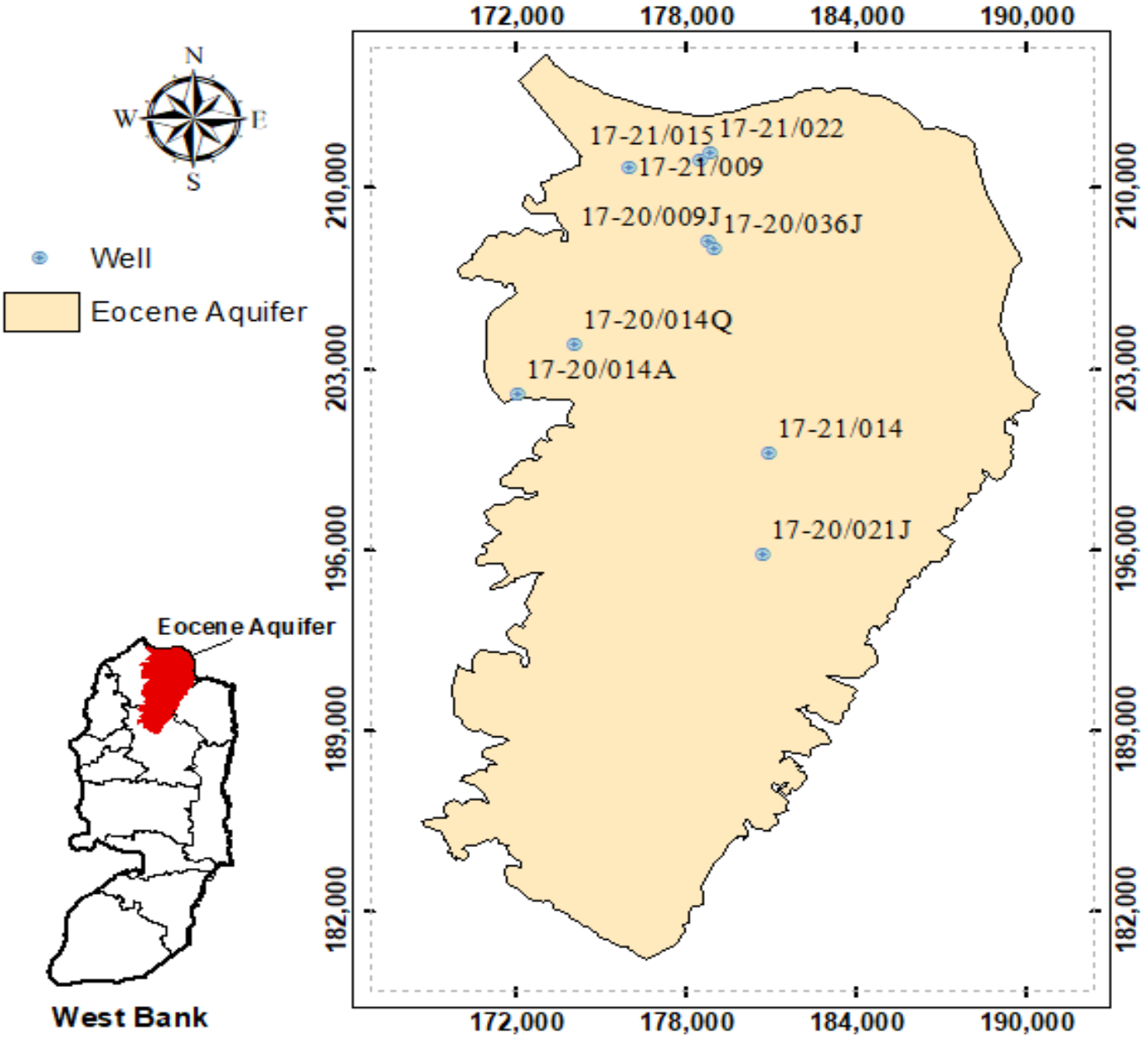

Figure B.2

The water table fluctuation for well 17-21/009.

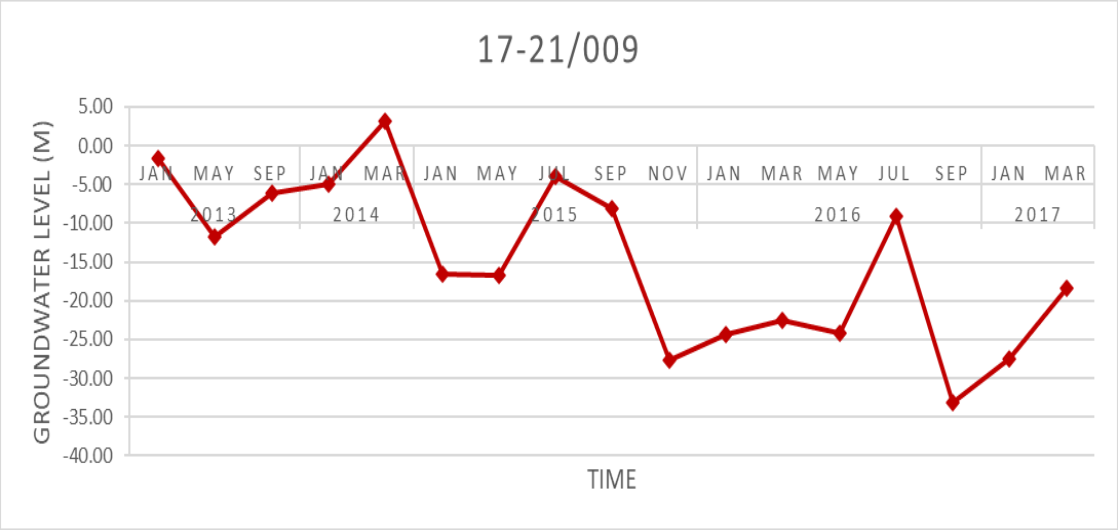

Figure B.3

The water table fluctuation for well 17-21/014.

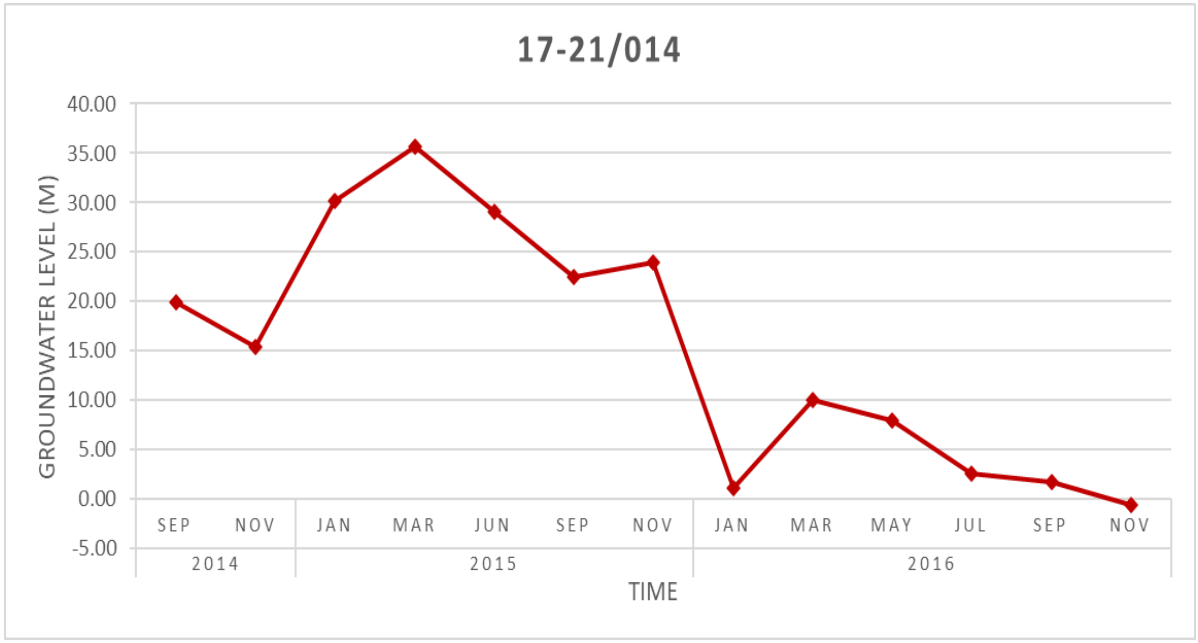

Figure B.4

The water table fluctuation for well 17-20/009J.

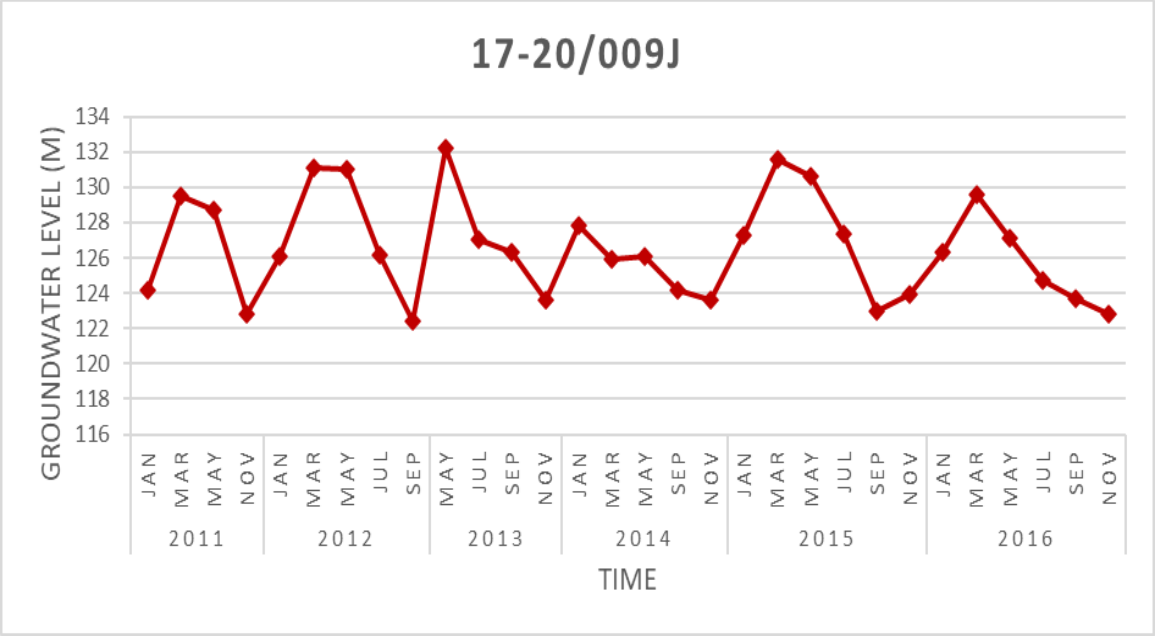

Figure B.5

The water table fluctuation for well 17-20/014A.

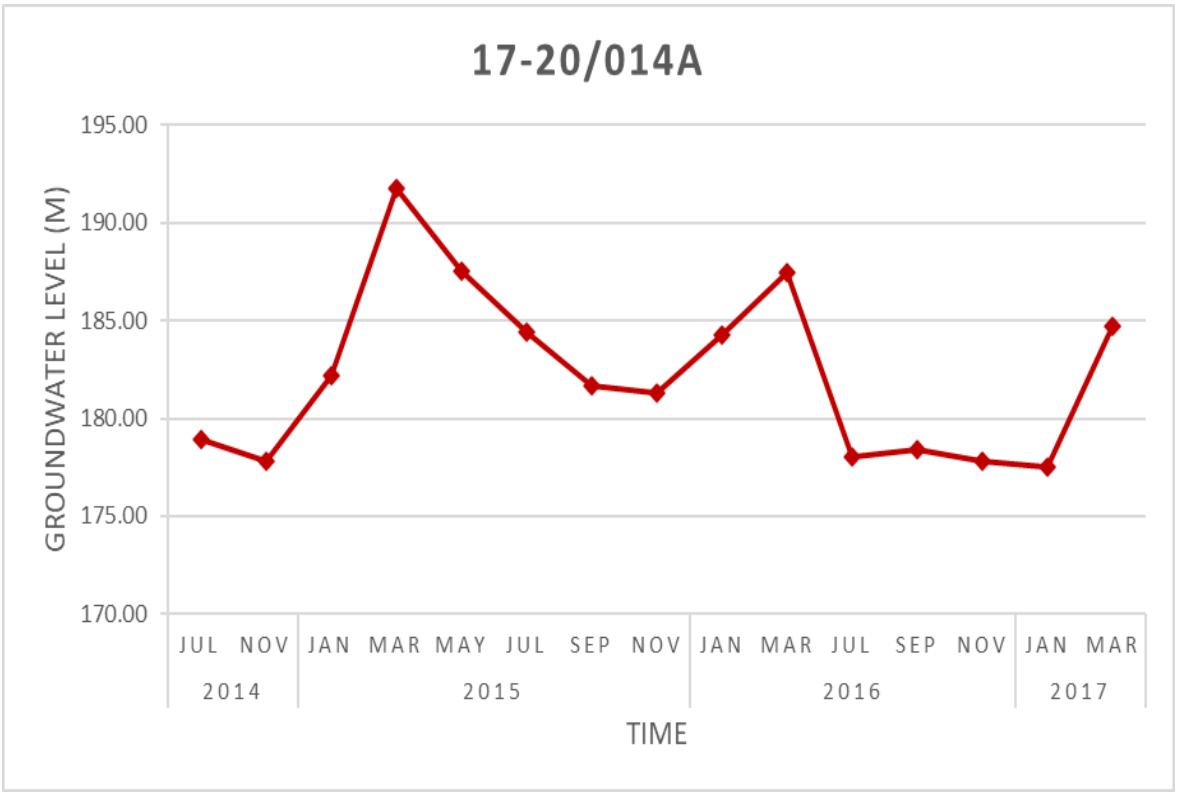

Figure B.6

The water table fluctuation for well 17-21/015.

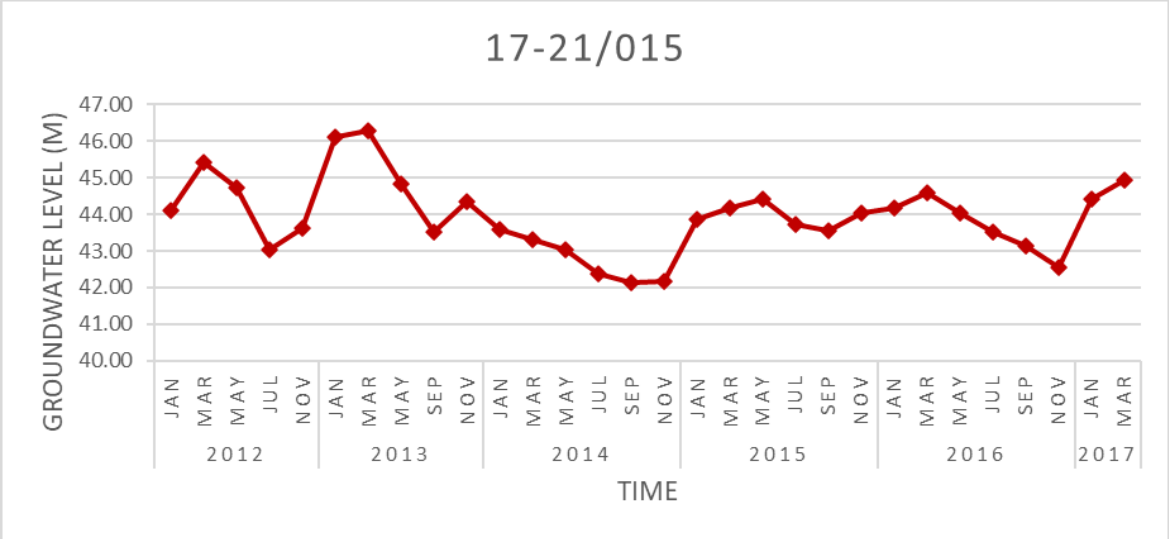

Figure B.7

The water table fluctuation for well 17-20/036J.

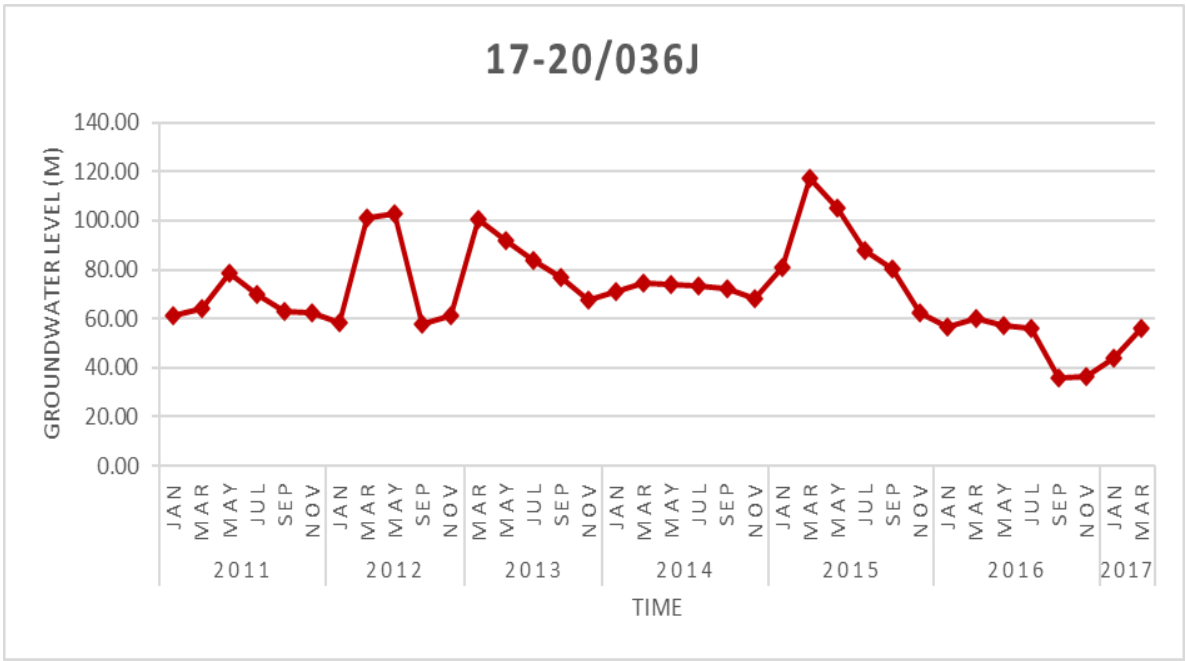

Figure B.8

The water table fluctuation for well 17-21/022.

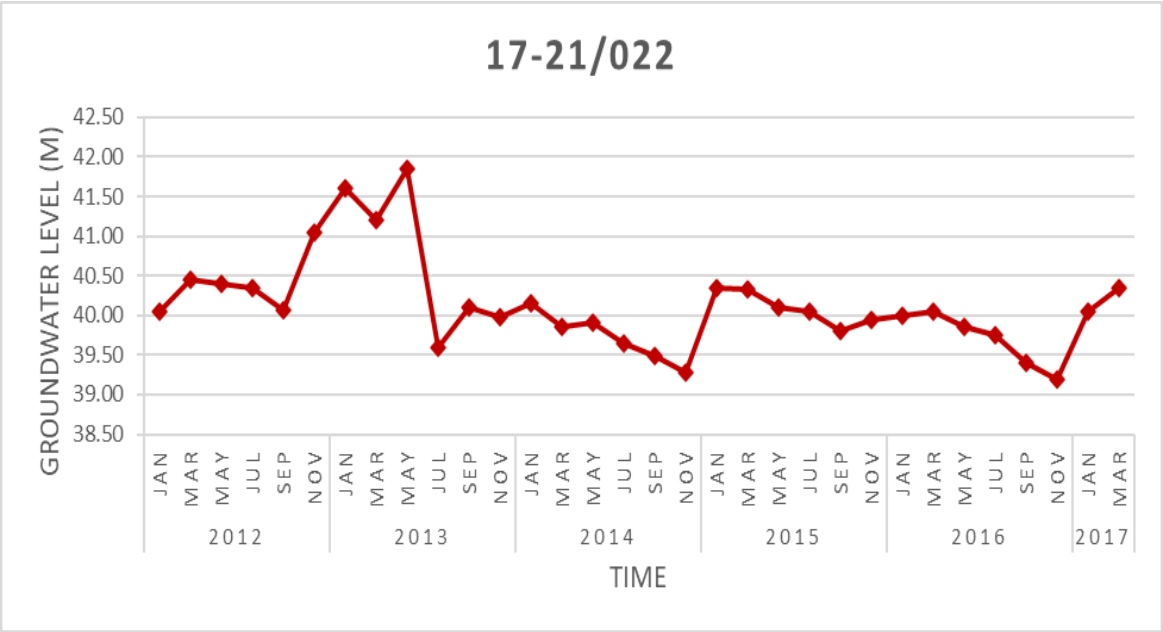

Figure B.9

The water table fluctuation for well 17-20/014Q.

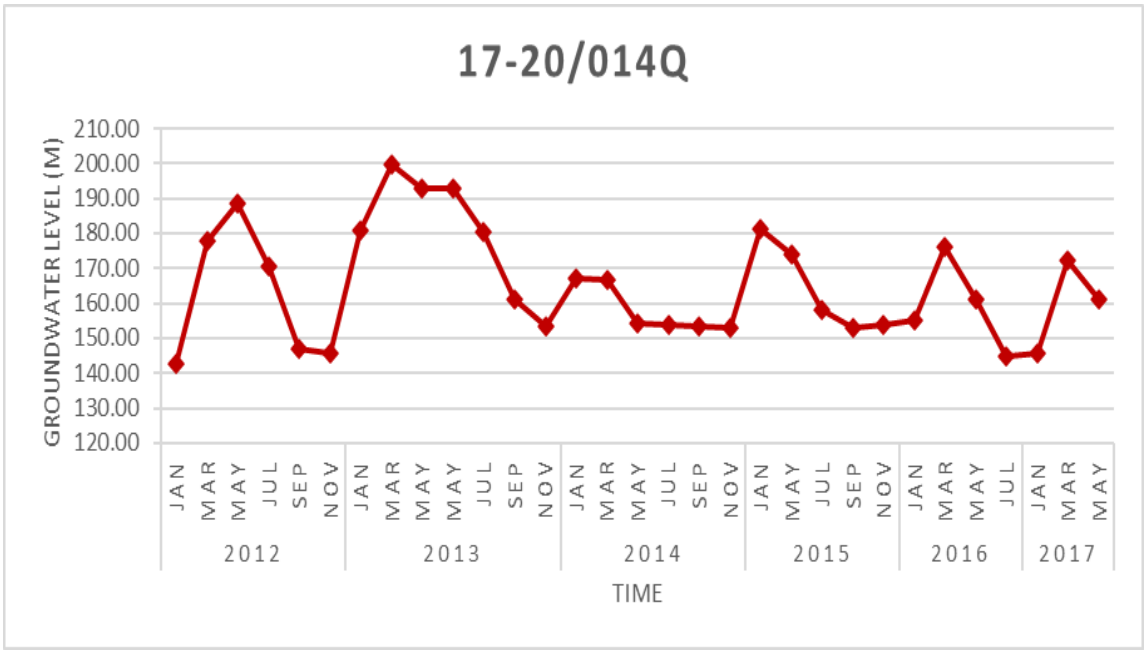

Figure B.10

The water table fluctuation for well 17-20/021J.

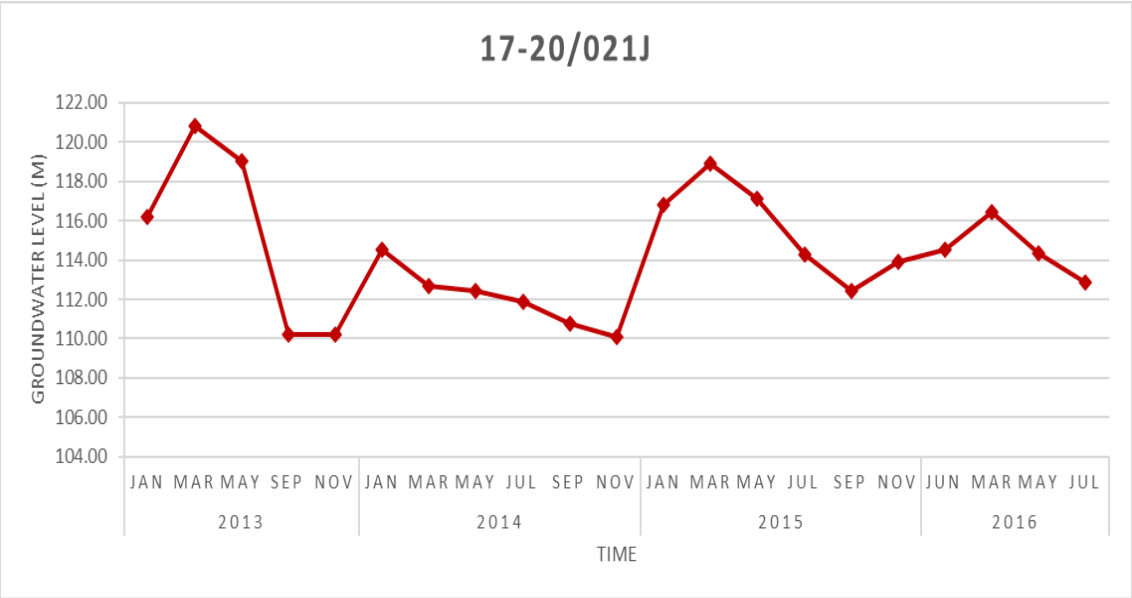

Figure B.11

The variation in the depth to water table for well (17-21/014) located within the Eocene Aquifer.

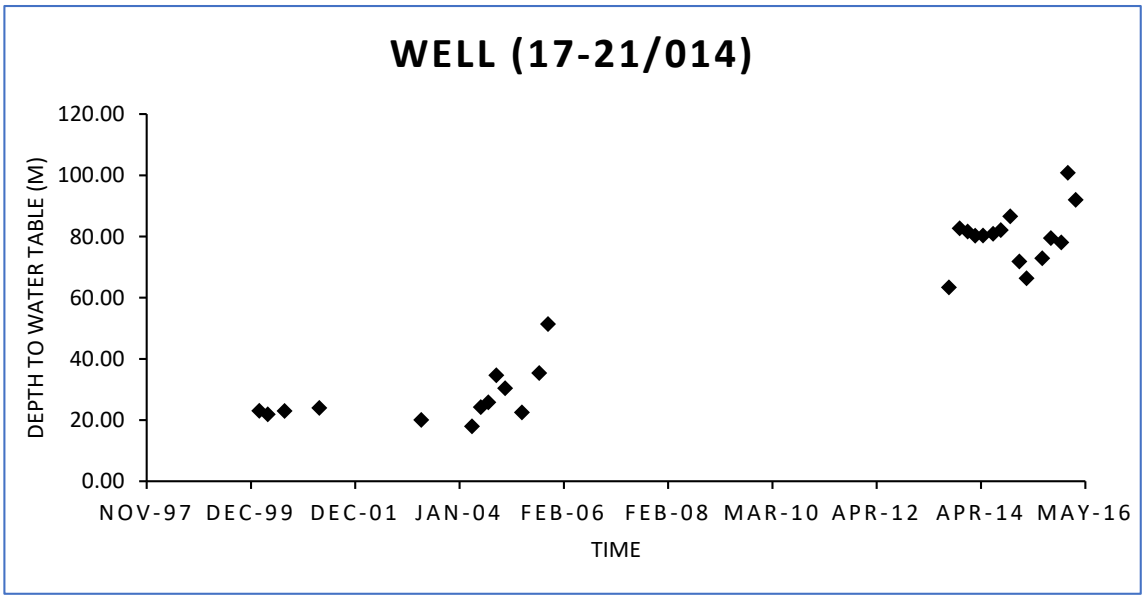

Figure B.12

The variation in the depth to water table for well (17-20/009J) located within the Eocene Aquifer.

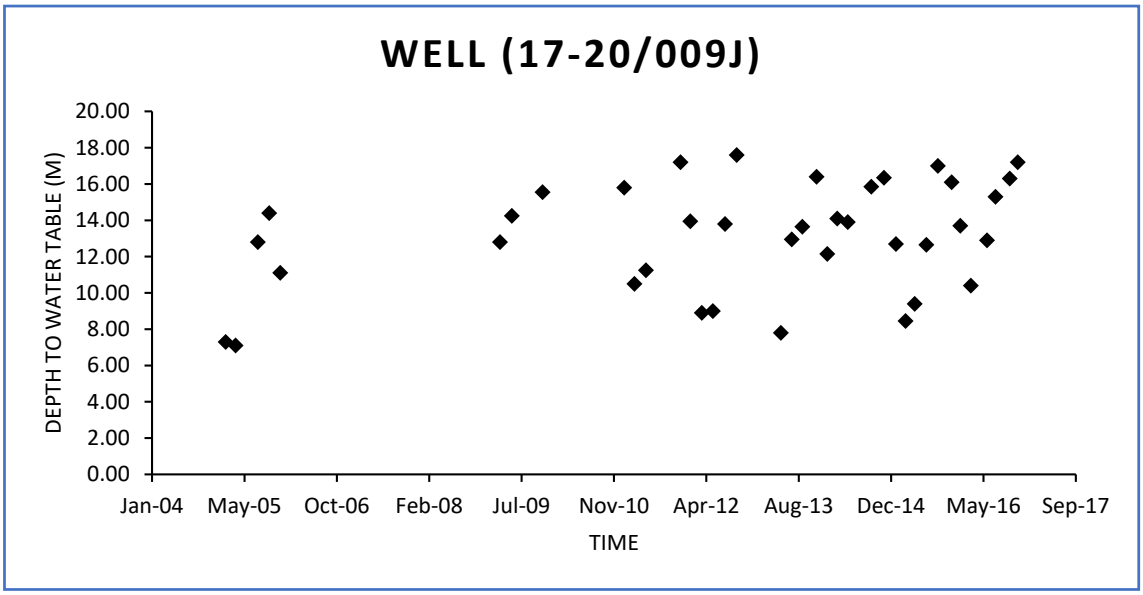

Figure B.13

The variation in the depth to water table for well (17-20/014A) located within the Eocene Aquifer.

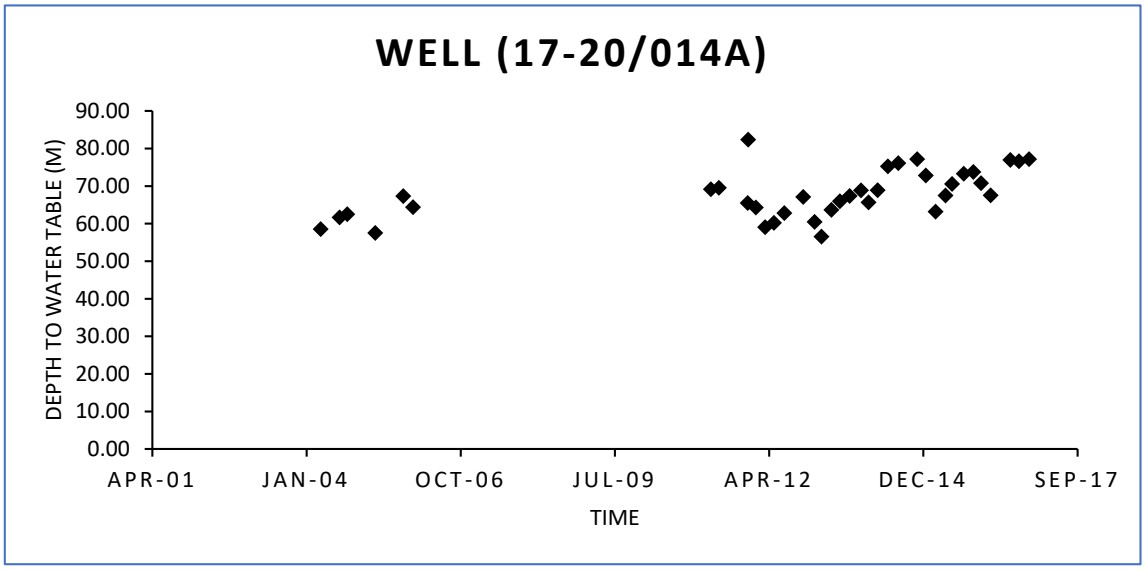

Figure B.14

The variation in the depth to water table for well (17-21/009) located within the Eocene Aquifer.

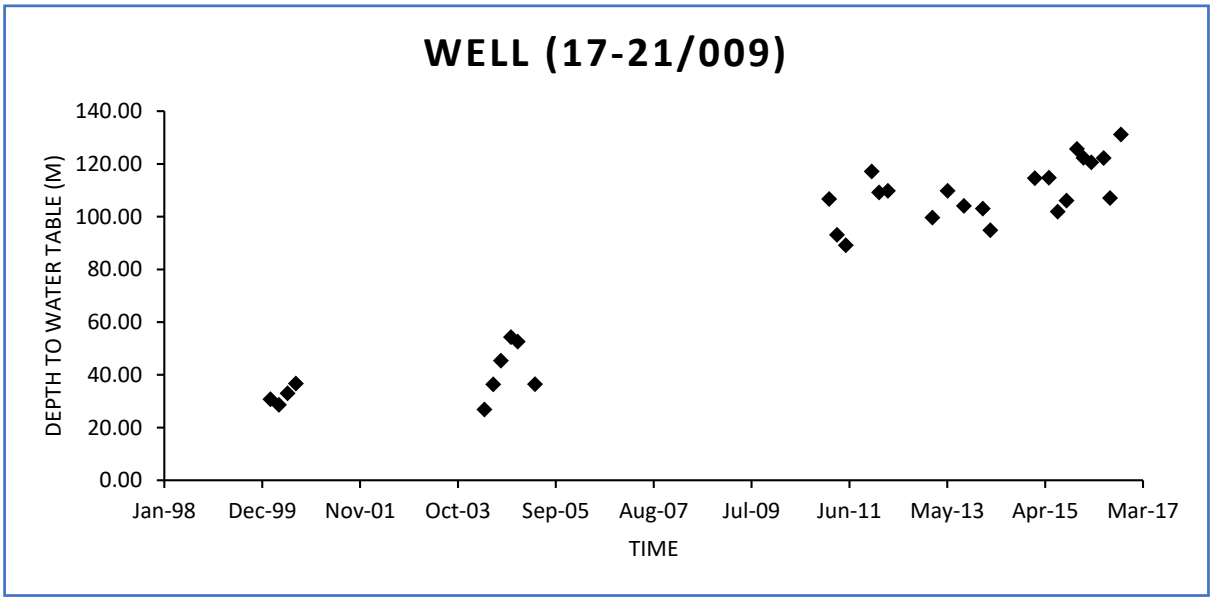

Figure B.15

The variation in the depth to water table for well (17-21/009) located within the Eocene Aquifer.

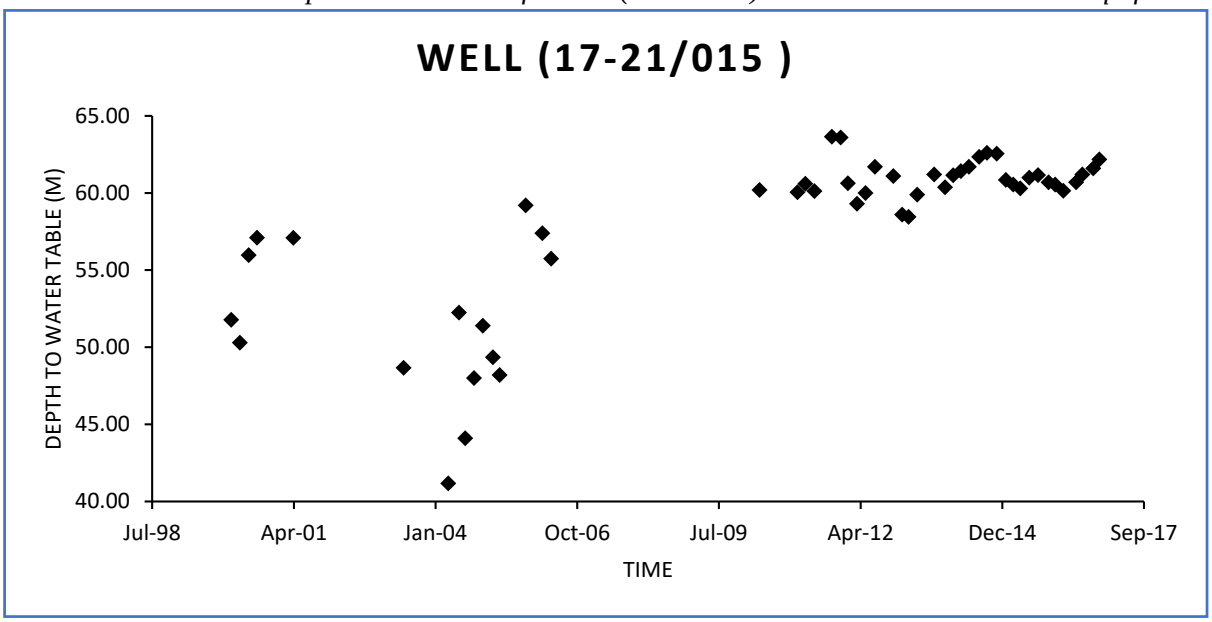

Figure B.16

The variation in the depth to water table for well (17-20/036J) located within the Eocene Aquifer

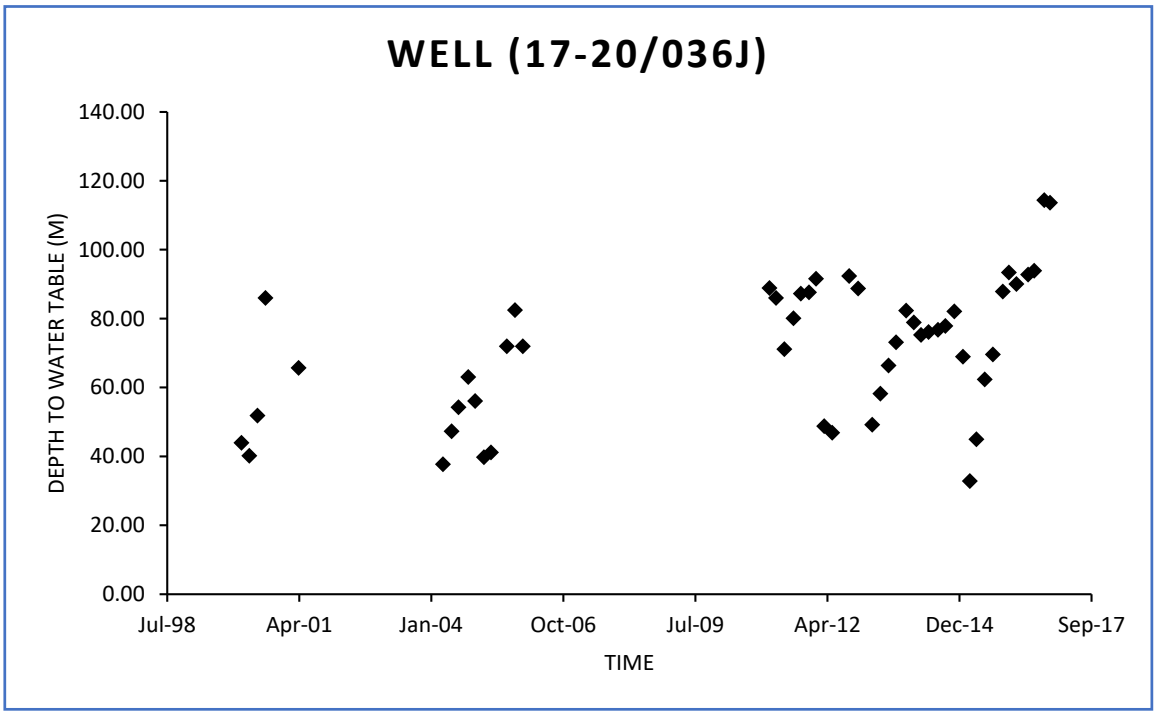

Figure B.17

The variation in the depth to water table for well (17-20/014Q) located within the Eocene Aquifer.

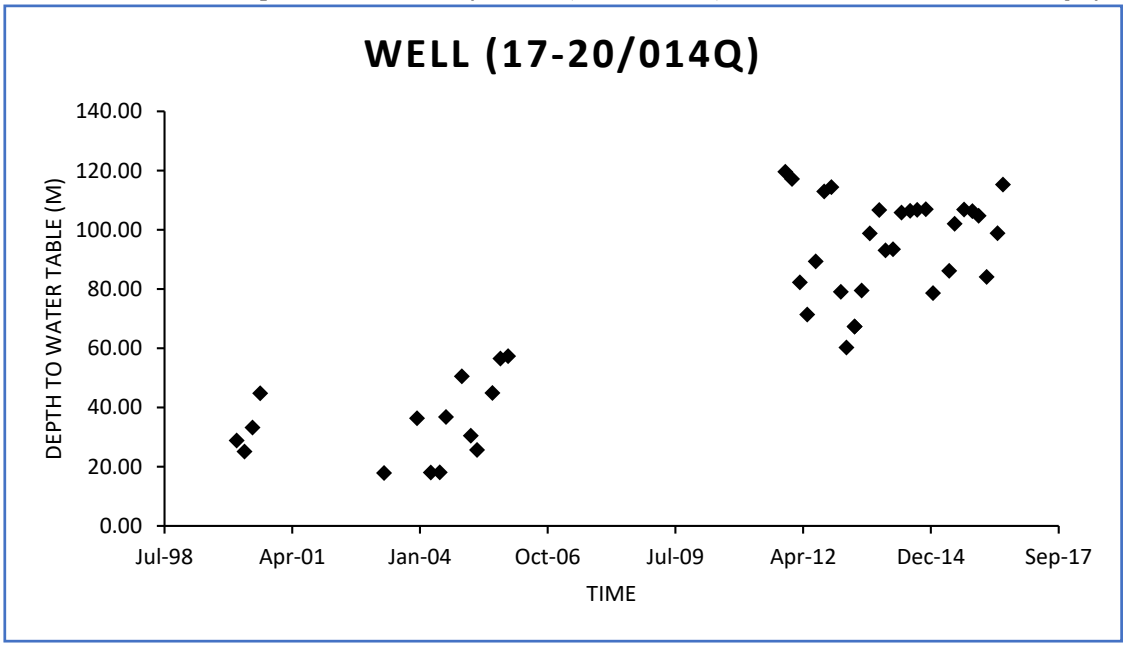

Figure B.18

The variation in the depth to water table for well (17-20/021J) located within the Eocene Aquifer.

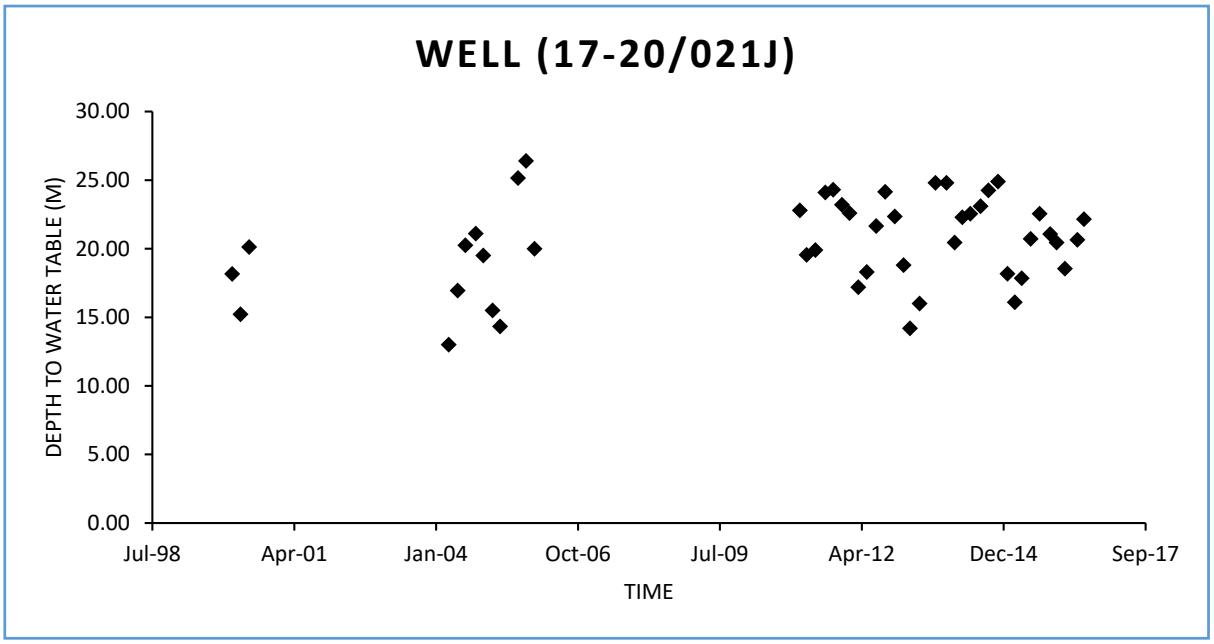

Figure B.19

The variation in the depth to water table for well (17-21/022) located within the Eocene Aquifer.

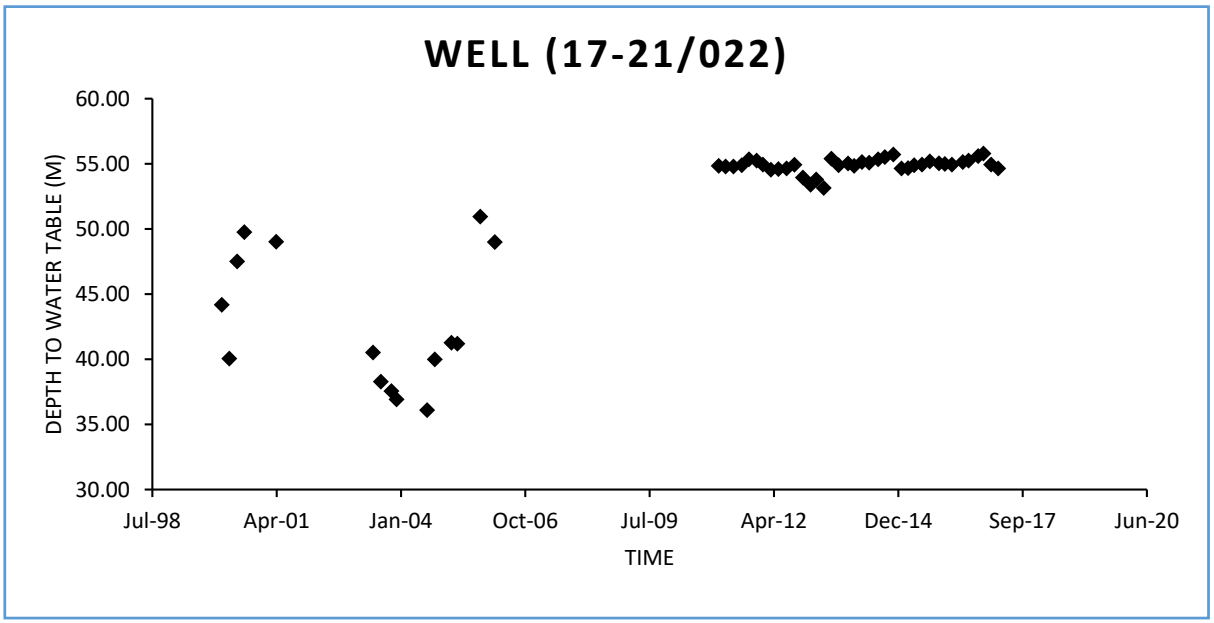

Appendix C. Water Demand Distribution

Figure C.1

The agricultural water demand for the communities located within the Eocene Aquifer for the study period.

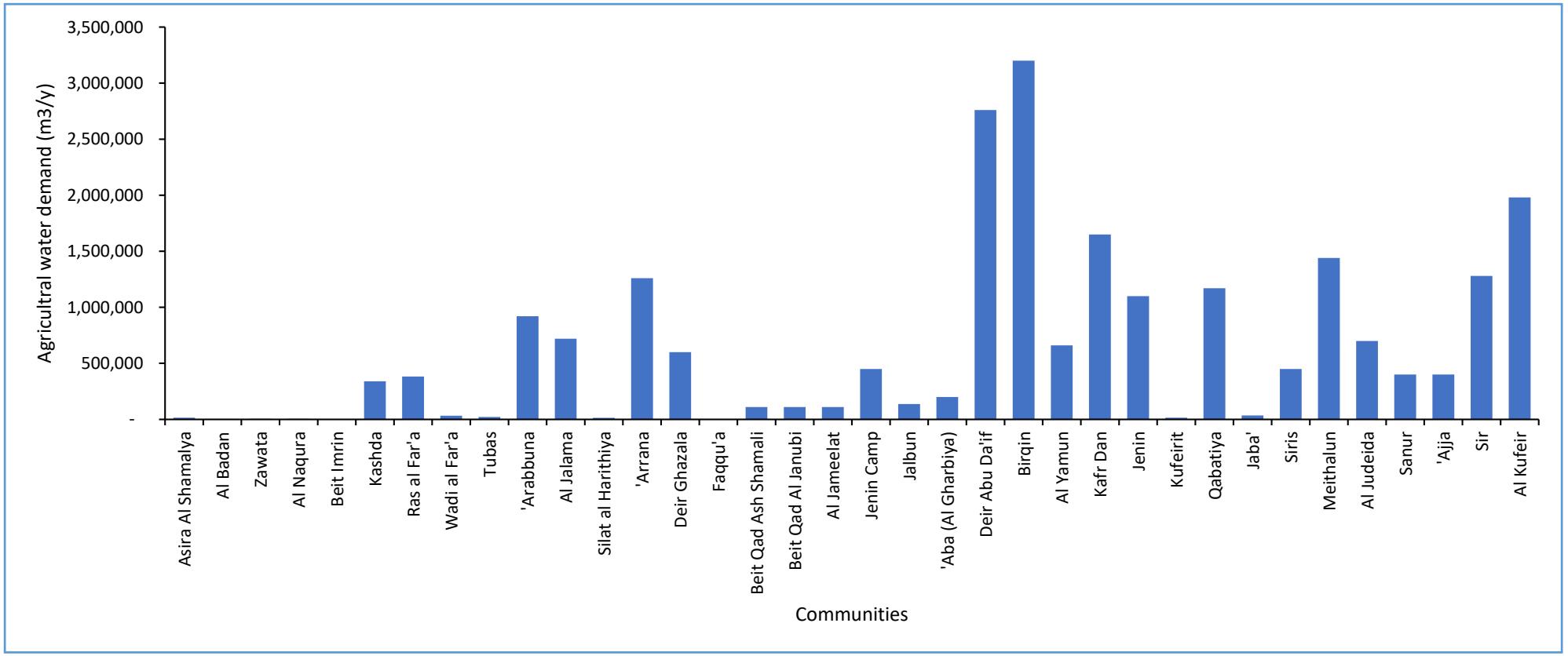

Figure C.2

The water demand of sheeps for the communities within the Eocene Aquifer for the study period.

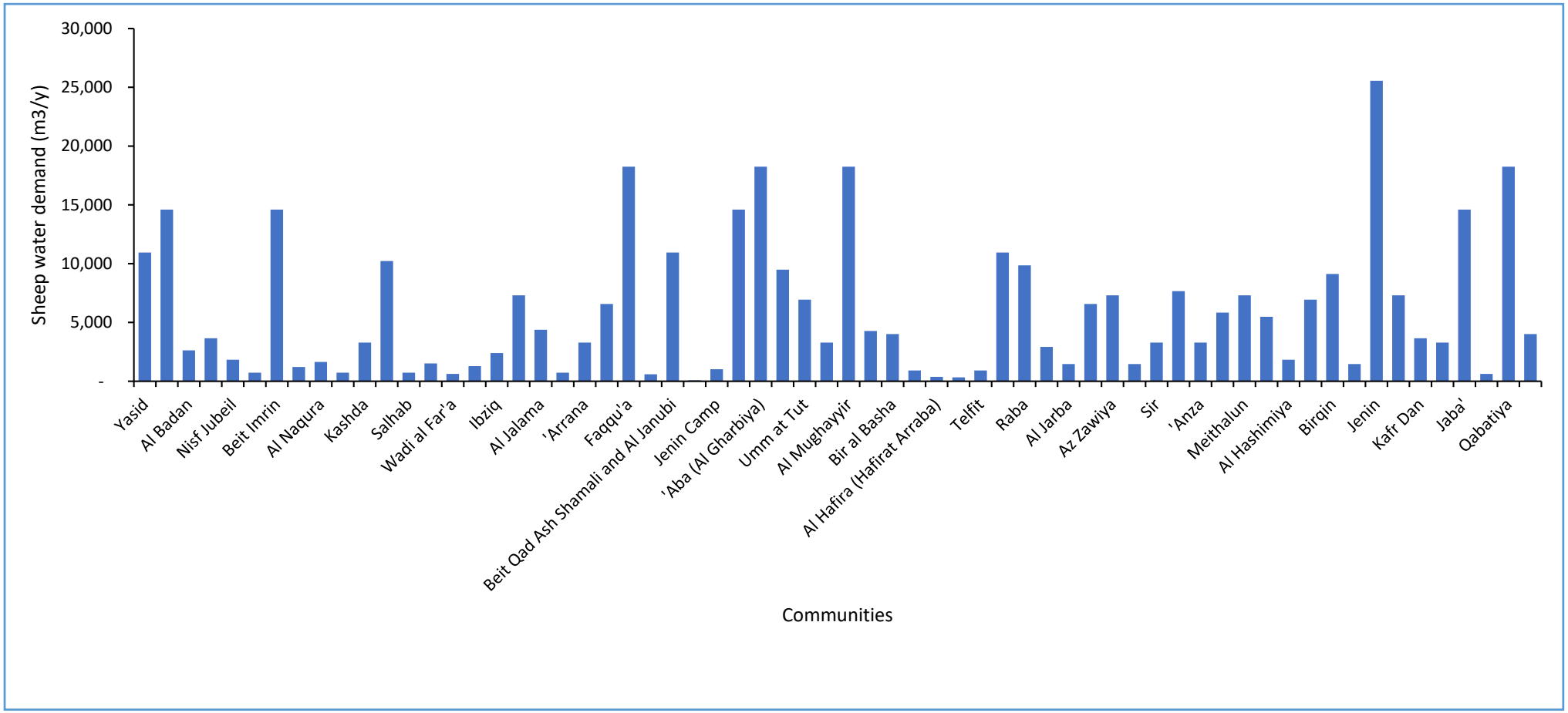

Figure C.3

The water demand of cows for the communities within the Eocene Aquifer for the study period.

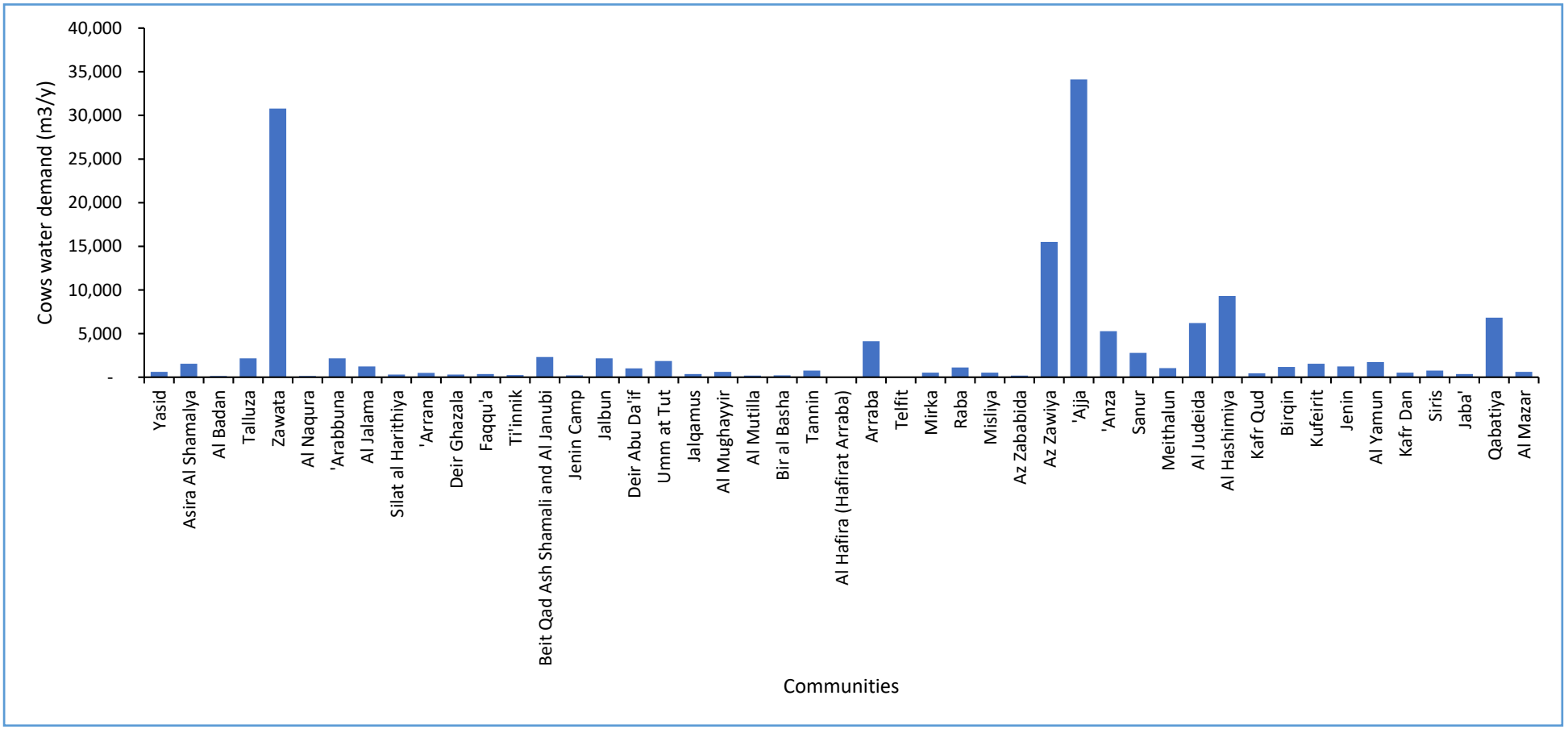

Figure C.4

The water demand of poultry for the communities within the Eocene Aquifer for the study period.

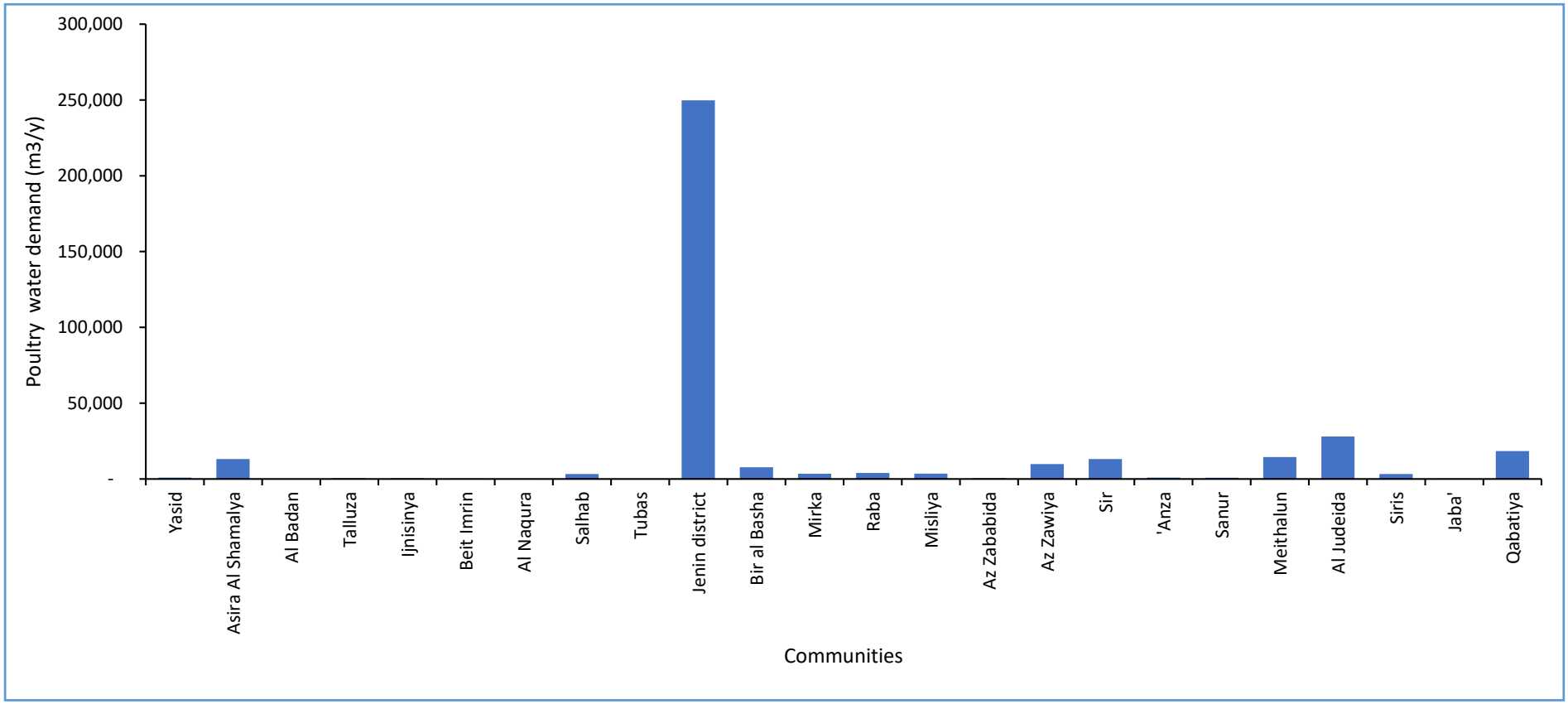

Appendix D. Swb Results

Figure D.1

The distribution of groundwater recharge for the Eocene Aquifer for January/2020.

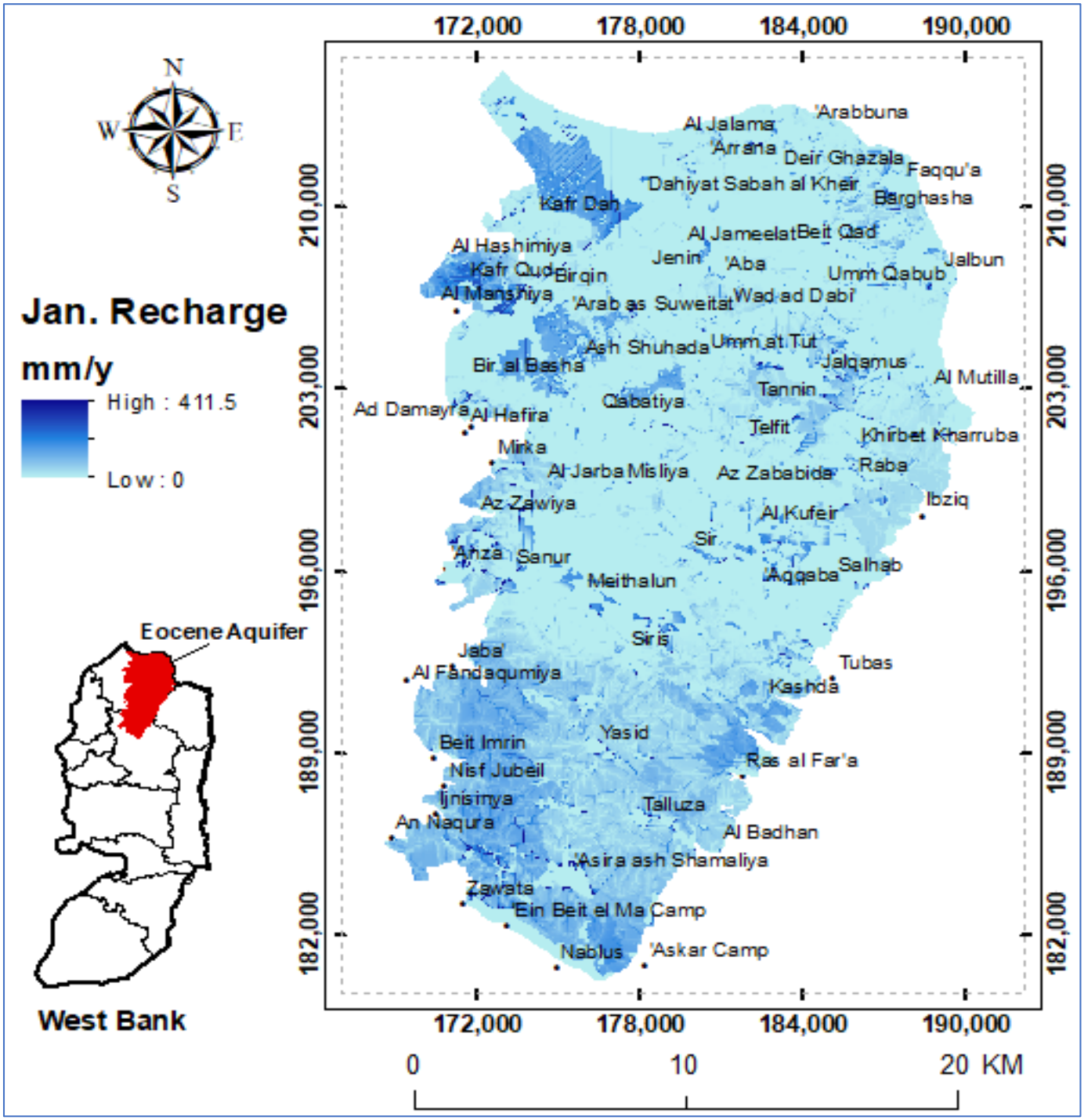

Figure D.2

The distribution of groundwater recharge for the Eocene Aquifer for February/2020.

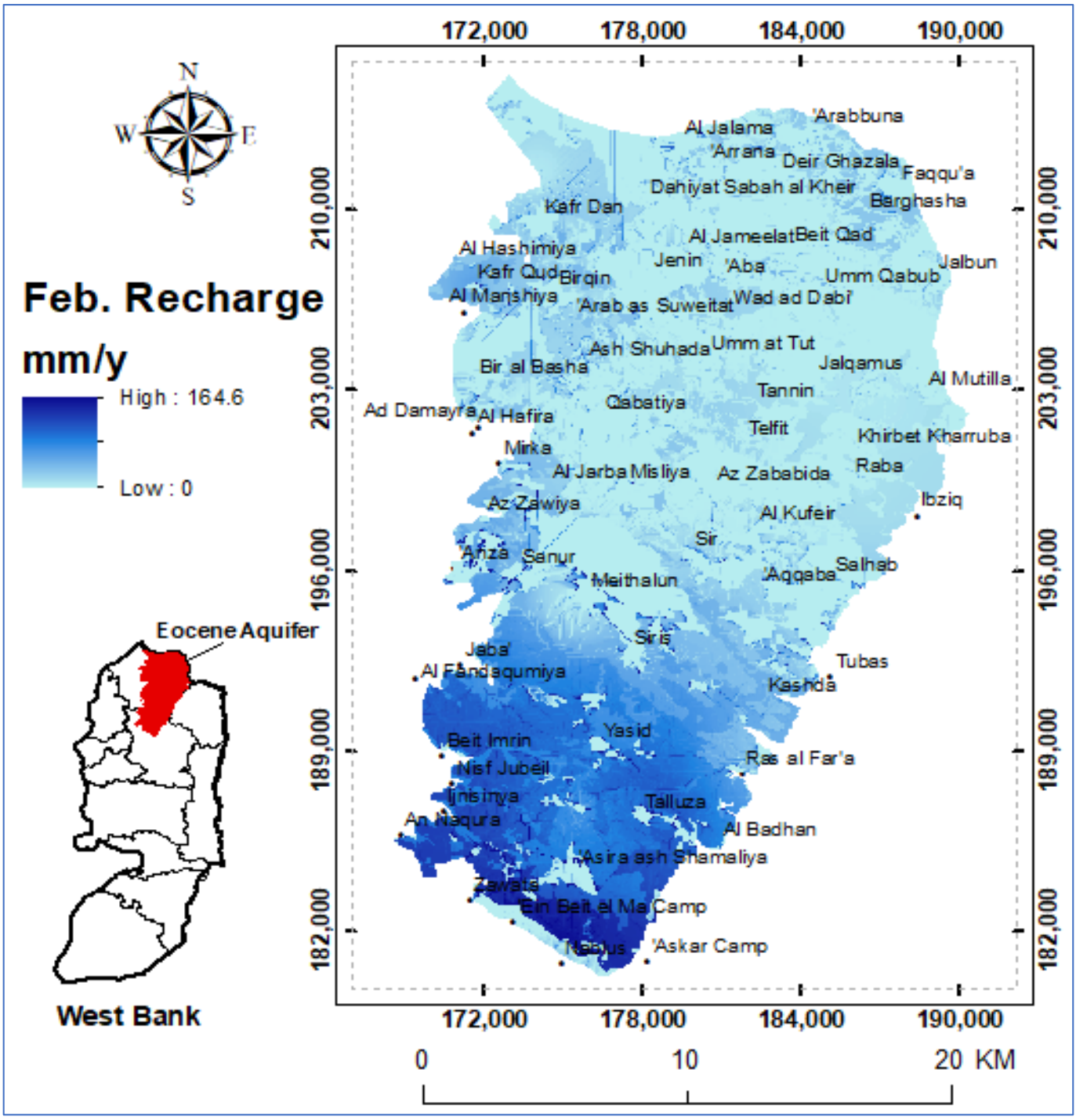

Figure D.3

The distribution of groundwater recharge for the Eocene Aquifer for March/2020.

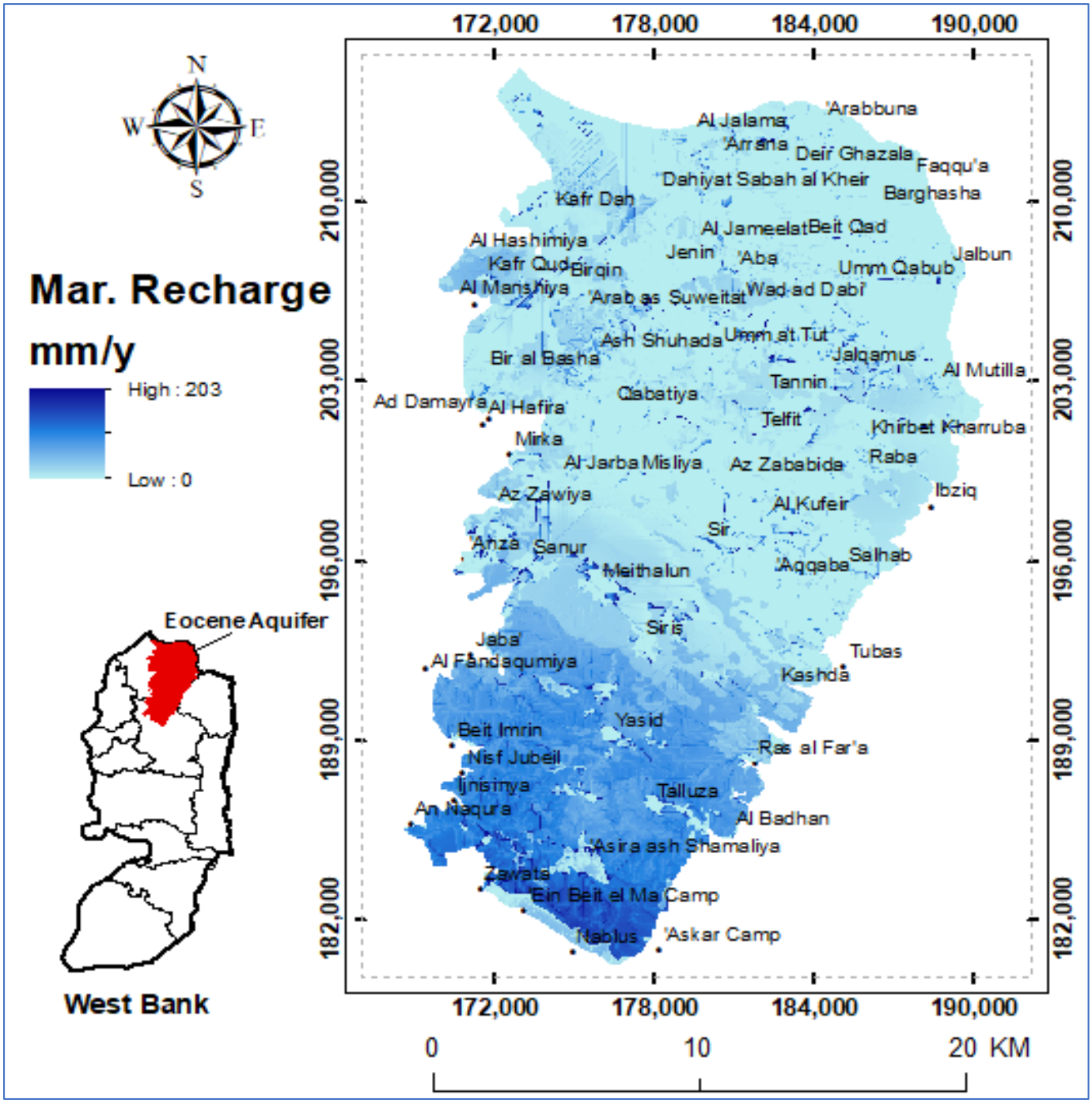

Figure D.4

The distribution of groundwater recharge for the Eocene Aquifer for April/2020.

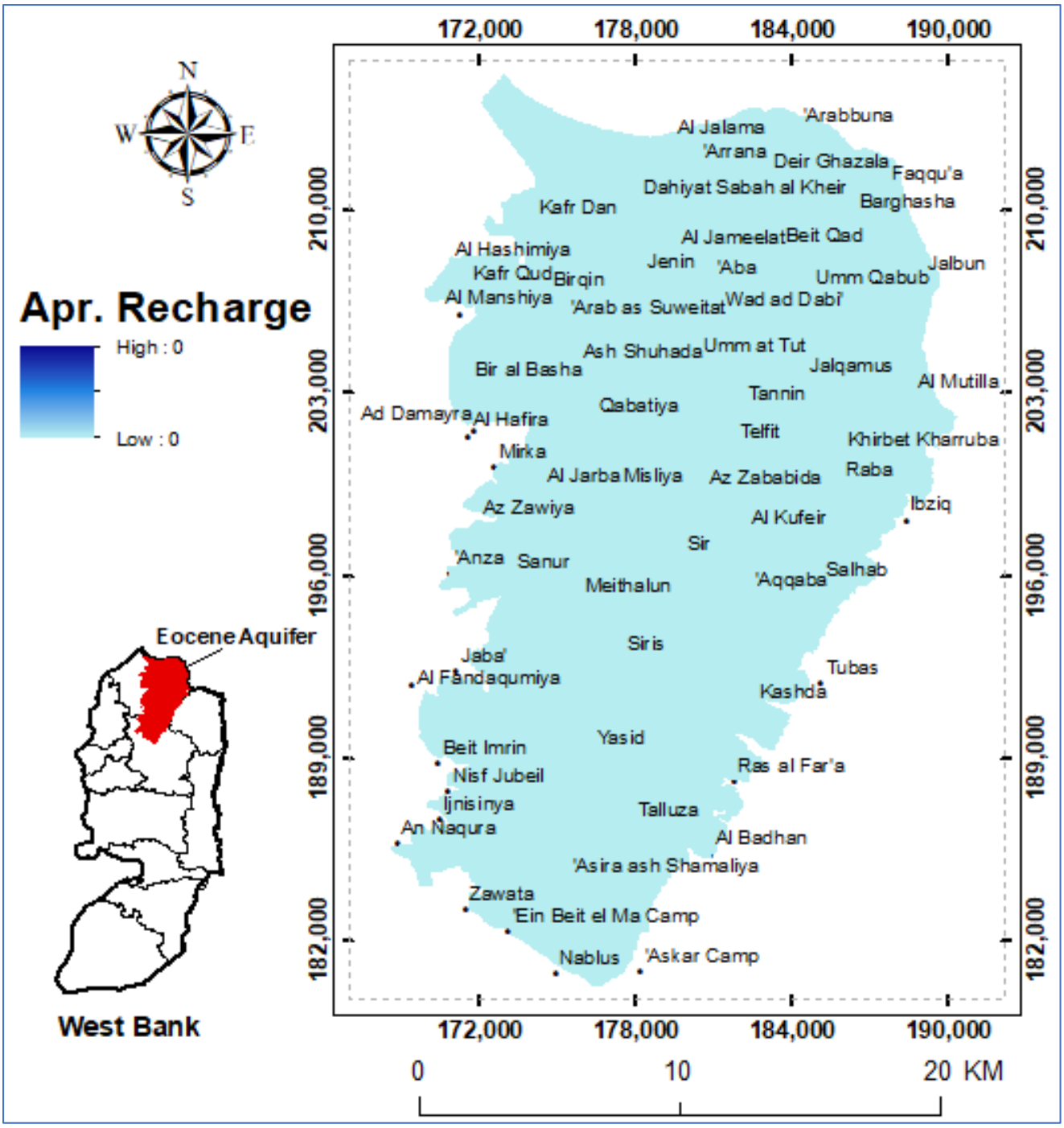

Figure D.5

The distribution of groundwater recharge for the Eocene Aquifer for May/2020.

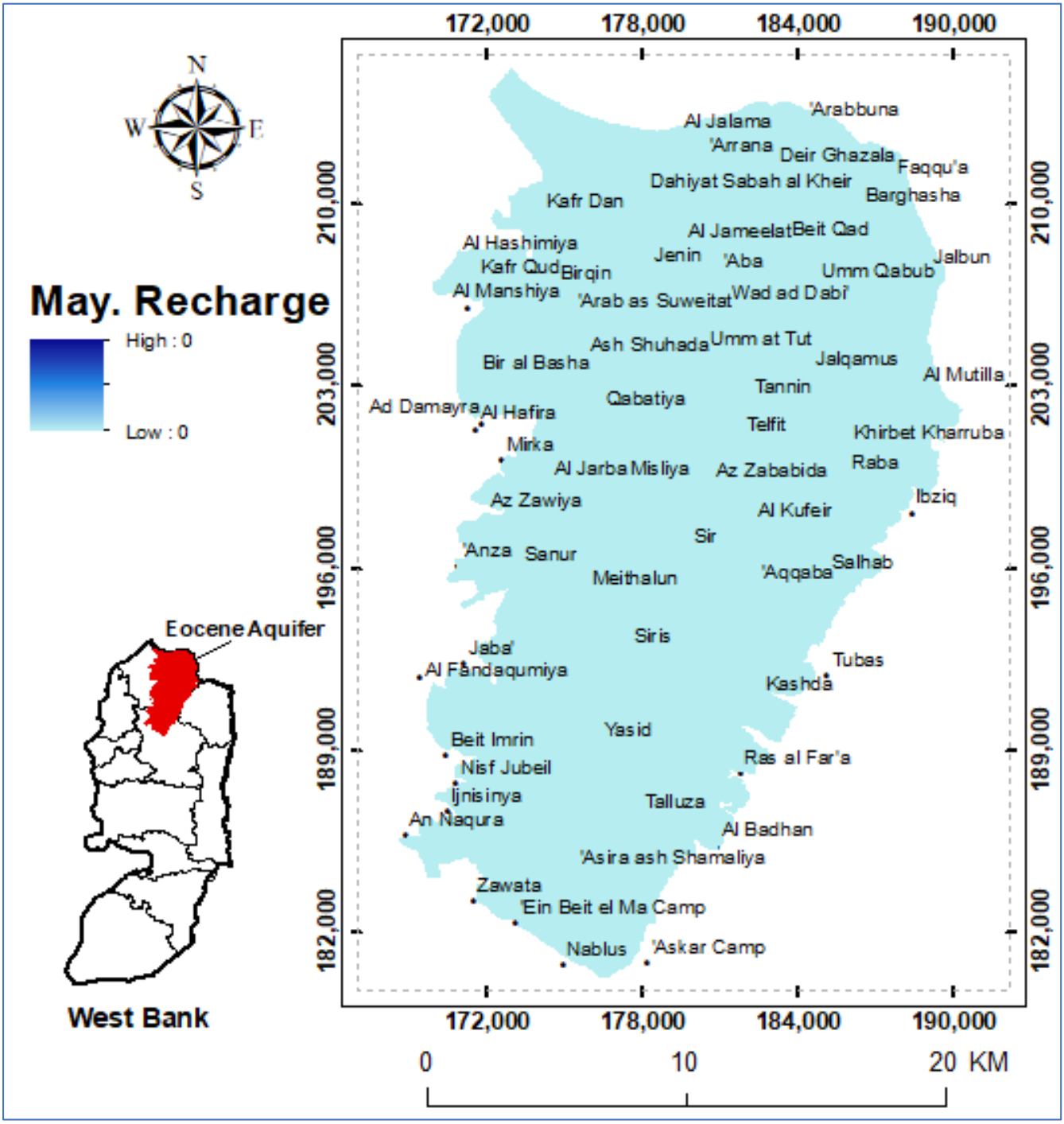

Figure D.6

The distribution of groundwater recharge for the Eocene Aquifer for June/2020.

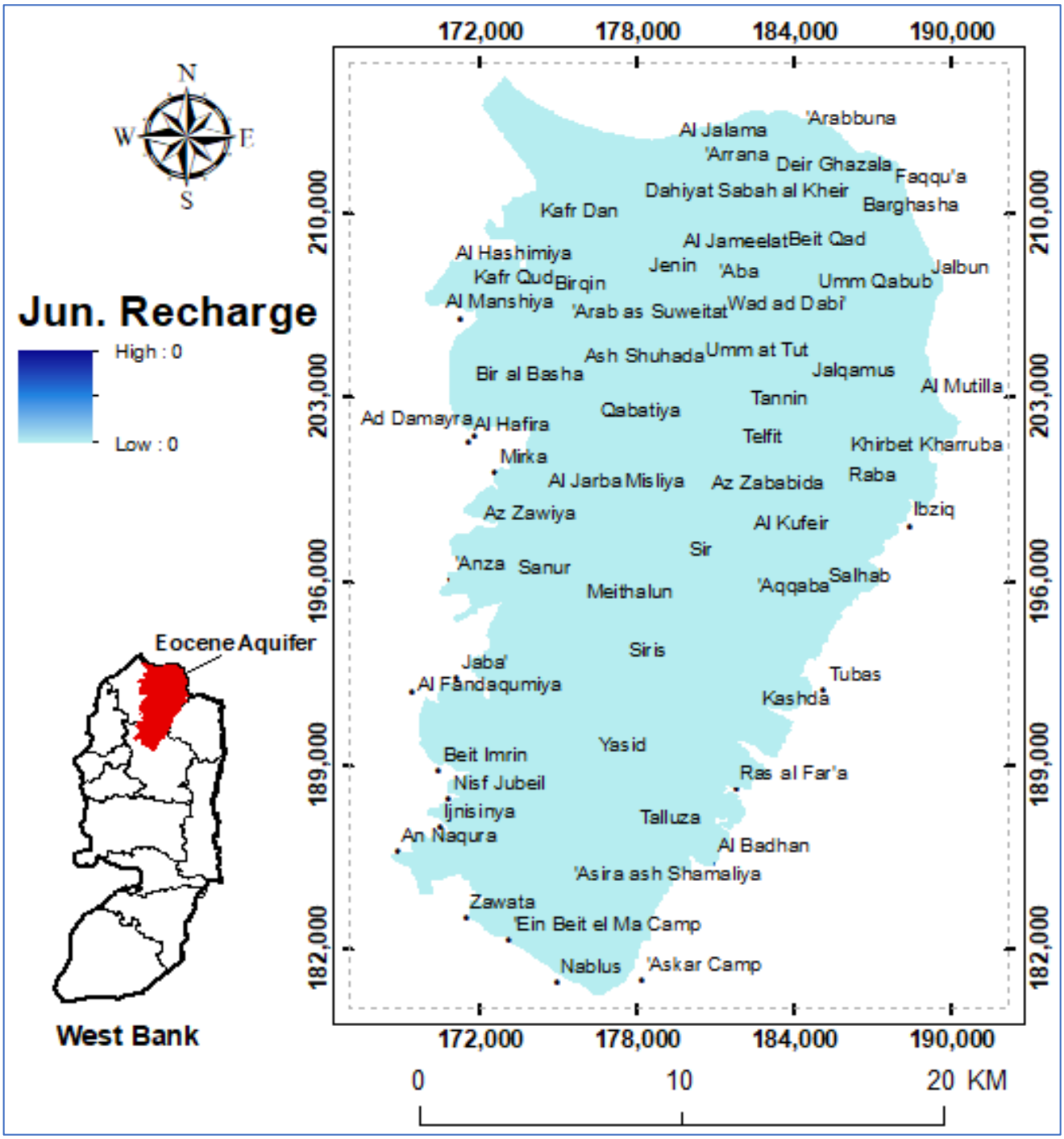

Figure D.7

The distribution of groundwater recharge for the Eocene Aquifer for July/2020.

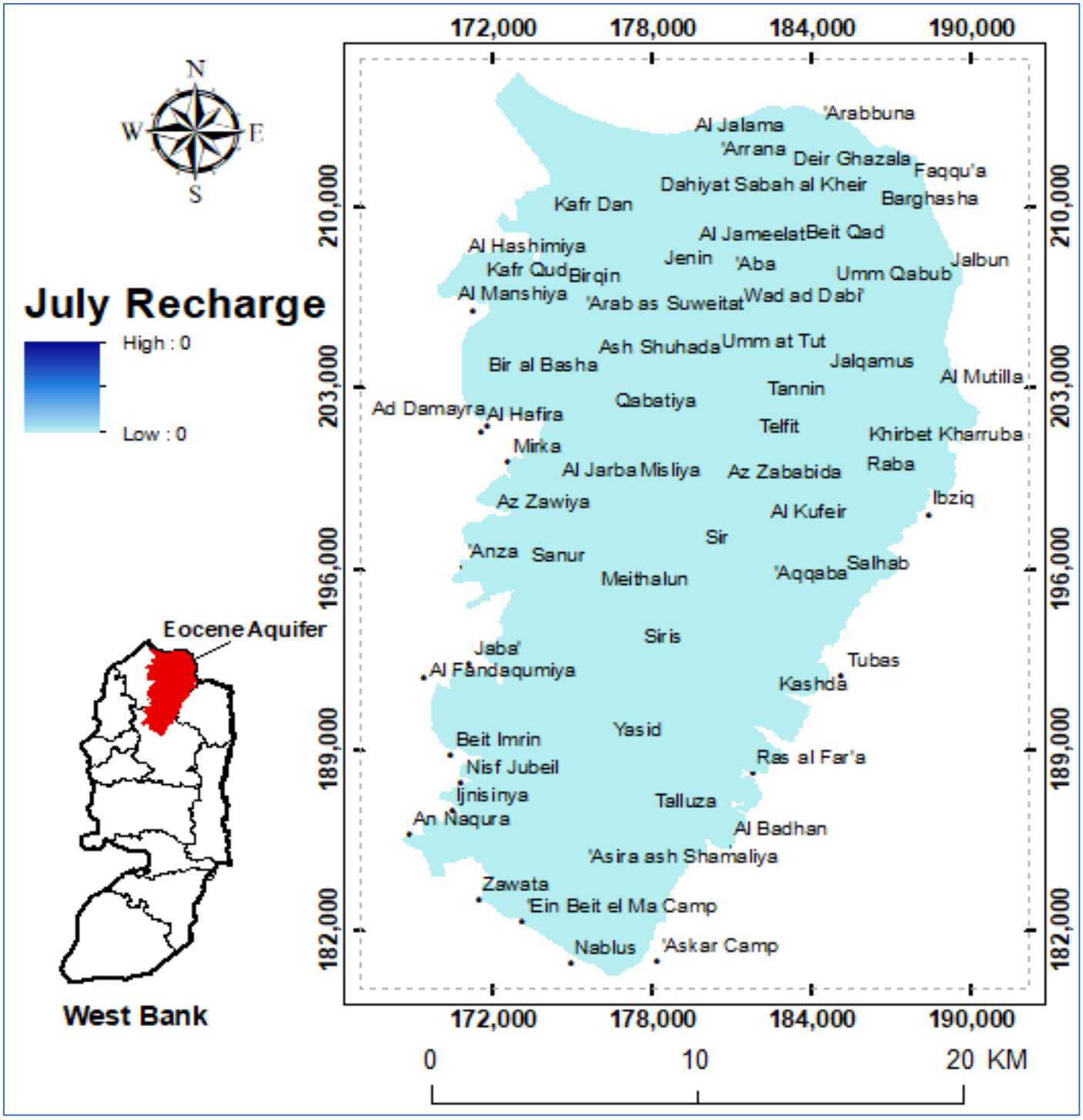

Figure D.8

The distribution of groundwater recharge for the Eocene Aquifer for August/2020.

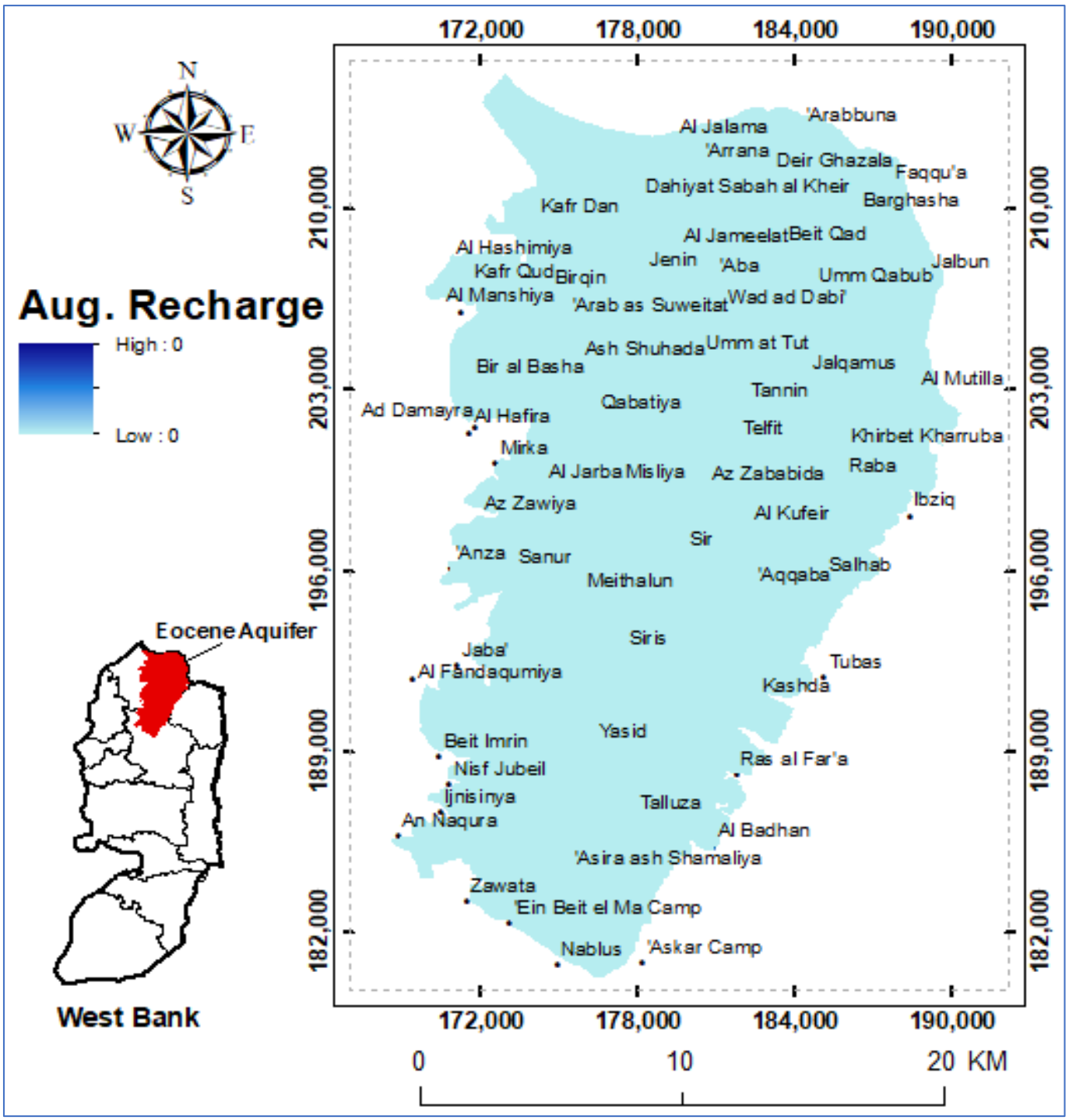

Figure D.9

The distribution of groundwater recharge for the Eocene Aquifer for September/2020.

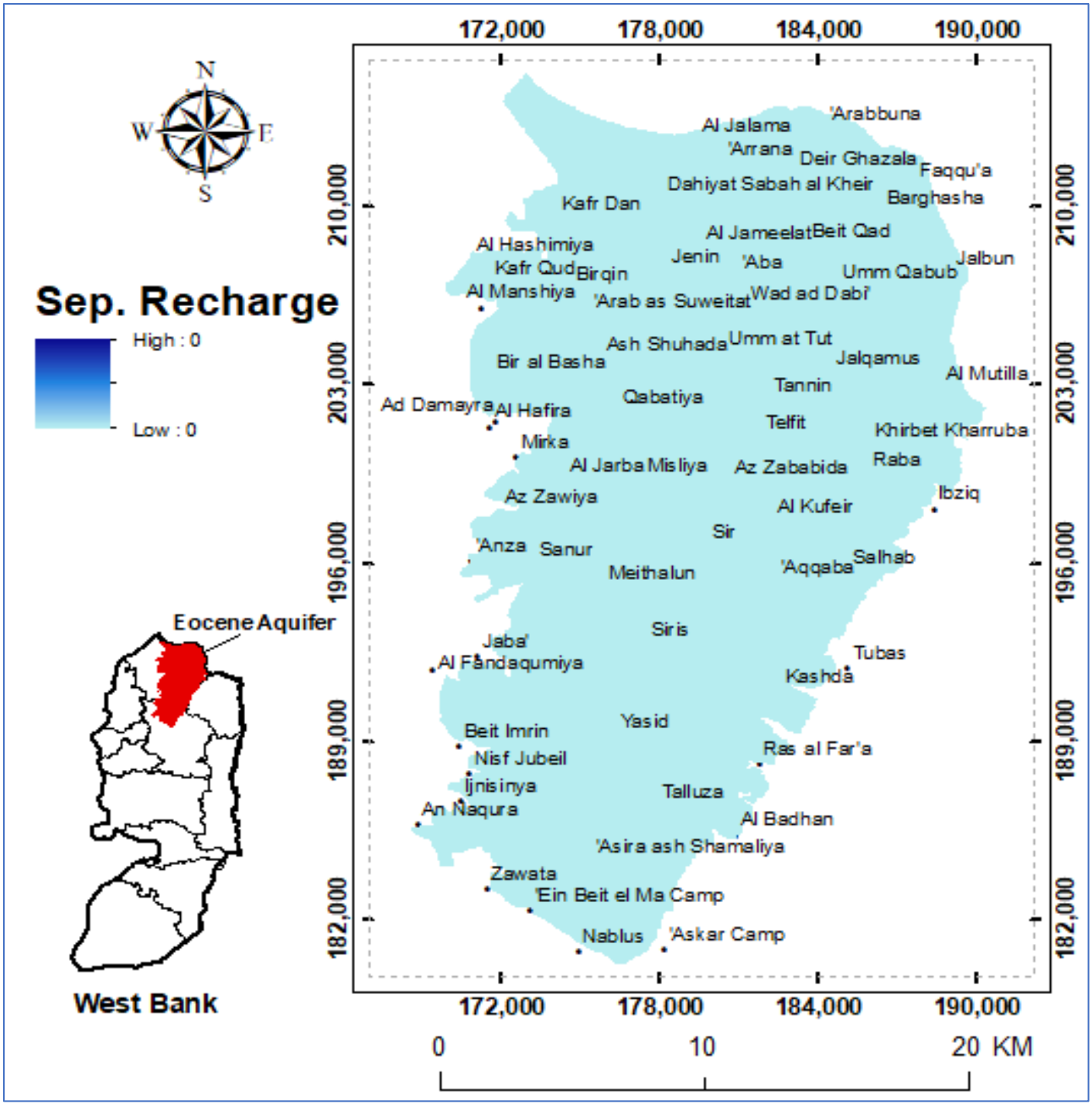

Figure D.10

The distribution of groundwater recharge for the Eocene Aquifer for October/2020.

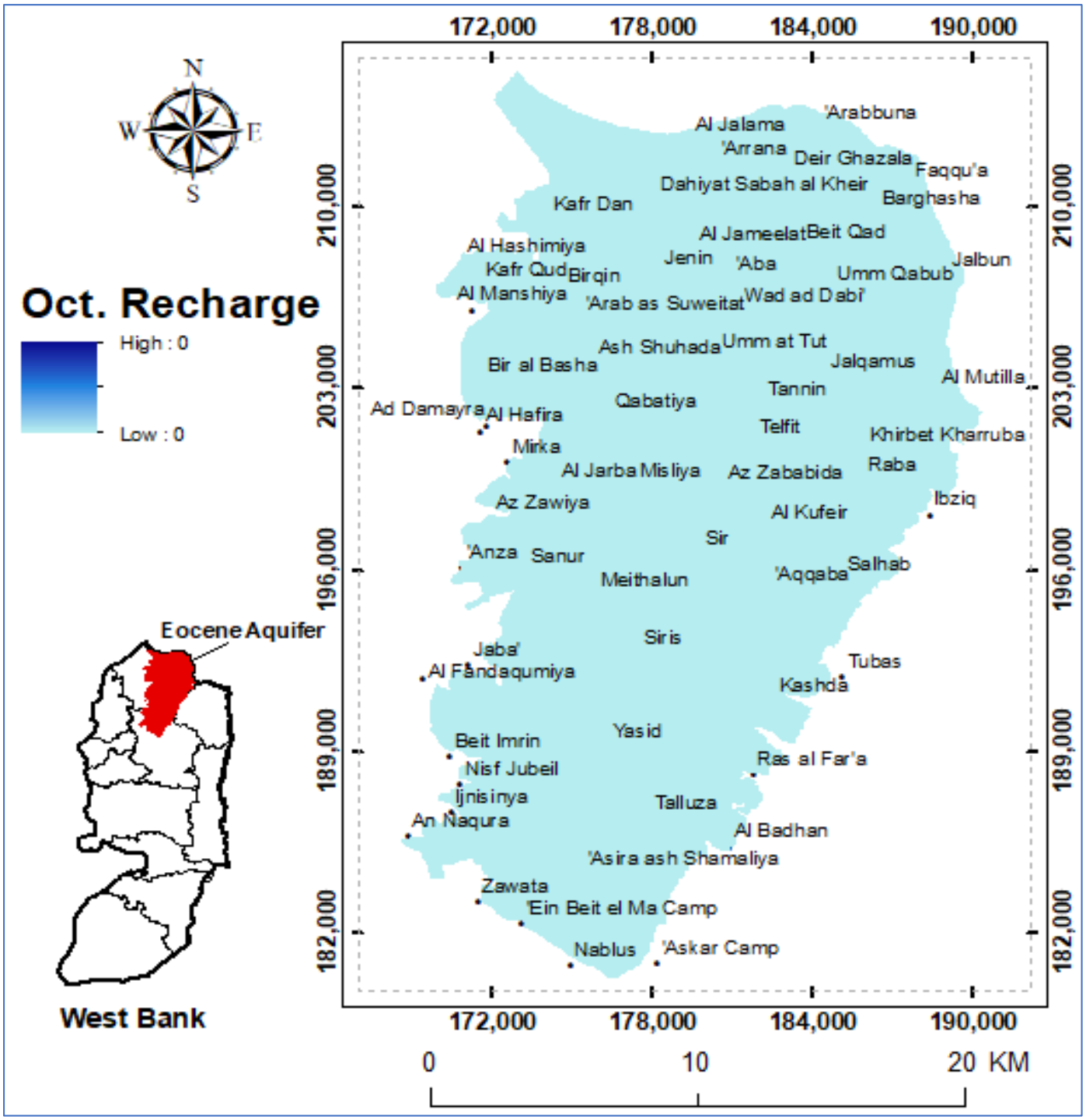

Figure D.11

The distribution of groundwater recharge for the Eocene Aquifer for November/2020.

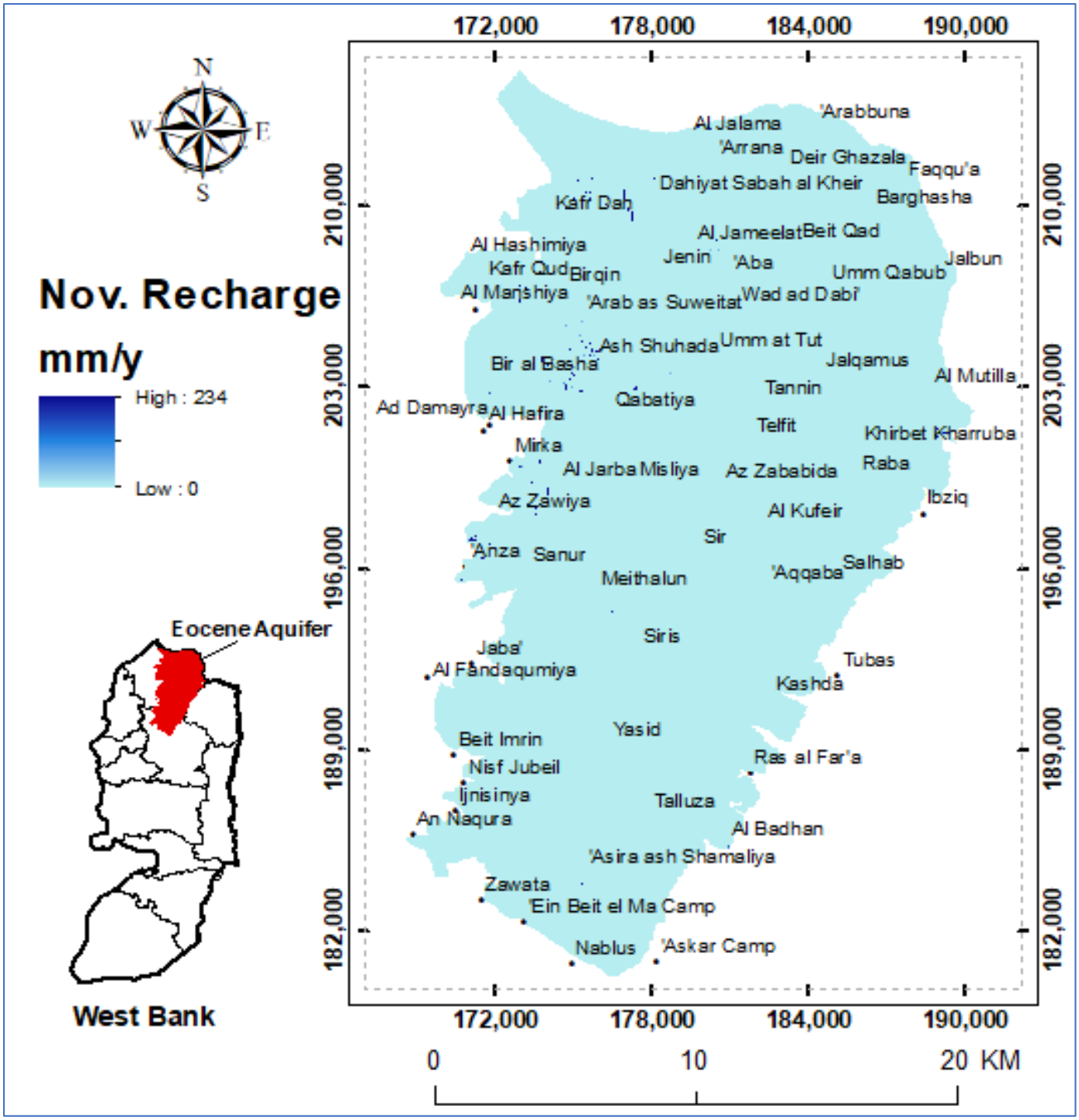

Figure D.12

The distribution of groundwater recharge for the Eocene Aquifer for December/2020.

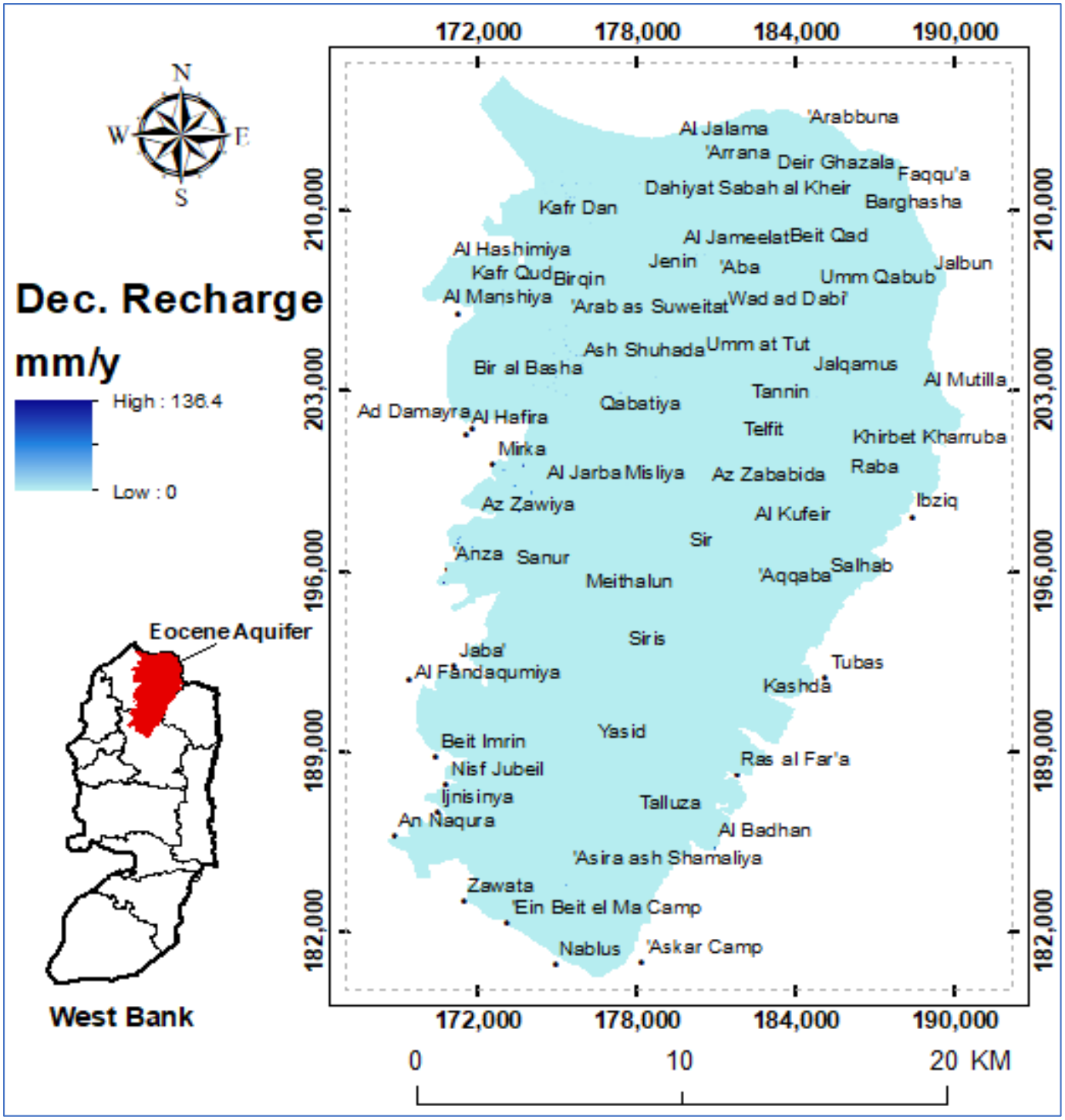

Figure D.13

The relationship between groundwater recharge and rainfall.

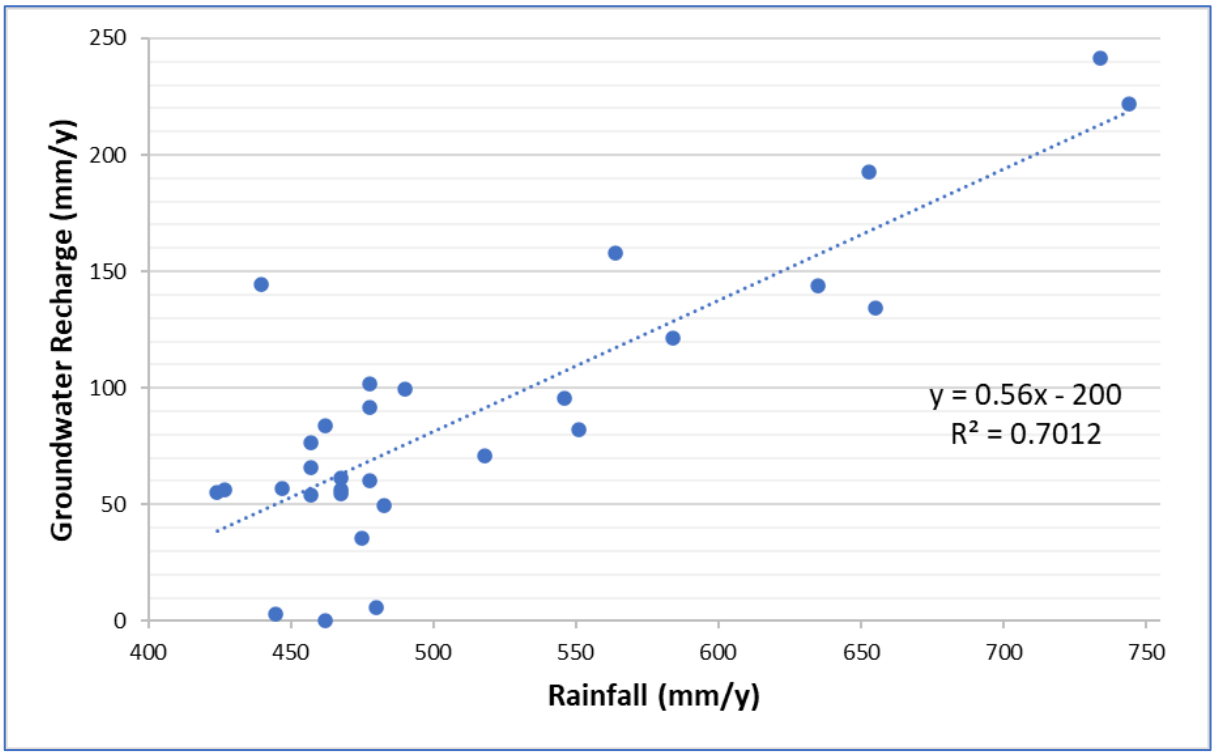

Figure D.14

The relationship between groundwater recharge and rainfall, with neglected zero recharge points

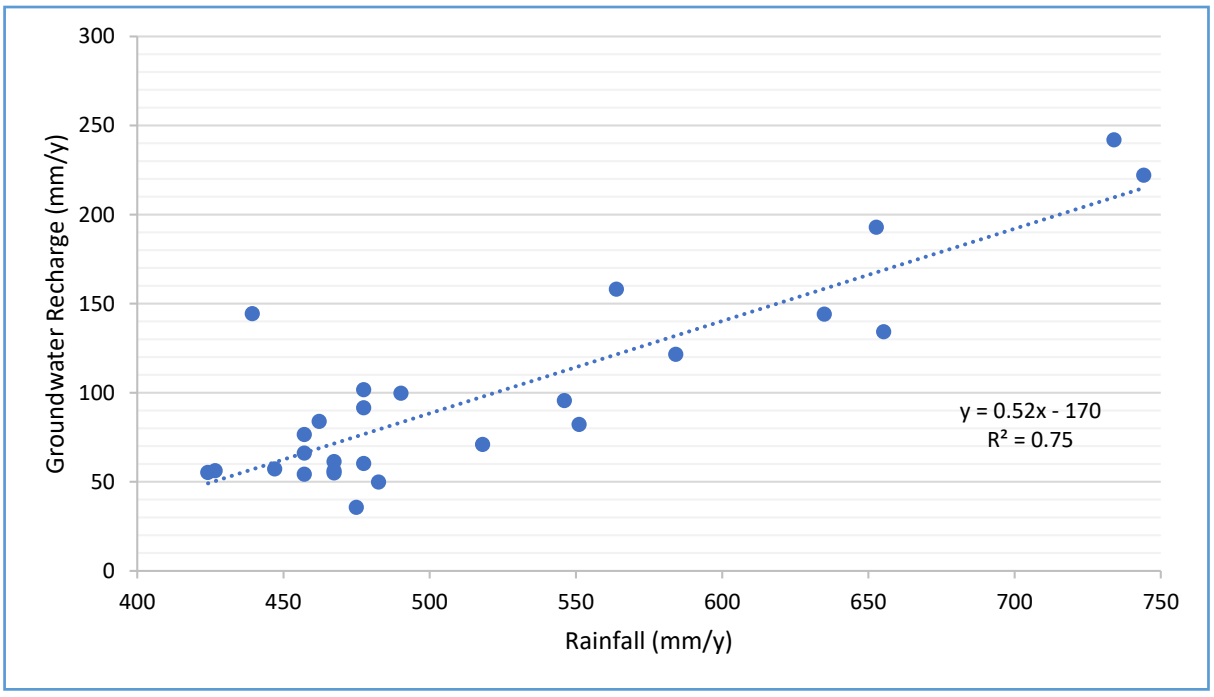

Figure D.15

The distribution of recharge for the land use types located within the Eocene Aquifer.

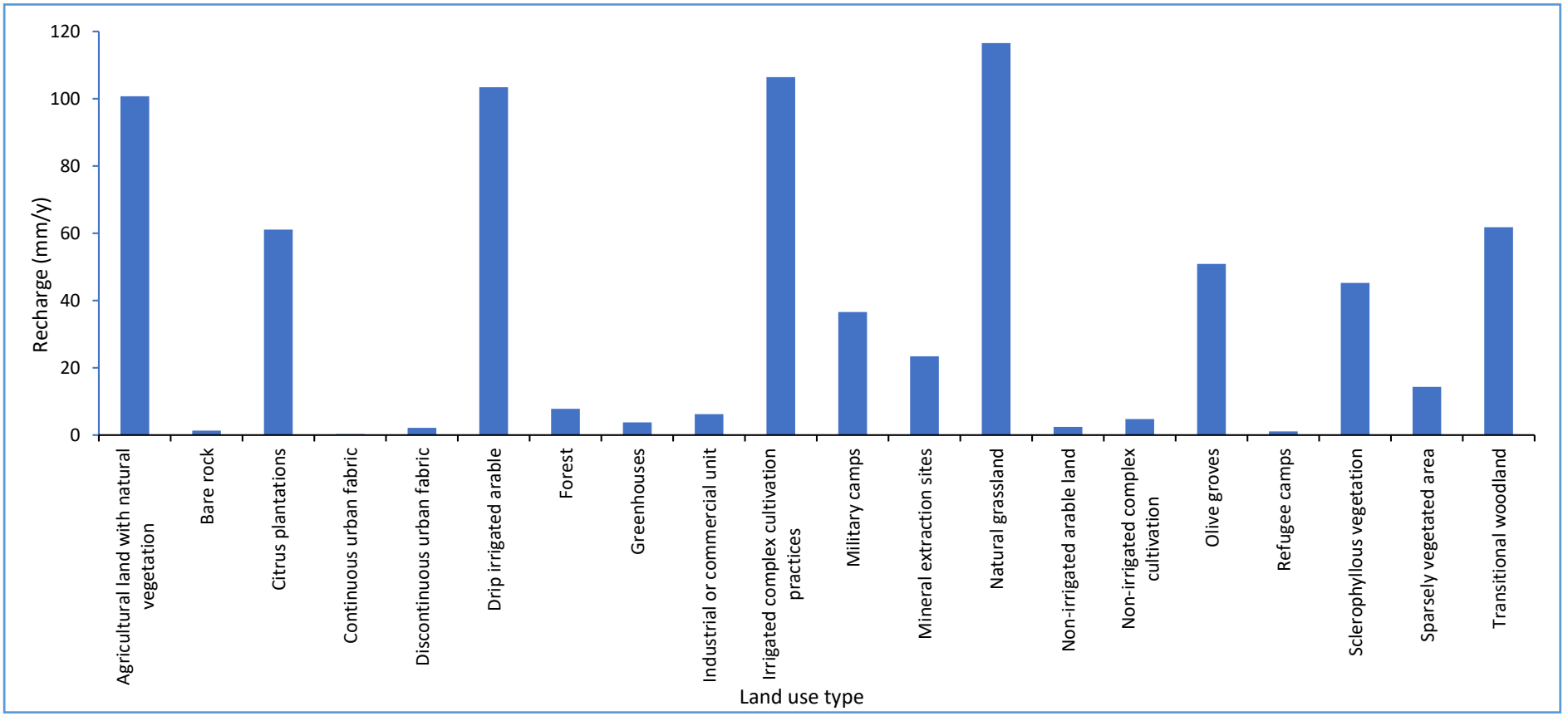

Figure D.16

The distribution of percentage of recharge for the land use types located within the Eocene Aquifer

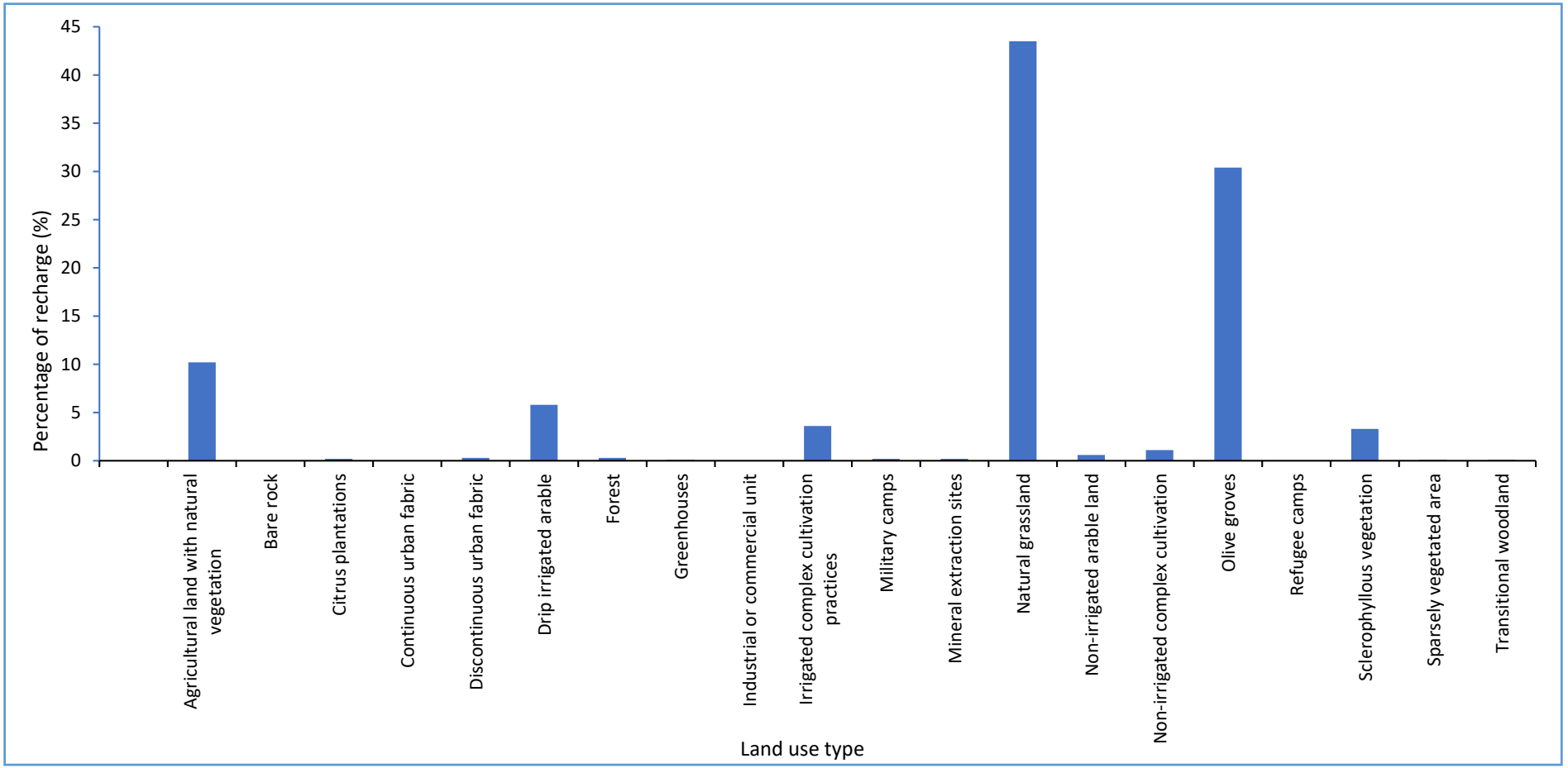

Appendix E. Tables

Table E.1

The land use lookup table.

LU Code	Description of Land use	CN II	Max Recharge	Interception		Root Depth
		HSG D	HSG D	(Growing Season)	(Non-Growing Season)	HSG D
101	Commercial and business and discontinuous urban fabric	96	1.2	0	0	2.22
104	Bare Rock	98	1.2	0	0	2.22
105	The assumed northern area	96	1.2	0	0	2.22
110	Colonies	96	1.2	0	0	2.22
111	Continuous Urban Fabric	96	1.2	0	0	2.22
112	Greenhouses	98	1.2	0	0	2.22
113	Refugee Camps	96	1.2	0	0	2.22
118	Agricultural Land with Natural Vegetation	80	1.2	0.04	0	2.22
124	Drip Irrigated Arable	89	1.2	0.05	0.05	0.83
148	Citrus Plantations	81	1.2	0.07	0.07	2.22
150	Military Camps	85	1.2	0.02	0	3.33
160	Olive Groves	79	1.2	0.05	0.05	2.22
161	Irrigated Complex Cultivation Practices	89	1.2	0.05	0.05	0.83
162	Natural Grass Land	81	1.2	0.05	0	2.45
163	Sparsely Vegetated Area	89	1.2	0.02	0	2.22
166	Non-Irrigated Arable Land	94	1.2	0	0	2.45

173	Non-Irrigated Complex Cultivation	94	1.2	0	0	2.22
175	Forest	77	1.2	0.07	0.07	3.9
240	Mineral Extraction Sites	91	1.2	0	0	2
250	Sclerophyllous vegetation and Woodland	77	1.2	0.05	0	2.22

Table E.2

The equivalent land use description for the Eocene Aquifer in the USDA tables for the curve number.

Land Use in Study Area	Its Equivalent in USDA
Commercial and business and discontinuous urban fabric	High Intensity
Bare Rock	High Intensity
The assumed northern area	High Intensity
Colonies	High Intensity
Continuous Urban Fabric	High Intensity
Greenhouses	High Intensity
Refugee Camps	High Intensity
Agricultural Land with Natural Vegetation	Pasture, grassland, or range
Drip Irrigated Arable	Row Crops
Citrus Plantations	Orchard and tree
Military Camps	Pasture, grassland, or range fair
Olive Groves	Orchard and tree
Irrigated Complex Cultivation Practices	Row Crops
Natural Grassland	Grassland (assume pasture, good condition)
Sparsely Vegetated Area	Grassland (assume pasture, poor condition)
Non-Irrigated Arable Land	Fallow land
Non-Irrigated Complex Cultivation	Fallow land
Forest	Forest
Mineral Extraction Sites	Barren
Sclerophyllous vegetation	Shrubland
Transitional Woodland	Shrubland

Table E.3

The runoff curve number values after adjusting -2%, -1%, and -0.5% from the original

LU Code	Description of Land Use	Original CN	CN (-2%)	CN (-1%)	CN (-0.5%)
		HSG D	HSG D	HSG D	HSG D
101	Commercial and business and discontinuous urban fabric	96	94.08	95.04	95.52
104	Bare Rock	98	96.04	97.02	97.51
105	The assumed northern area	96	94.08	95.04	95.52
110	Colonies	96	94.08	95.04	95.52
111	Continuous Urban Fabric	96	94.08	95.04	95.52
112	Greenhouses	98	96.04	97.02	97.51
113	Refugee Camps	96	94.08	95.04	95.52
118	Agricultural Land with Natural Vegetation	80	78.4	79.2	79.6
124	Drip Irrigated Arable	89	87.22	88.11	88.555
148	Citrus Plantations	81	79.38	80.19	80.6
150	Military Camps	85	83.3	84.15	84.575

160	Olive Groves	79	77.42	78.21	78.605
161	Irrigated Complex Cultivation Practices	89	87.22	88.11	88.555
162	Natural Grass Land	81	79.38	80.19	80.6
163	Sparsely Vegetated Area	89	87.22	88.11	88.555
166	Non-Irrigated Arable Land	94	92.12	93.06	93.53
173	Non-Irrigated Complex Cultivation	94	92.12	93.06	93.53
175	Forest	77	75.46	76.23	76.615
240	Mineral Extraction Sites	91	89.18	90.09	90.545
250	Sclerophyllous vegetation and Woodland	77	75.46	76.23	76.23

Table E.4

Calculations of agricultural water demand for the Eocene Aquifer.

Communities	**Irrigated Cultivated Areas (Dunum)**	**Water Consumption (m^3/y.dunum)**	**Water demand (m^3/y)**
Asira Al Shamalya	50	300	15,000
Al Badan	12	300	3,600
Zawata	16	300	4,800
Al Naqura	14	300	4,200
Beit Imrin	5	300	1,500
Kashda	340	1000	340,000
Ras al Far'a	332	1150	381,800
Wadi al Far'a	33	1000	33,000
Tubas	21	1000	21,000
'Arabbuna	800	1150	920,000
Al Jalama	800	900	720,000
Silat al Harithiya	15	900	13,500
'Arrana	1400	900	1,260,000
Deir Ghazala	600	1000	600,000
Faqqu'a	5	600	3,000
Beit Qad Ash Shamali	100	1100	110,000
Beit Qad Al Janubi	100	1100	110,000
Al Jameelat	100	1100	110,000
Jenin Camp	450	1000	450,000
Jalbun	250	550	137,500
'Aba (Al Gharbiya)	200	1000	200,000
Deir Abu Da'if	2300	1200	2,760,000
Birqin	3200	1000	3,200,000
Al Yamun	600	1100	660,000
Kafr Dan	1500	1100	1,650,000
Jenin	1000	1100	1,100,000
Kufeirit	16	900	14,400
Qabatiya	1300	900	1,170,000
Jaba'	50	700	35,000
Siris	500	900	450,000
Meithalun	1800	800	1,440,000
Al Judeida	1000	700	700,000
Sanur	500	800	400,000
'Ajja	500	800	400,000
Sir	1600	800	1,280,000
Al Kufeir	2200	900	1,980,000
		Sum	**22,678,300**

Table E.5

Calculations of water demand for sheeps for the Eocene Aquifer.

Communities	Number of Sheep	Average Typical Water Uses by Sheep (L/sheep.day)	Water Demand (m^3/y)
Yasid	3000	10	10,950
Asira Al Shamalya	4000	10	14,600
Al Badan	720	10	2,628
Talluza	1000	10	3,650
Nisf Jubeil	500	10	1,825
Ijnisinya	200	10	730
Beit Imrin	4000	10	14,600
Zawata	330	10	1,205
Al Naqura	450	10	1,643
Beit Iba	200	10	730
Kashda	900	10	3,285
Aqqaba	2800	10	10,220
Salhab	200	10	730
Ras al Far'a	415	10	1,515
Wadi al Far'a	170	10	621
Tubas	350	10	1,278
Ibziq	655	10	2,391
'Arabbuna	2000	10	7,300
Al Jalama	1200	10	4,380
Silat al Harithiya	200	10	730
'Arrana	900	10	3,285
Deir Ghazala	1800	10	6,570
Faqqu'a	5000	10	18,250
Ti'innik	160	10	584
Beit Qad Ash Shamali and Al Janubi	3000	10	10,950
Al Jameelat	20	10	73
Jenin Camp	280	10	1,022
Jalbun	4000	10	14,600
'Aba (Al Gharbiya)	5000	10	18,250
Deir Abu Da'if	2600	10	9,490
Umm at Tut	1900	10	6,935
Jalqamus	900	10	3,285
Al Mughayyir	5000	10	18,250
Al Mutilla	1170	10	4,271
Bir al Basha	1100	10	4,015
Tannin	250	10	913
Al Hafira (Hafirat Arraba)	100	10	365

Arraba	88	10	321
Telfit	250	10	913
Mirka	3000	10	10,950
Raba	2700	10	9,855
Misliya	800	10	2,920
Al Jarba	400	10	1,460
Az Zababida	1800	10	6,570
Az Zawiya	2000	10	7,300
Al Kufeir	400	10	1,460
Sir	900	10	3,285
'Ajja	2100	10	7,665
'Anza	900	10	3,285
Sanur	1600	10	5,840
Meithalun	2000	10	7,300
Al Judeida	1500	10	5,475
Al Hashimiya	500	10	1,825
Kafr Qud	1900	10	6,935
Birqin	2500	10	9,125
Kufeirit	400	10	1,460
Jenin	7000	10	25,550
Al Yamun	2000	10	7,300
Kafr Dan	1000	10	3,650
Siris	900	10	3,285
Jaba'	4000	10	14,600
Al Fandaqumiya	170	10	621
Qabatiya	5000	10	18,250
Al Mazar	1100	10	4,015
		Sum	**377,330**

Table E.6

Calculations of water demand for cows for the Eocene Aquifer.

Communities	Number of Cows	Average Typical Water Use by Cow (L/cow.day)	Water Demand (m^3/y)
Yasid	20	85	621
Asira Al Shamalya	50	85	1,551
Al Badan	5	85	155
Talluza	70	85	2,172
Zawata	992	85	30,777
Al Naqura	5	85	155
'Arabbuna	70	85	2,172
Al Jalama	40	85	1,241
Silat al Harithiya	10	85	310
'Arrana	16	85	496
Deir Ghazala	10	85	310
Faqqu'a	12	85	372
Ti'innik	8	85	248
Beit Qad Ash Shamali and Al Janubi	75	85	2,327
Jenin Camp	7	85	217
Jalbun	70	85	2,172
Deir Abu Da'if	33	85	1,024
Umm at Tut	60	85	1,862
Jalqamus	12	85	372
Al Mughayyir	20	85	621
Al Mutilla	6	85	186
Bir al Basha	7	85	217
Tannin	25	85	776
Al Hafira (Hafirat Arraba)	2	85	62
Arraba	133	85	4,126
Telfit	2	85	62
Mirka	17	85	527
Raba	36	85	1,117
Misliya	17	85	527
Az Zababida	6	85	186
Az Zawiya	500	85	15,513
'Ajja	1100	85	34,128
'Anza	170	85	5,274
Sanur	90	85	2,792
Meithalun	34	85	1,055
Al Judeida	200	85	6,205
Al Hashimiya	300	85	9,308

Kafr Qud	15	85	465
Birqin	38	85	1,179
Kufeirit	50	85	1,551
Jenin	40	85	1,241
Al Yamun	56	85	1,737
Kafr Dan	17	85	527
Siris	25	85	776
Jaba'	12	85	372
Qabatiya	220	85	6,826
Al Mazar	20	85	621
		Sum	**146,531**

Table E.7

Calculations of poultry water demand for the Eocene Aquifer.

Communities	Number of Chickens	Average Typical Water Use by Poultry (L/poultry.day)	Water Demand (m^3/y)
Yasid	14,000	0.18	920
Asira Al Shamalya	200,000	0.18	13,140
Al Badan	2,400	0.18	158
Talluza	8,000	0.18	526
Ijnisinya	10,000	0.18	657
Beit Imrin	5,000	0.18	329
Al Naqura	2,700	0.18	177
Salhab	50,000	0.18	3,285
Tubas	2,100	0.18	138
Jenin district	3,801,600	0.18	249,765
Bir al Basha	118,000	0.18	7,753
Mirka	53,000	0.18	3,482
Raba	60,000	0.18	3,942
Misliya	54,000	0.18	3,548
Az Zababida	10,000	0.18	657
Az Zawiya	150,000	0.18	9,855
Sir	200,000	0.18	13,140
'Anza	14,000	0.18	920
Sanur	12,000	0.18	788
Meithalun	220,000	0.18	14,454
Al Judeida	427,000	0.18	28,054
Siris	50,000	0.18	3,285
Jaba'	5,000	0.18	329
Qabatiya	280,000	0.18	18,396
		Sum	**377,696**

Table E.8

Calculations of domestic water demand for the Eocene Aquifer.

Number of populations	Average daily consumption (L/day.capita)	water demand (m^3/y)
230,400	85.6	7,198,618

Table E.9

Results of the sensitivity analysis for recharge corresponding to curve number values by ±5 and ±10%.

LU Code	Description of land use	CN (adjusted)	CN (-5%)	RPS	CN (-10%)	RPS	CN (5%)	RPS	CN (10%)	RPS
		HSG D	HSG D	%	HSG D	%	HSG D	%	HSG D	%
101	Commercial and business and discontinuous urban fabric	95.52	90.744	293.43	85.968	253.85	100.296	-108.27	105.072	-132.15
104	Bare Rock	97.51	92.6345	293.43	87.759	253.85	102.3855	-108.27	107.261	-132.15
105	The assumed northern area	95.52	90.744	293.43	85.968	253.85	100.296	-108.27	105.072	-132.15
110	Colonies	95.52	90.744	293.43	85.968	253.85	100.296	-108.27	105.072	-132.15
111	Continuous Urban Fabric	95.52	90.744	293.43	85.968	253.85	100.296	-108.27	105.072	-132.15
112	Greenhouses	97.51	92.6345	293.43	87.759	253.85	102.3855	-108.27	107.261	-132.15
113	Refugee Camps	95.52	90.744	293.43	85.968	253.85	100.296	-108.27	105.072	-132.15
118	Agricultural Land with Natural Vegetation	79.6	75.62	293.43	71.64	253.85	83.58	-108.27	87.56	-132.15
124	Drip Irrigated Arable	88.555	84.12725	293.43	79.6995	253.85	92.98275	-108.27	97.4105	-132.15
148	Citrus Plantations	80.6	76.57	293.43	72.54	253.85	84.63	-108.27	88.66	-132.15
150	Military Camps	84.575	80.34625	293.43	76.1175	253.85	88.80375	-108.27	93.0325	-132.15
160	Olive Groves	78.605	74.67475	293.43	70.7445	253.85	82.53525	-108.27	86.4655	-132.15
161	Irrigated Complex Cultivation Practices	88.555	84.12725	293.43	79.6995	253.85	92.98275	-108.27	97.4105	-132.15
162	Natural Grass Land	80.6	76.57	293.43	72.54	253.85	84.63	-108.27	88.66	-132.15
163	Sparsely Vegetated Area	88.555	84.12725	293.43	79.6995	253.85	92.98275	-108.27	97.4105	-132.15
166	Non-Irrigated Arable Land	93.53	88.8535	293.43	84.177	253.85	98.2065	-108.27	102.883	-132.15
173	Non-Irrigated Complex Cultivation	93.53	88.8535	293.43	84.177	253.85	98.2065	-108.27	102.883	-132.15

175	Forest	76.615	72.78425	293.43	68.9535	253.85	80.44575	-108.27	84.2765	-132.15
240	Mineral Extraction Sites	90.545	86.01775	293.43	81.4905	253.85	95.07225	-108.27	99.5995	-132.15
250	Sclerophyllous vegetation and Woodland	76.615	72.78425	293.43	68.9535	253.85	80.44575	-108.27	84.2765	-132.15

Table E.10

The relationship between land use and recharge rate.

Land Use Type	Area (km^2)	Percentage of Area	Recharge (mm/y)	Percentage of Recharge
Olive groves	139	30.30%	50.87	30.4%
Natural grassland	87	19.00%	116.53	43.5%
Non-irrigated arable land	55.64	12.13%	2.46	0.6%
Non-irrigated complex cultivation	54.88	12.00%	4.77	1.1%
Discontinuous urban fabric	34.9	7.61%	2.18	0.3%
Agricultural land with natural vegetation	23.5	5.11%	100.72	10.2%
Sclerophyllous vegetation	16.91	3.68%	45.25	3.3%
Drip irrigated arable	13	2.83%	103.4	5.8%
Forest	10.4	2.26%	7.8	0.3%
Irrigated complex cultivation practices	7.84	1.71%	106.4	3.6%
Greenhouses	3.4	0.75%	3.77	0.1%
Bare rock	2.83	0.62%	1.34	0.0%
Sparsely vegetated area	2.16	0.47%	14.32	0.1%
Continuous urban fabric	1.77	0.38%	0.3	0.0%
Mineral extraction sites	1.74	0.38%	23.44	0.2%
Military camps	1.15	0.25%	36.6	0.2%
Citrus plantations	0.67	0.15%	61.1	0.2%
Refugee camps	0.51	0.11%	1.08	0.0%
Industrial or commercial unit	0.49	0.11%	6.23	0.0%
Transitional woodland	0.49	0.11%	61.8	0.1%

Appendix F. Swb Model Tutorial

1) After extraction of the SWB software, the files are arranged as follows:

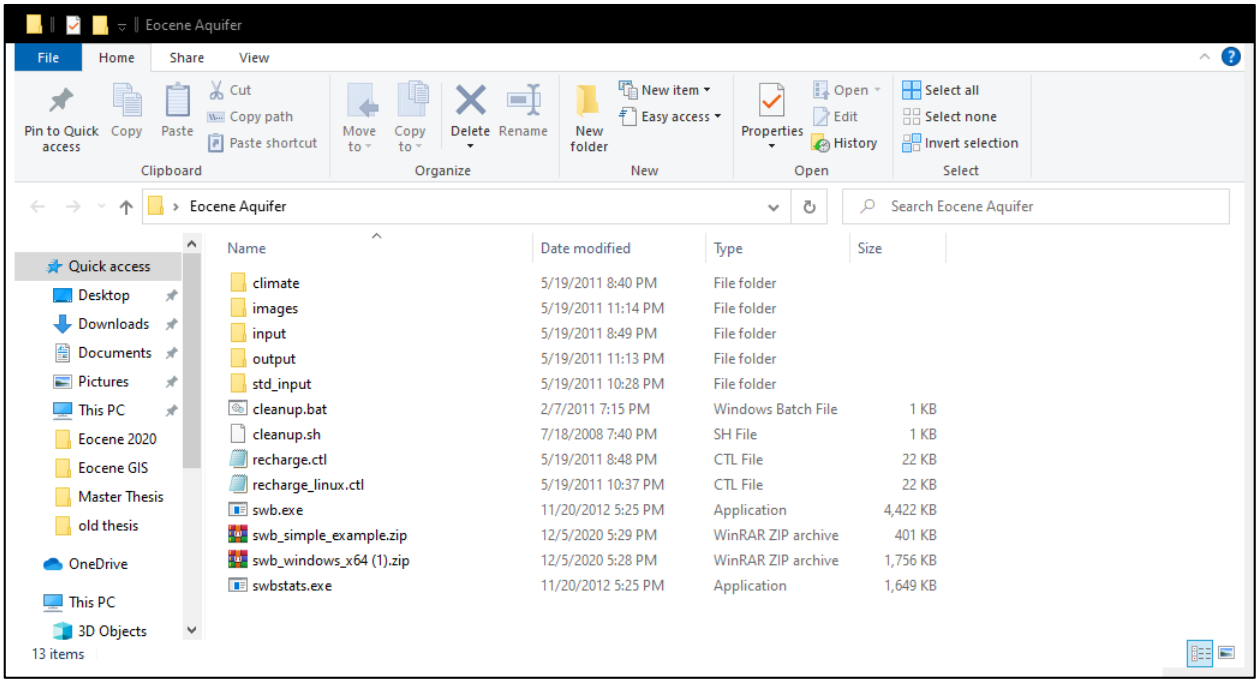

2) Place the ASCII gridded files (AWC, HSG, flow direction, FSM, and land use) that were processed using ArcMap into a file named Input.

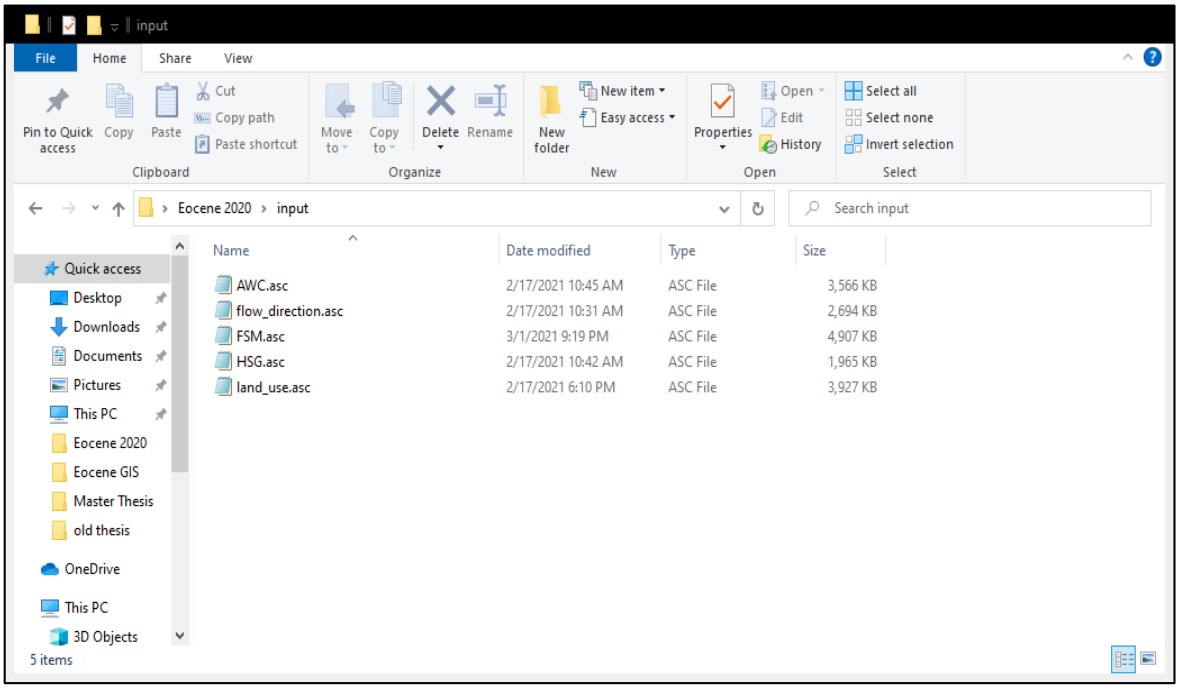

3) Place the land use lookup table and the soil moisture retention grid in a file named Std Input. The land use lookup table must be in text format (*.txt). When you need to make any modifications to this table, open it in Excel format, and upon completion, convert it to text format. The soil moisture retention grid is attached to the package of the code in ASCII file format and it does not need any modification.

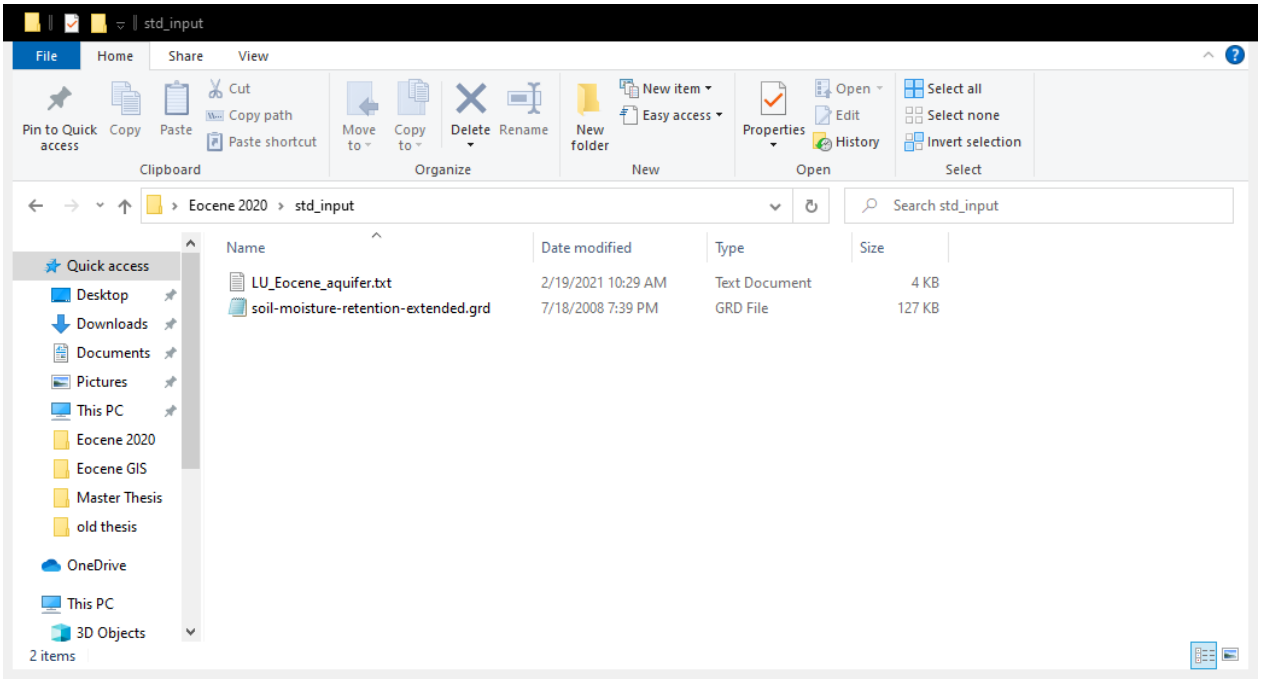

4) Place the ASCII files for daily rainfall in a file named Climate. A climate file contains a file named temp in which daily temperature data (maximum and minimum) are entered in ASCII file format.

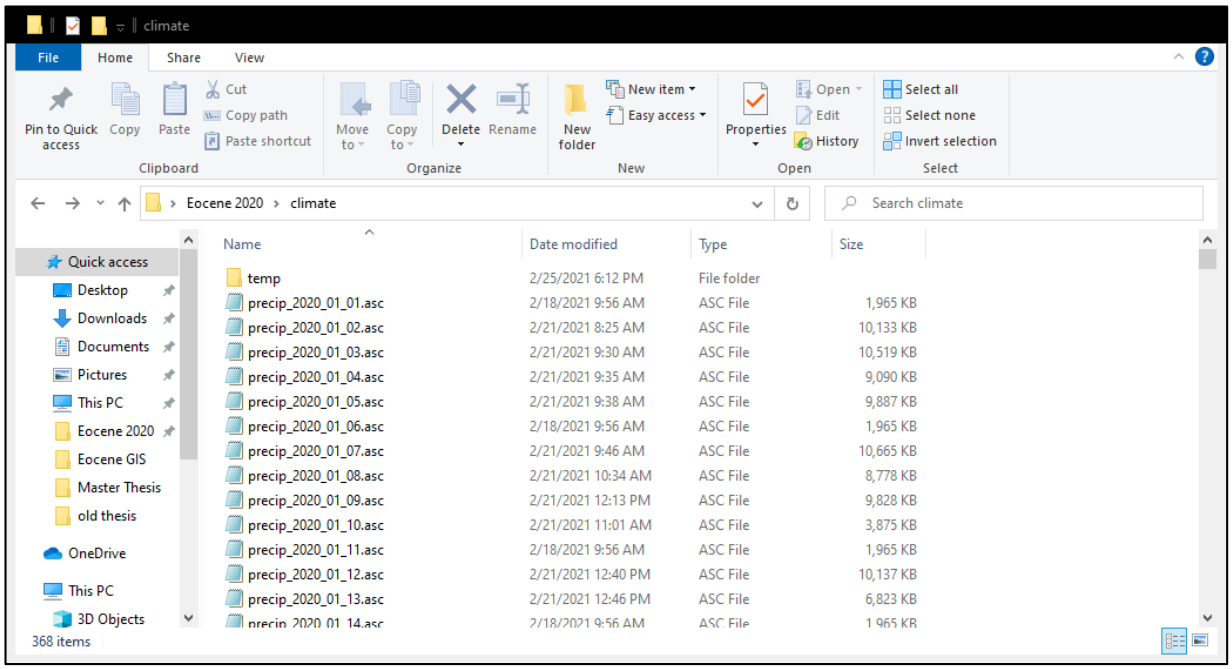

5) Before you start writing the code, create a new text file that contains the code to be written. After writing the code, make sure to convert the text file (*.txt) into a control file (*.ctl) because SWB code will not run if the control file is still in text format.

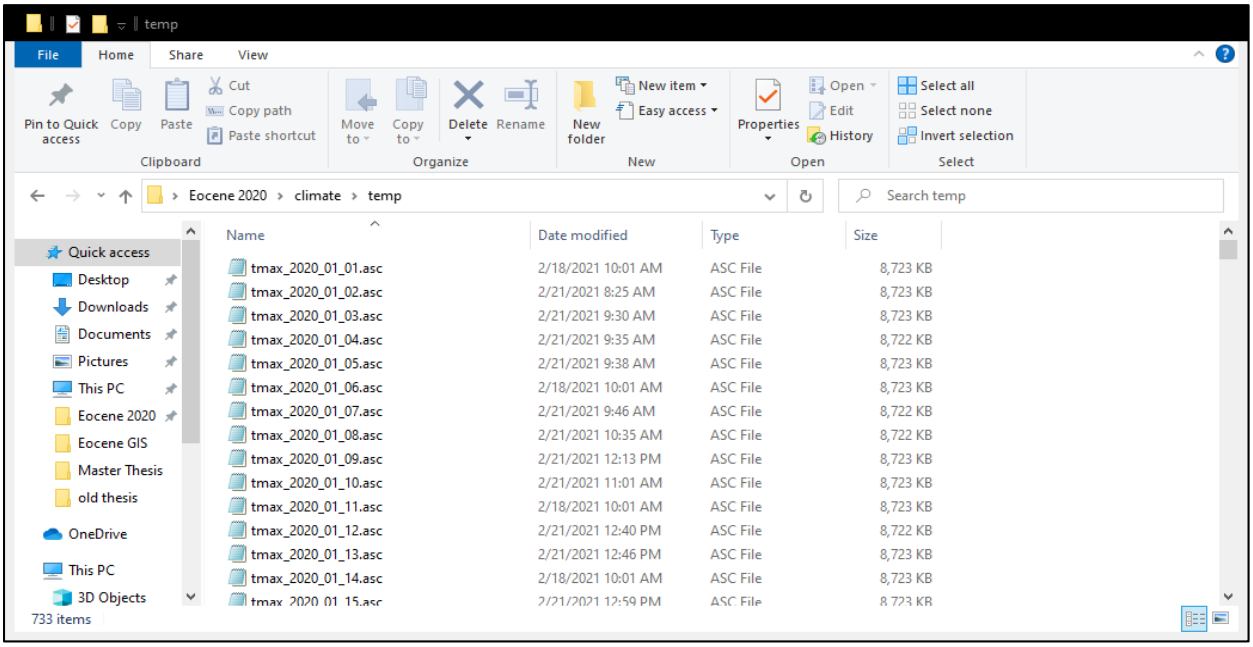

6) It is necessary to use the SWB code tutorial to learn how to write the code for the study area. The following text represents the SWB code for the Eocene Aquifer:

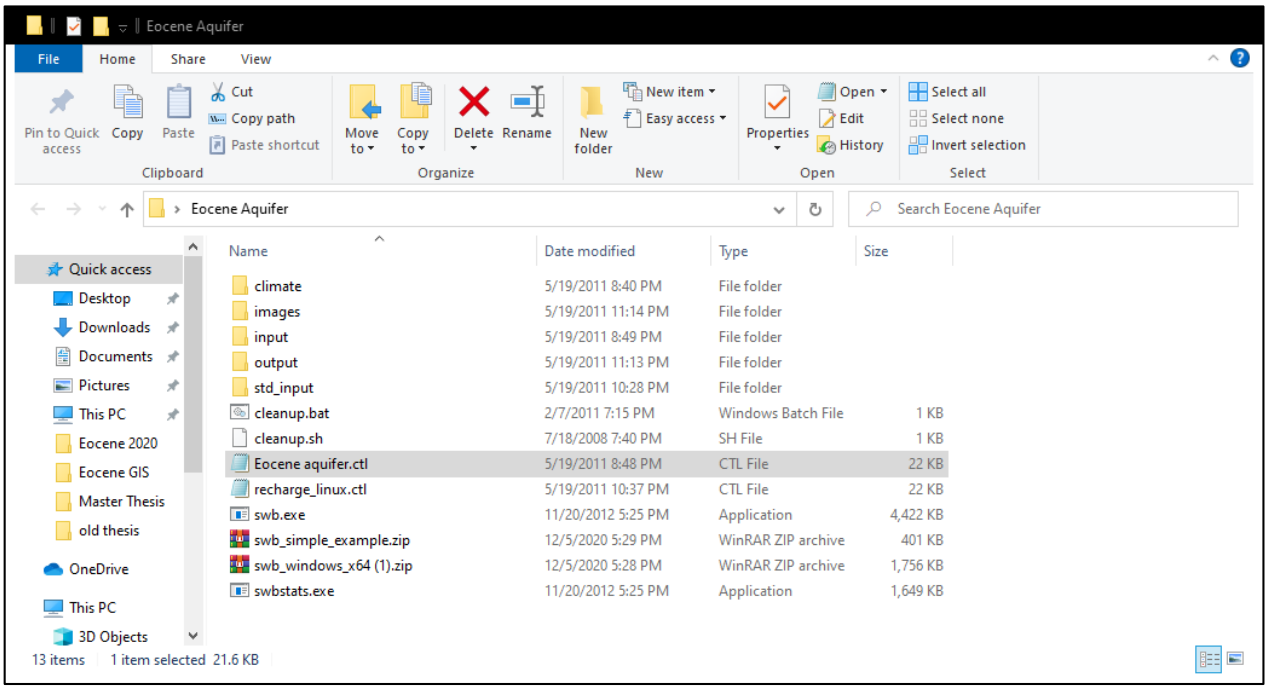

MODEL DOMAIN DEFINITION

NX NY X0 Y0 X1 Y1 Size

GRID 818 1228 167462.50940719 178907.12327103 192002.50940719 215747.12327103 30

#***

LENGTH UNITS

GRID_LENGTH_UNITS METERS

#***

OUTPUT CONTROL

TURN OFF SCREEN OUTPUT?

SUPPRESS_SCREEN_OUTPUT

#***

GROWING SEASON

GROWING_SEASON 305 120 TRUE

#***

ANSI_COLORS FALSE

#***

RLE_MULTIPLIER 10000

#***

PRECIPITATION

PRECIPITATION ARC_GRID climate\precip

#***

TEMPERATURE

TEMPERATURE ARC_GRID climate\temp\tmax climate\temp\tmin

#***

OUTPUT GRID FILENAME SUFFIX

OUTPUT_GRID_SUFFIX asc

#***

INITIAL ABSTRACTION METHOD

INITIAL_ABSTRACTION_METHOD TR55

#***

INITIAL CONTINUOUS FROZEN GROUND INDEX

INITIAL_FROZEN_GROUND_INDEX CONSTANT 0.0

#***

FROZEN GROUND THRESHOLD CFGI VALUE

UPPER_LIMIT_CFGI 83.

LOWER_LIMIT_CFGI 56.

#***

FLOW DIRECTION

FLOW_DIRECTION ARC_GRID input\flow_direction.asc

#***

SOIL GROUP

SOIL_GROUP ARC_GRID input\HSG.asc

#***

LAND USE/COVER CLASSIFICATION

LAND_USE ARC_GRID input\land_use.asc

#***

Land Use LOOKUP table:

LAND_USE_LOOKUP_TABLE std_input\LU_Eocene_aquifer.txt

#***

BASE SOIL WATER CAPACITY

WATER_CAPACITY ARC_GRID input\AWC.asc

#***

SOIL MOISTURE ACCOUNTING METHOD

SM T-M std_input\soil-moisture-retention-extended.grd

#***

INITIAL SOIL MOISTURE

INITIAL_SOIL_MOISTURE ARC_GRID input\FSM.asc

#***

INITIAL SNOW COVER

INITIAL_SNOW_COVER CONSTANT 0

#***

SOLUTION METHOD

RUNOFF C-N DOWNHILL

#**********

EVAPOTRANSPIRATION METHOD

ET HARGREAVES 32.20 32.55

#**********

PLOTTING CUSTOMIZATION

DISLIN_PARAMETERS RECHARGE

SET_Z_AXIS_RANGE DAILY 0 1.5 0.1

SET_Z_AXIS_RANGE MONTHLY 0 7 1.0

SET_Z_AXIS_RANGE ANNUAL 0 20 2.

Z_AXIS_TITLE RECHARGE, IN INCHES

#

DISLIN_PARAMETERS ACT_ET

SET_Z_AXIS_RANGE DAILY 0 0.8 0.05

SET_Z_AXIS_RANGE MONTHLY 0 10. 0.5

SET_Z_AXIS_RANGE ANNUAL 0 40. 5.0

#SET_DEVICE PDF

#SET_FONT Helvetica-Bold

Z_AXIS_TITLE ACTUAL ET, IN INCHES

#

DISLIN_PARAMETERS POT_ET

```
SET_Z_AXIS_RANGE DAILY 0 0.8 0.05

SET_Z_AXIS_RANGE MONTHLY 0 10. 0.5

SET_Z_AXIS_RANGE ANNUAL 0 45. 5.

#SET_DEVICE WMF

#SET_FONT Courier New Italic

Z_AXIS_TITLE POTENTIAL ET, IN INCHES

#

#DISLIN_PARAMETERS RUNOFF_OUTSIDE

#SET_Z_AXIS_RANGE DAILY 0 5. 0.5

#SET_Z_AXIS_RANGE MONTHLY 0 12. 0.5

#SET_Z_AXIS_RANGE ANNUAL 0 25. 5.

#Z_AXIS_TITLE RUNOFF OUT OF GRID, IN INCHES

#

#DISLIN_PARAMETERS SNOWCOVER

#SET_Z_AXIS_RANGE DAILY 0 12. 0.5

#Z_AXIS_TITLE SNOW COVER, IN INCHES (WATER EQUIVALENT)

#

DISLIN_PARAMETERS SM_APWL

SET_Z_AXIS_RANGE DAILY -20. 0. 2.0

Z_AXIS_TITLE ACCUMULATED POTENTIAL WATER LOSS, IN INCHES

SET_COLOR_TABLE RRAIN
```

```
#***************************************************************
# OUTPUT OPTIONS
# Format for specifying output options is:
# "OUTPUT_OPTIONS variable_name daily_option monthly_option annual_option",
# where the possible values for each option are:
# NONE, GRAPH (or PLOT), GRID, or BOTH
OUTPUT_OPTIONS RECHARGE NONE BOTH BOTH
OUTPUT_OPTIONS SM_APWL NONE NONE PLOT
OUTPUT_OPTIONS SNOWCOVER NONE NONE NONE
OUTPUT_OPTIONS INTERCEPTION NONE GRID BOTH
OUTPUT_OPTIONS RUNOFF_OUTSIDE NONE NONE BOTH
OUTPUT_OPTIONS ACT_ET NONE NONE BOTH
OUTPUT_OPTIONS POT_ET NONE NONE BOTH
OUTPUT_OPTIONS GROSS_PRECIP NONE NONE GRID
OUTPUT_OPTIONS AVG_TEMP NONE NONE GRID
OUTPUT_OPTIONS INFLOW NONE NONE GRID
OUTPUT_OPTIONS OUTFLOW NONE NONE GRID
OUTPUT_OPTIONS CHG_IN_SOIL_MOIS NONE NONE GRID
#***************************************************************
# OUTPUT GRID FILE FORMAT
OUTPUT_FORMAT ARC_GRID
```

#**

SOLVE_NO_TS_FILE 2020 2020

#

EOJ

#

7) To run the model:

a) Open a command prompt.

b) Type CD (change directory) and copy the path of the file that contains the control file for the code, and press enter.

c) Type the following command: swb control_file_name.ctl (swb Eocene_aquifer.ctl)

d) Press enter. The SWB will now run the complete model. This could take hours depending on the cell size and resolution.

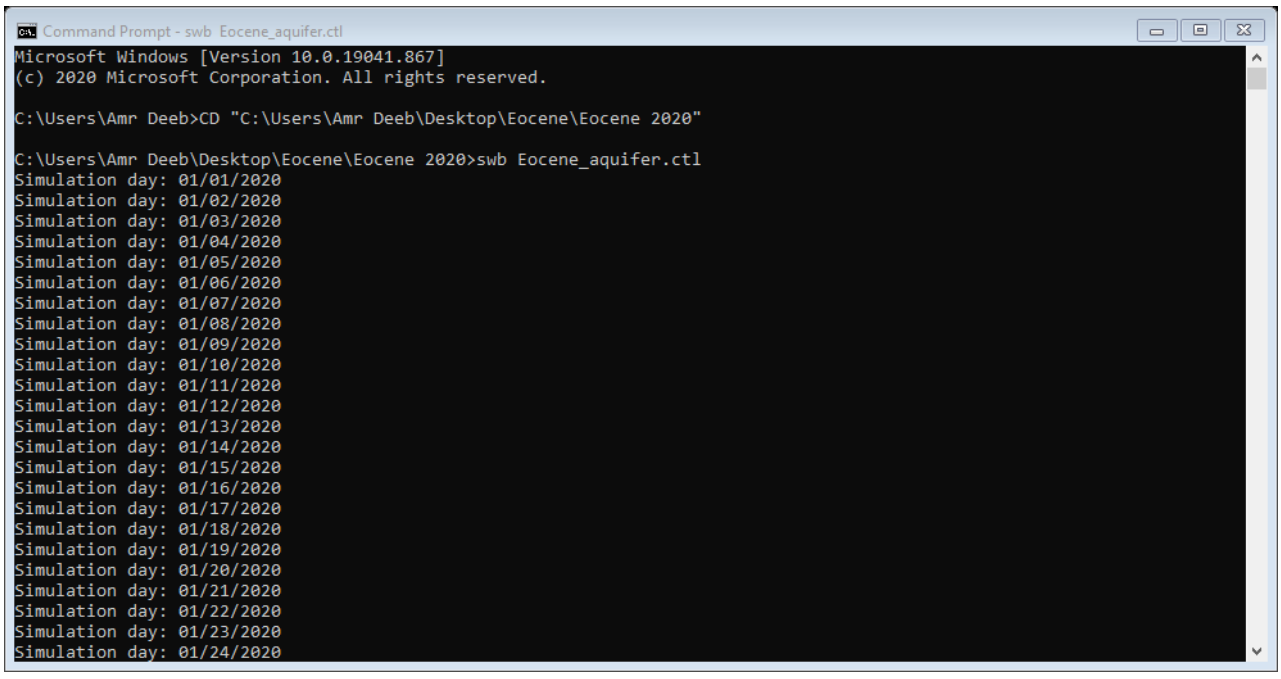

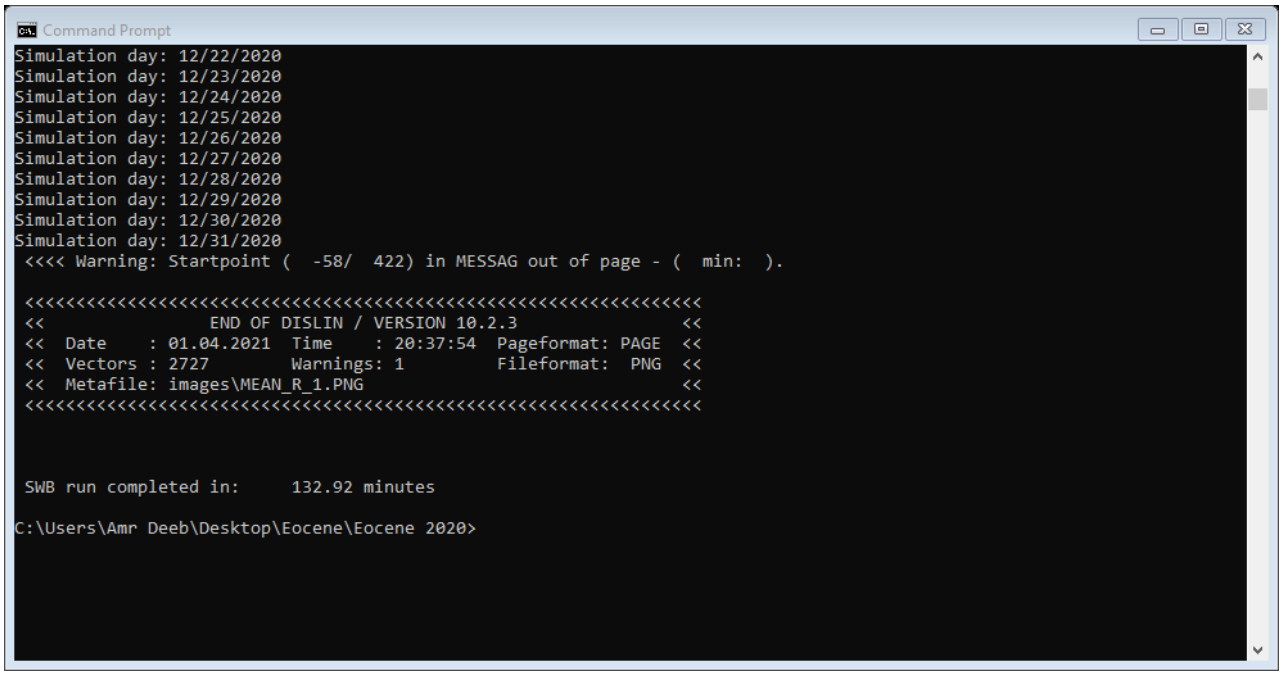
Command Prompt
Simulation day: 12/22/2020
Simulation day: 12/23/2020
Simulation day: 12/24/2020
Simulation day: 12/25/2020
Simulation day: 12/26/2020
Simulation day: 12/27/2020
Simulation day: 12/28/2020
Simulation day: 12/29/2020
Simulation day: 12/30/2020
Simulation day: 12/31/2020
<<<< Warning: Startpoint (-58/ 422) in MESSAG out of page - (min:).
<<<<<<<<<<<<<<<<<<<<<<<<<<<<<<<<<<<<<<<<<<<<<<<<<<<<<<<<<<<<<<<<<<<<<<<
<< END OF DISLIN / VERSION 10.2.3 <<
<< Date : 01.04.2021 Time : 20:37:54 Pageformat: PAGE <<
<< Vectors : 2727 Warnings: 1 Fileformat: PNG <<
<< Metafile: images\MEAN_R_1.PNG <<
<<<<<<<<<<<<<<<<<<<<<<<<<<<<<<<<<<<<<<<<<<<<<<<<<<<<<<<<<<<<<<<<<<<<<<<
SWB run completed in: 132.92 minutes
C:\Users\Amr Deeb\Desktop\Eocene\Eocene 2020>

جامعة النجاح الوطنية

كلية الدراسات العليا

نمذجة تغذية المياه الجوفية للحوض الجوفي الايوسيني (فلسطين) باستخدام برنامج (SWB) المطور من قبل هيئة المسح الجيولوجي الأمريكية

إعداد

عمرو عادل ديب

إشراف

د. محمد نهاد المصري

قدمت هذه الأطروحة استكمالا لمتطلبات الحصول على درجة الماجستير في هندسة المياه والبيئة بكلية الدراسات العليا في جامعة النجاح الوطنية، نابلس، فلسطين.

2021

نمذجة تغذية المياه الجوفية للحوض الجوفي الايوسيني (فلسطين) باستخدام برنامج (SWB) المطور من قبل هيئة المسح الجيولوجي الأمريكية

إعداد

عمرو عادل ديب

إشراف

د. محمد نهاد المصري

الملخص

تعتبر المياه الجوفية هي المصدر الرئيسي للمياه العذبة في فلسطين. إن إعادة تغذية المياه الجوفية هي عملية هيدرولوجية تحدث عندما تتسرب المياه إلى باطن الأرض وتصل إلى منطقة التشبع. تبدأ هذه العملية بحدوث هطول الأمطار على سطح الأرض، تليها عملية تسرب المياه إلى منطقة الجذور. تعد تغذية المياه الجوفية أحد مكونات الدورة الهيدرولوجية، لكنها أقلها فهماً؛ لأنها متغيرة بدرجة كبيرة مكانياً وزمانياً ويصعب قياسها بشكل مباشر. ومع ذلك، فإن معرفة وقياس كمية تغذية الحوض الجوفي أمر حيوي ومهم للغاية لعملية إدارة المياه الجوفية. استخدم هذا البحث كود توازن المياه في التربة (SWB) الذي طورته هيئة المسح الجيولوجي الأمريكية (USGS)، لمحاكاة التغذية المحتملة للمياه الجوفية للحوض الجوفي الايوسيني لعام 2020. يقع الحوض الجوفي الايوسيني في الجزء الشمالي من الضفة الغربية، فلسطين. تتمثل ميزات كود SWB في أنه من السهل الحصول على المدخلات التي يحتاجها هذا الكود، ويقدر الكود كمية إعادة تغذية المياه الجوفية بدقة بناءً على التوزيعات المكانية والزمانية. تم اختيار الدقة المكانية لنموذج SWB بخلايا موحدة 30 م × 30 م.

من أجل نمذجة إعادة التغذية، تم تقسيم مدى الخزان الجوفي إلى خلايا مربعة منتظمة. نجح نموذج SWB في تقدير كمية إعادة التغذية بناءً على التغيرات المكانية والزمانية لعام 2020 بقيمة 50.70 ملم / سنة (1.996 بوصة / سنة) ومجموع إعادة التغذية السنوي لكامل الحوض الجوفي الايوسيني خلال فترة الدراسة هو 23.25 مليون متر مكعب. بلغت كمية التغذية حوالي 10.07٪ من حجم هطول الأمطار. يختلف معدل إعادة الشحن باختلاف أنواع استخدامات الأراضي. تم التحقق من نموذج SWB باستخدام طريقة Water Table Fluctuation (WTF) وطريقة Water Demand Calculation (WDC) من خلال مقارنة نتائج قيم إعادة التغذية المحتملة التي تم الحصول عليها من نموذج SWB مع قيم إعادة التغذية التي تم الحصول عليها من طرق WTF وWDC. أظهر البحث توافق كبير بين نموذج SWB وطرق التحقق. تم تعديل قيم رقم المنحنى (CN) يدويًا بنسبة −2٪، و −1٪، و −0.5٪ لأنواع استخدامات الأراضي، لإيجاد أفضل توافق لطريقة WTF وللحصول على نتائج أكثر واقعية. تم تقييم أداء نموذج SWB بعد عملية التحقق باستخدام الخطأ النسبي (RE) وجودة التوافق بين قيم إعادة التغذية المحاكاة الناتجة عن نموذج SWB وقيم إعادة التغذية المرصودة الناتجة عن طريقة WTF. تم تقدير الكمية الإجمالية السنوية للطلب على المياه في منطقة الحوض الجوفي الايوسيني بحوالي 28.29 مليون متر مكعب، حيث أثبتت نتائج البحث أن مستوى المياه الجوفية في الحوض الجوفي الإيوسيني يتناقص مع الزمن بسبب العجز المائي السنوي، والذي تم تقديره بحوالي حوالي 5.04 مليون متر مكعب. تم إجراء تحليل الحساسية لفحص كيفية تأثير النسبة المئوية للتغير في قيم رقم المنحنى على النسبة المئوية للتغير في إعادة التغذية. تم تعديل قيم رقم المنحنى لجميع استخدامات الأراضي بنسبة ± 5٪ و ± 10٪. أظهرت النتائج أن تغذية المياه الجوفية حساسة للغاية للتغيرات الصغيرة في قيم رقم المنحنى ولها تأثير كبير على نتائج النموذج. تحدث أعلى معدلات التغذية في الأجزاء الجنوبية والشمالية الغربية

من الحوض الجوفي الايوسيني. بينما أدنى معدلات التغذية تحدث في وسط وشمال الحوض الجوفي. يتوافق هذا مع التوزيع المكاني لهطول الأمطار وأنواع استخدامات الأراضي في المنطقة. أوصى البحث بضرورة وضع خطة لإدارة المياه الجوفية في الحوض الجوفي الايوسيني بناءً على نتائج نموذج SWB من أجل إدارة موارد المياه المتجددة والمستدامة في هذا الحوض الجوفي وزيادة منسوب المياه الجوفية من خلال تحقيق التوازن بين التغذية والضخ الكلي، ووضع خطط وقائية لحماية المياه الجوفية من التلوث، وفهم التأثير السلبي لتحويل مناطق التغذية العالية إلى مناطق سكنية على الوضع المائي في الخزان الجوفي.